CHAPTER IV

RESULTS AND DISCUSSION

Pharmaceutical applications of cyclodextrins (CDs) as additives and drug complexing agents have been rapidly growing. Abundance of drug molecules are capable of residing partially within the central cavity of a CD molecule, thus forming an inclusion complex. The interaction may alter the chemical and/or physical properties of the guest molecule and lead to improve stability, aqueous solubility, and bioavailability. The purpose of this research is to study the effects of CDs on the chemical stability of ranitidine HCl (R) in solution and solid state. Two CDs were included in this investigation, β - CD and 2HP-β-CD. Three preparation methods (co-grinding, freeze-drying, and kneading) and three molar ratios of R:CD (1:1, 1:2, and 2:1) were performed for the formation of inclusion complexes.

1. Preparations of Ranitidine HCl (R) : Cyclodextrin (β - CD, 2HP-β-CD) Inclusion Complexes

The appearance of ranitidine HCl is a white to pale yellow, slightly sulfur-mercaptan odor, crystalline powder. β - CD is a white, non-hygroscopic, free-flowing, crystalline powder. 2HP-β-CD is a white, fluffy, non-hygroscopic powder.

The R:CD products having both CDs as host molecules prepared by both co-grinding and freeze-drying methods were relatively easy to prepared. In the case of co-grinding method, the products were finely white powder. The products obtained by the freeze-drying method were white, fluffy powder when β-CD was used as the host, but they were white powder when 2HP-β-CD was used as the host.

The kneaded products of R:β-CD were pale yellow sticky mass but the kneaded mixtures of R:2HP-β-CD were white sticky viscous mass. Therefore, the products were dried without screening. The products of R:β-CD and R:2HP-β-CD were pale yellow and white hard mass, respectively, after they had been dried. They were very hard to pulverize to obtain a powder form. This might be due to the high water solubilities of both ranitidine HCl and CDs, especially 2HP-β-CD.

2. Ranitidine HCl : Cyclodextrin (β - CD, 2HP-β-CD) Inclusion Complex Characteristics

The characterization of solid state R:CD inclusion complexes were employed by FTIR spectroscopy, differential scanning calorimetry, and X-ray powder diffractometry. While the characterization of the complexes in solution was performed by proton nuclear magnetic resonance spectroscopy. Furthermore, the morphology of the pure components and the obtained products were investigated by scanning electron microscopy.

2.1 Fourier Transform Infrared Spectroscopy

FTIR spectroscopy is one of the useful technique for analyses of complexes. Upon complexation of the guest, shifts or changes in the spectrum occur.

R:β-CD system: The FTIR spectra of ranitidine HCl, β - CD, and the physical mixture are presented in Figure 12. While Figures 13-15, 16 and 17 showed the FTIR spectra of the R:CD products (three molar ratios) prepared by co-grinding (with various grinding times), freeze-drying, and kneading methods, respectively.

R:2-HP-β-CD system: The FTIR spectra of ranitidine HCl, 2HP-β-CD, and the physical mixture are shown in Figure 18. While Figures 19-21, 22 and 23 illustrate the FTIR spectra of the R:CD products (three molar ratios) prepared by

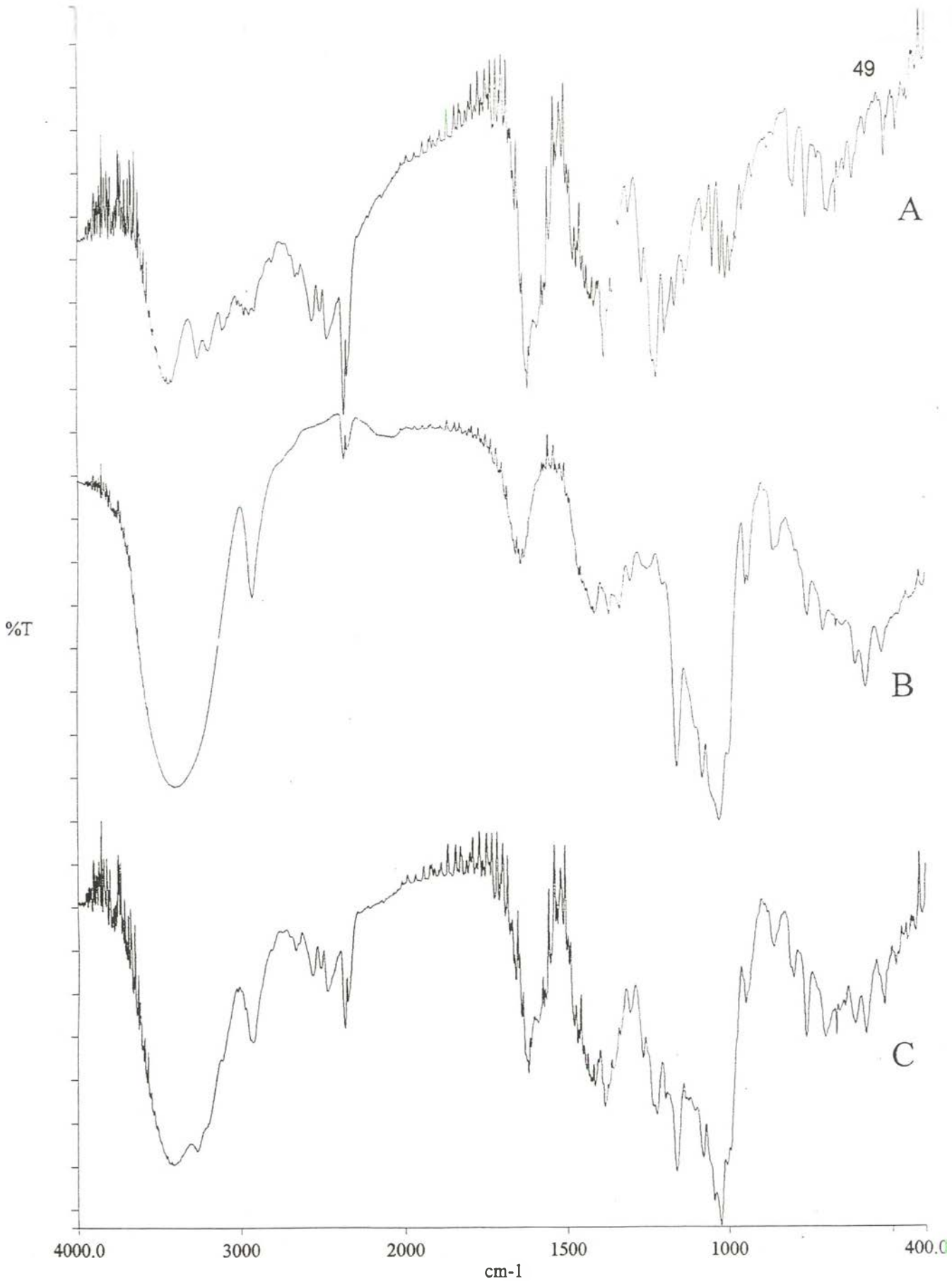

Figure 12. Infrared spectra in KBr pellet of ranitidine HCl, (A); β - CD, (B); and the physical mixture of ranitidine HCl and β -CD molar ratio 1:1, (C).

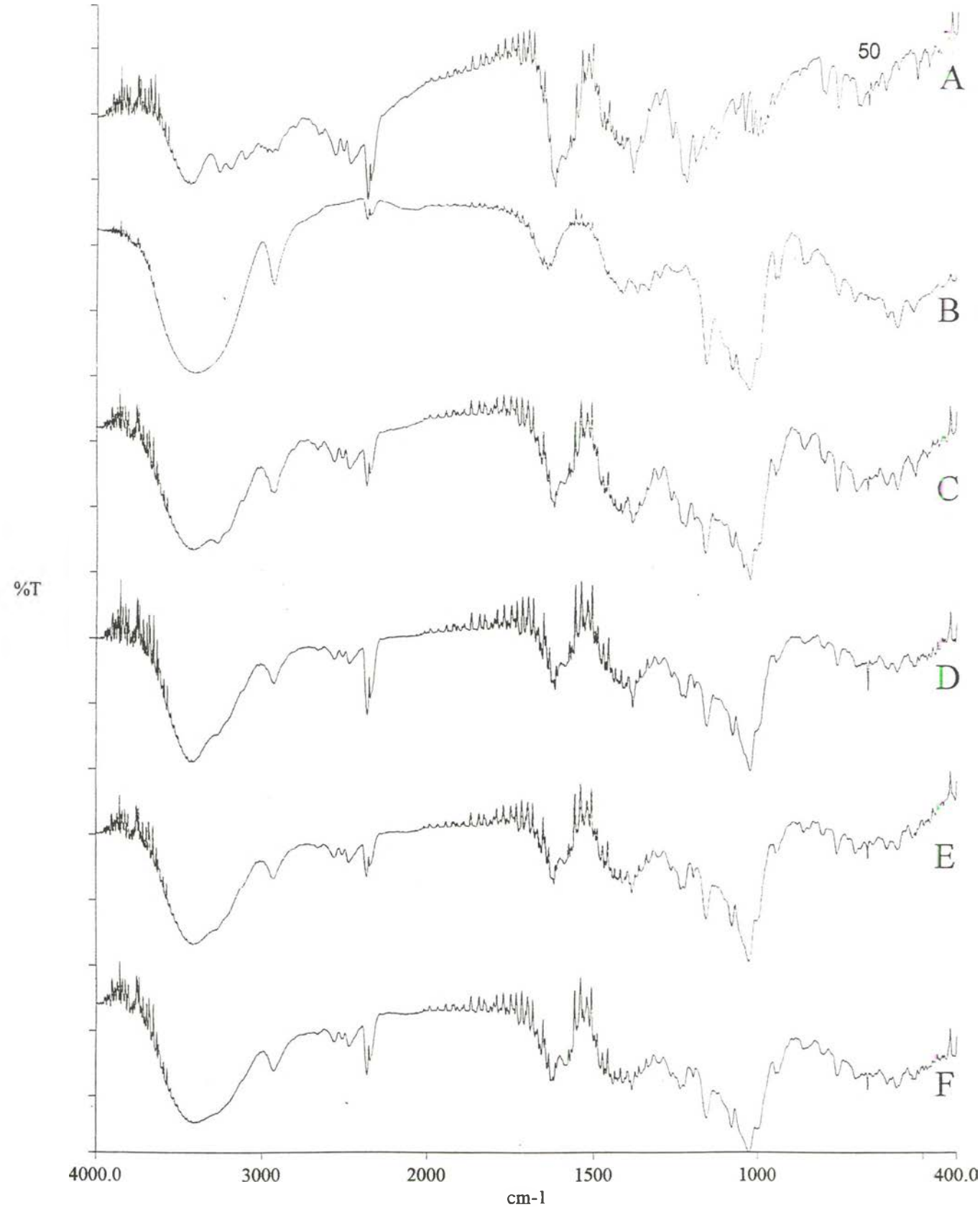

Figure 13. Infrared spectra in KBr pellet of ranitidine HCl : β- CD products (molar ratio 1:1) prepared by co-grinding method. [ranitidine HCl, (A); β -CD, (B); the physical mixture of ranitidine HCl and β -CD molar ratio 1:1, (C); co-grinding 30 min, (D); co-grinding 1 hr, (E); and co-grinding 3 hr, (F)].

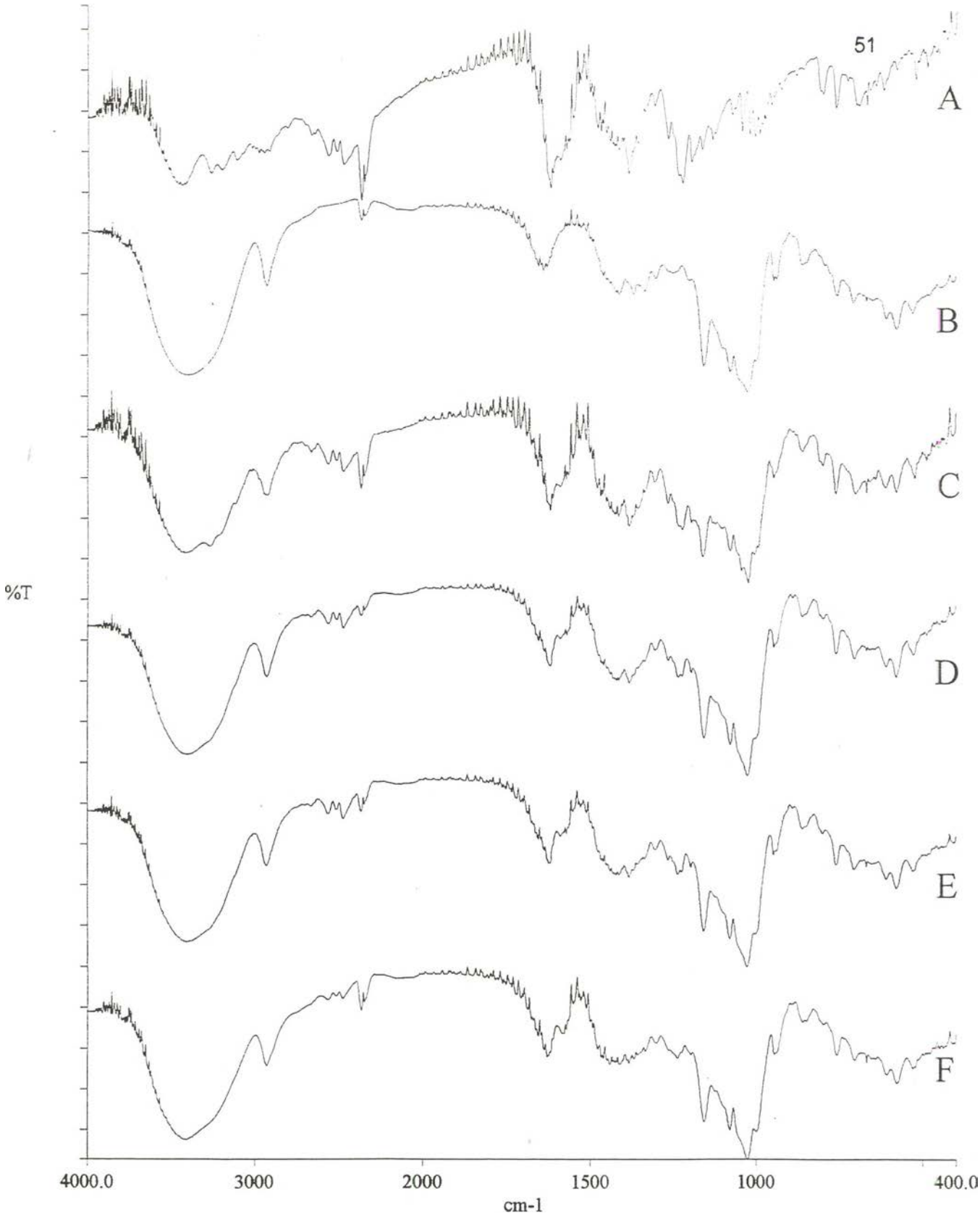

Figure 14. Infrared spectra in KBr pellet of ranitidine HCl : β- CD products (molar ratio 1:2) prepared by co-grinding method. [ranitidine HCl, (A); β -CD, (B); the physical mixture of ranitidine HCl and β -CD molar ratio 1:1, (C); co-grinding 30 min, (D); co-grinding 1 hr, (E); and co-grinding 3 hr, (F)].

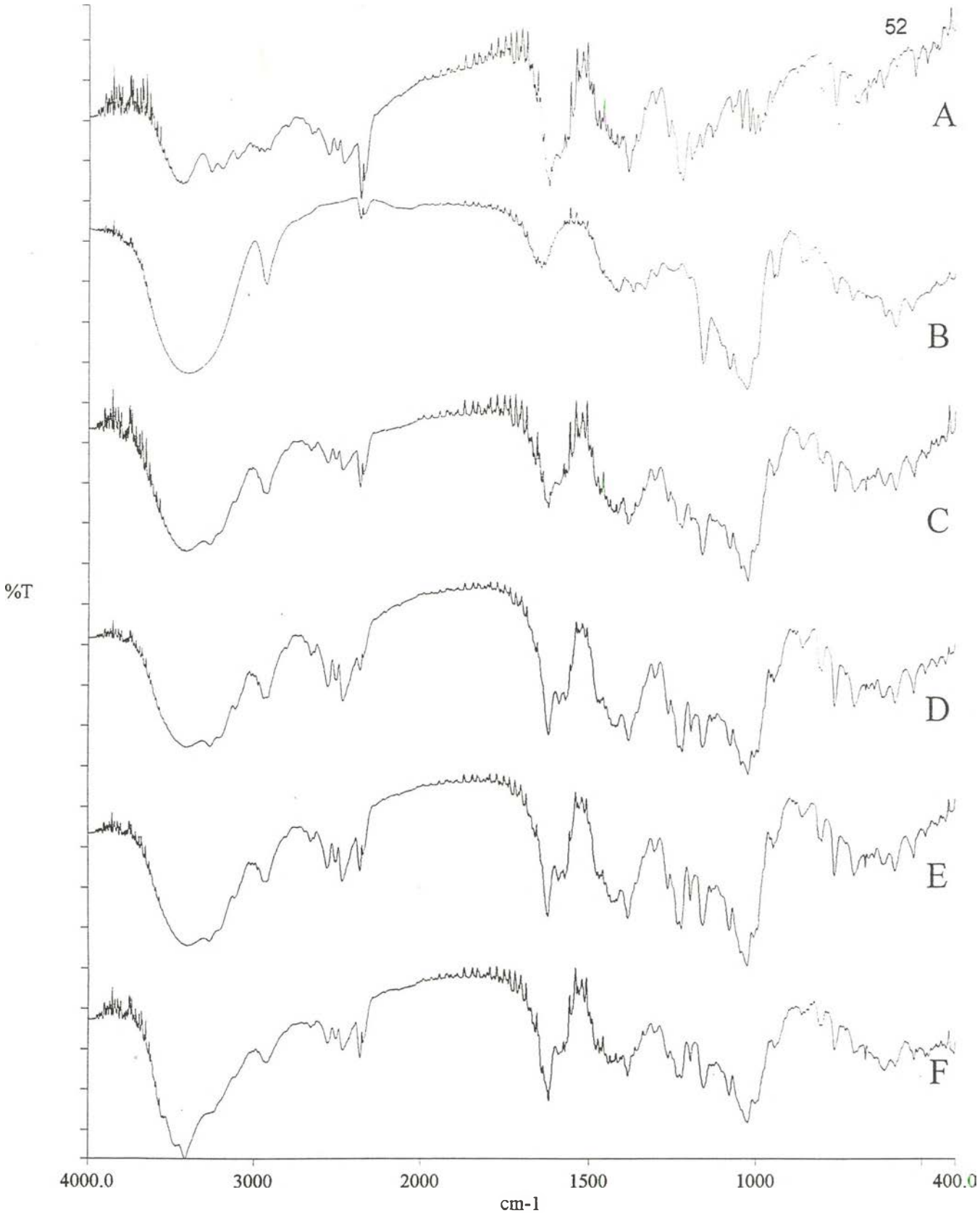

Figure 15. Infrared spectra in KBr pellet of ranitidine HCl : β- CD products (molar ratio 2:1) prepared by co-grinding method. [ranitidine HCl, (A); β -CD, (B); the physical mixture of ranitidine HCl and β -CD molar ratio 1:1, (C); co-grinding 30 min, (D); co-grinding 1 hr, (E); and co-grinding 3 hr, (F)].

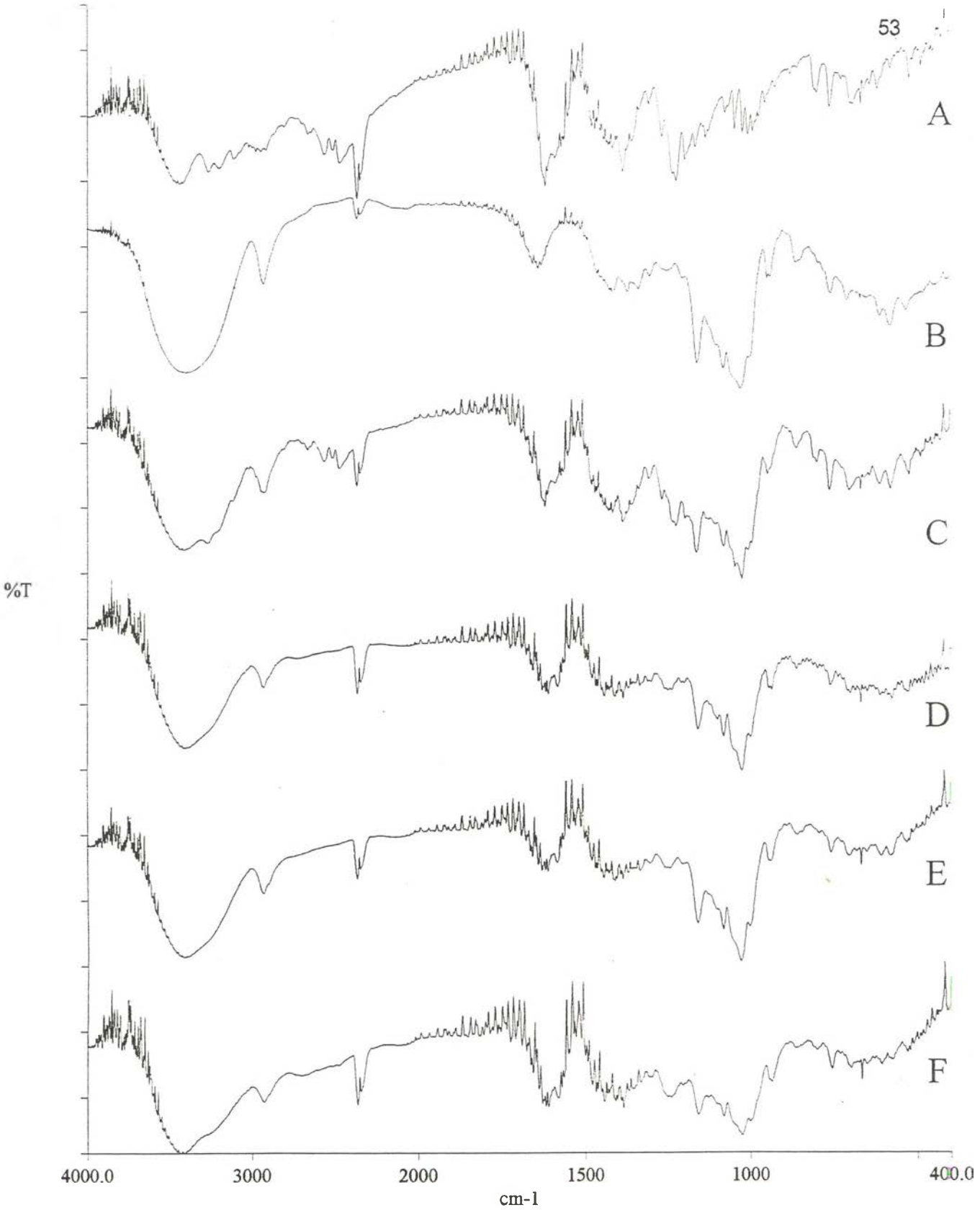

Figure 16. Infrared spectra in KBr pellet of ranitidine HCl : β- CD products prepared by freeze-drying method. [ranitidine HCl, (A); β -CD, (B); the physical mixture of ranitidine HCl and β -CD molar ratio 1:1, (C); molar ratio 1:1, (D); molar ratio 1:2, (E); and molar ratio 2:1, (F)].

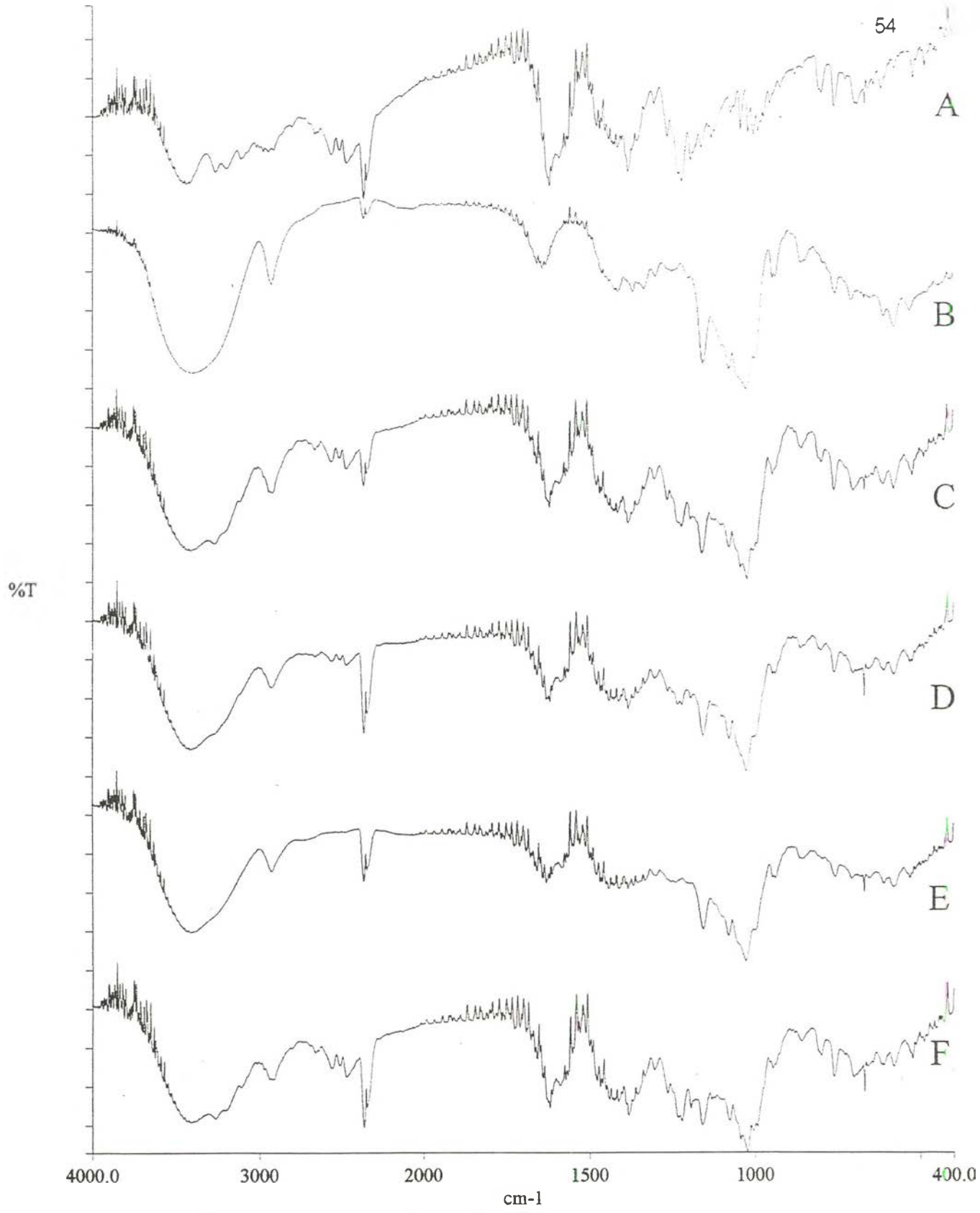

Figure 17. Infrared spectra in KBr pellet of ranitidine HCl : β- CD products prepared by kneading method. [ranitidine HCl, (A); β -CD, (B); the physical mixture of ranitidine HCl and β -CD molar ratio 1:1, (C); molar ratio 1:1, (D); molar ratio 1:2, (E); and molar ratio 2:1, (F)].

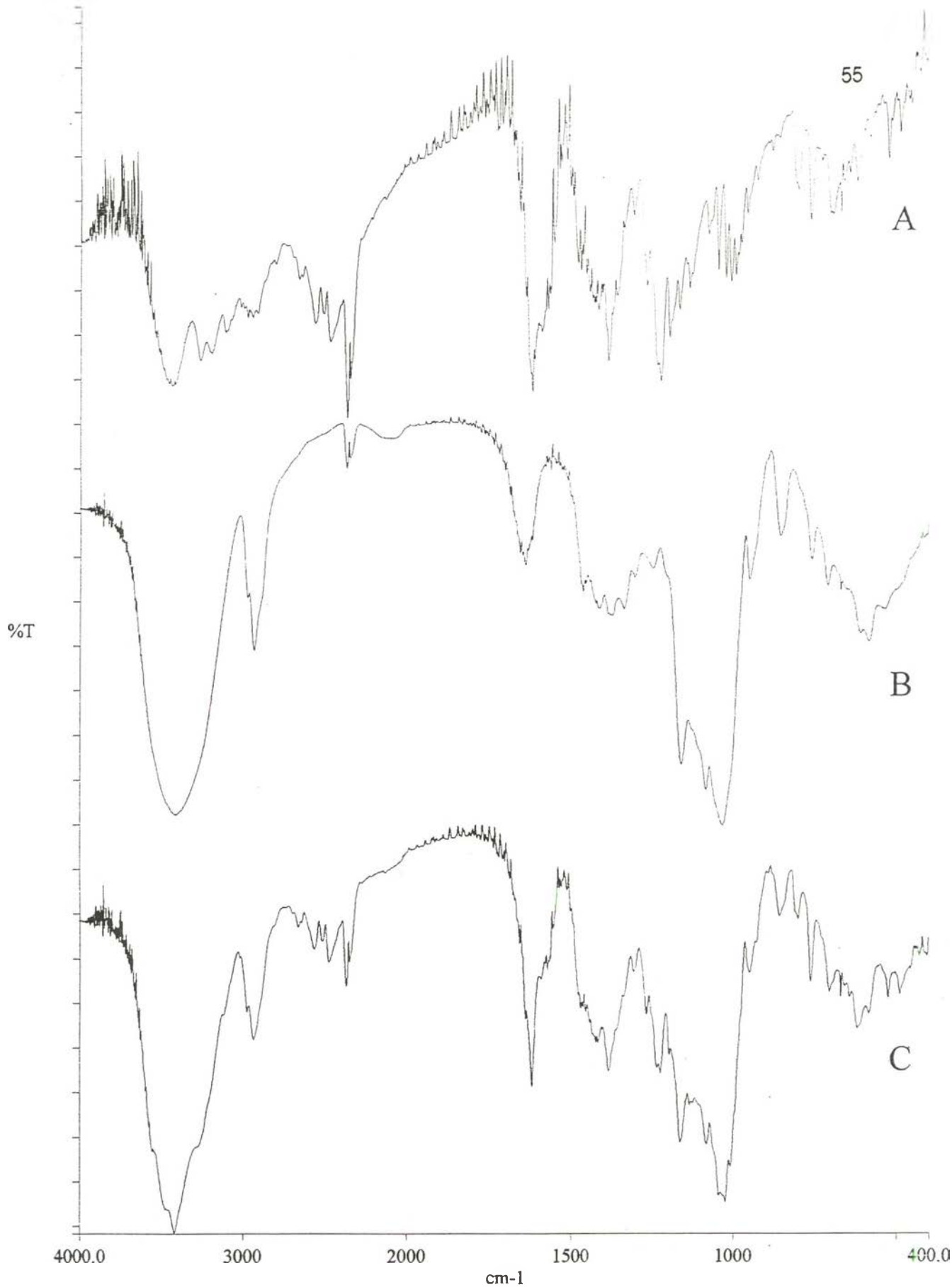

Figure 18. Infrared spectra in KBr pellet of ranitidine HCl, (A); 2HP-β-CD, (B); and the physical mixture of ranitidine HCl and 2HP-β-CD molar ratio 1:1 (C).

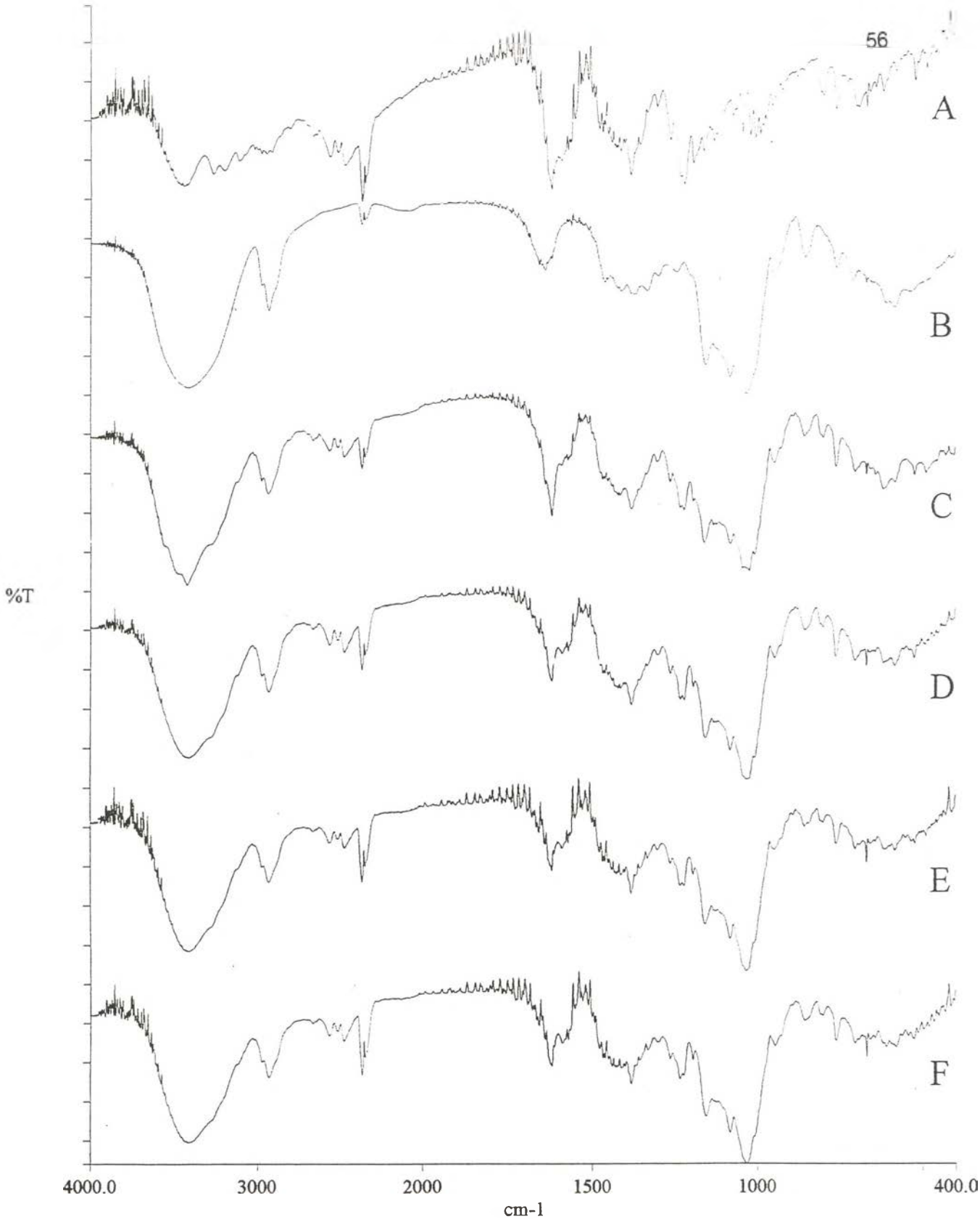

Figure 19. Infrared spectra in KBr pellet of ranitidine HCl : 2HP-β-CD products (molar ratio 1:1) prepared by co-grinding method. [ranitidine HCl, (A); 2HP-β-CD, (B); the physical mixture of ranitidine HCl and 2HP-β-CD molar ratio 1:1, (C); co-grinding 30 min, (D); co-grinding 1 hr, (E); and co-grinding 3 hr, (F)].

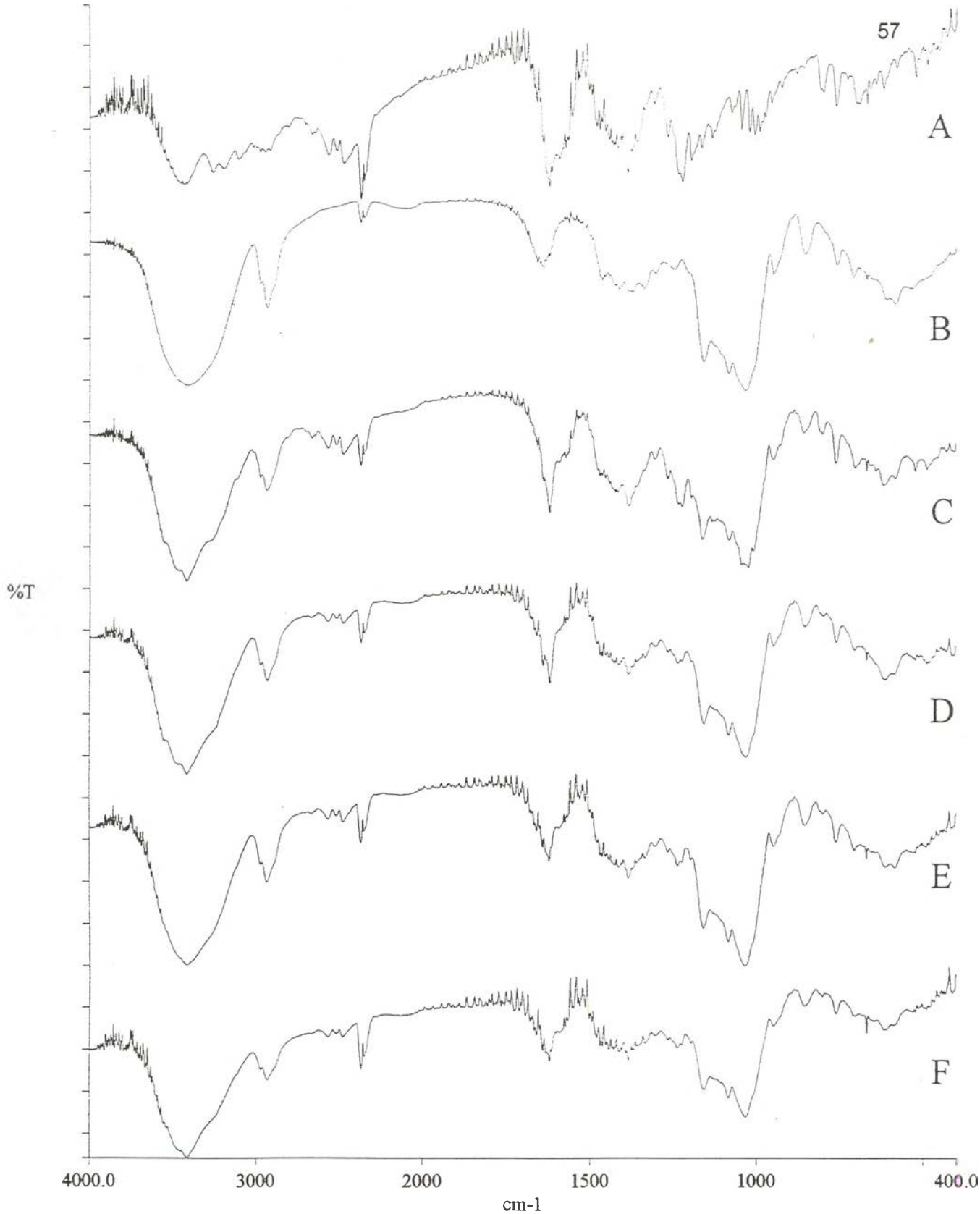

Figure 20. Infrared spectra in KBr pellet of ranitidine HCl : 2HP-β-CD products (molar ratio 1:2) prepared by co-grinding method. [ranitidine HCl, (A); 2HP-β-CD, (B); the physical mixture of ranitidine HCl and 2HP-β-CD molar ratio 1:1, (C); co-grinding 30 min, (D); co-grinding 1 hr, (E); and co-grinding 3 hr, (F)].

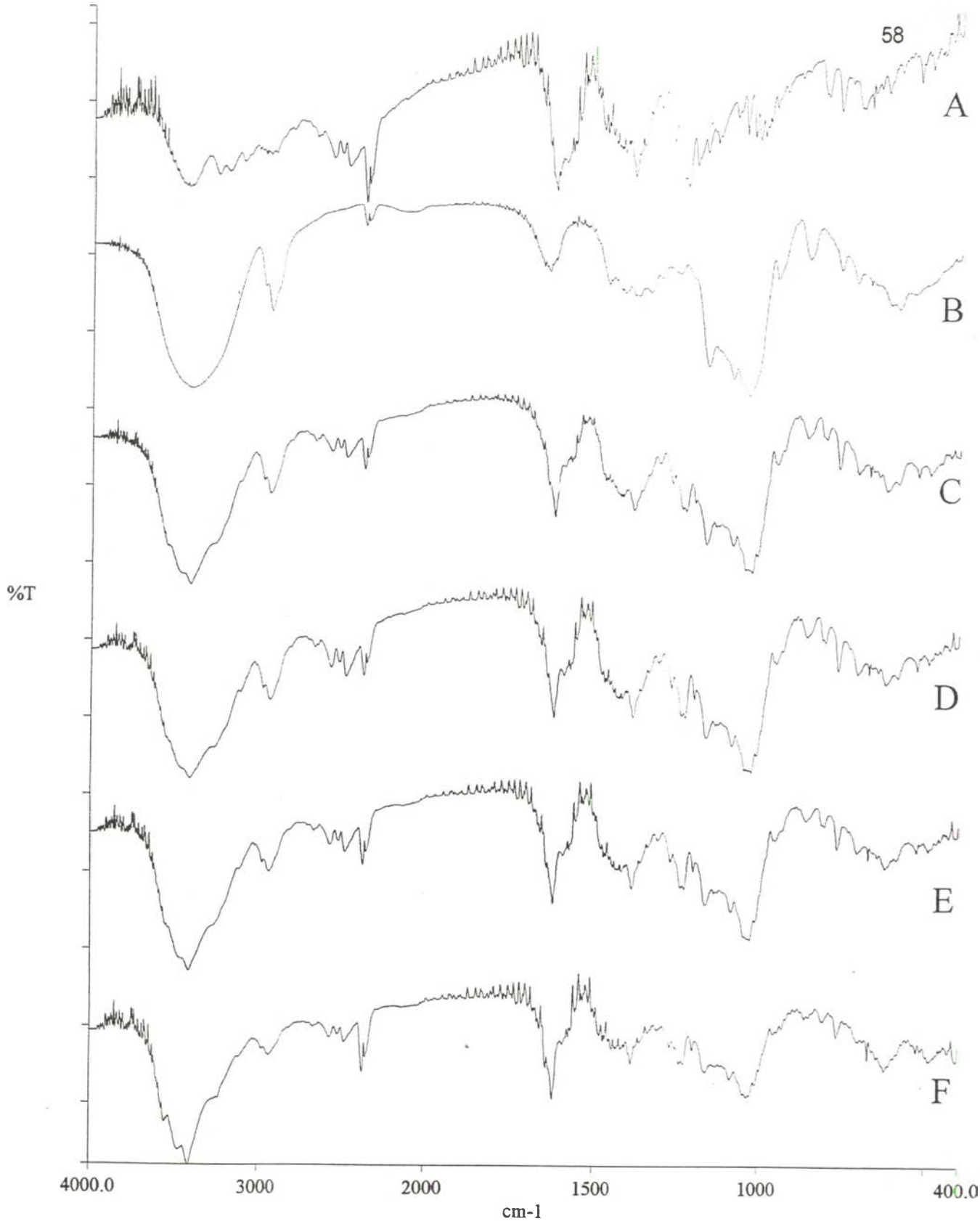

Figure 21. Infrared spectra in KBr pellet of ranitidine HCl : 2HP-β-CD products (molar ratio 2:1) prepared by co-grinding method. [ranitidine HCl, (A); 2HP-β-CD, (B); the physical mixture of ranitidine HCl and 2HP-β-CD molar ratio 1:1, (C); co-grinding 30 min, (D); co-grinding 1 hr, (E); and co-grinding 3 hr, (F)].

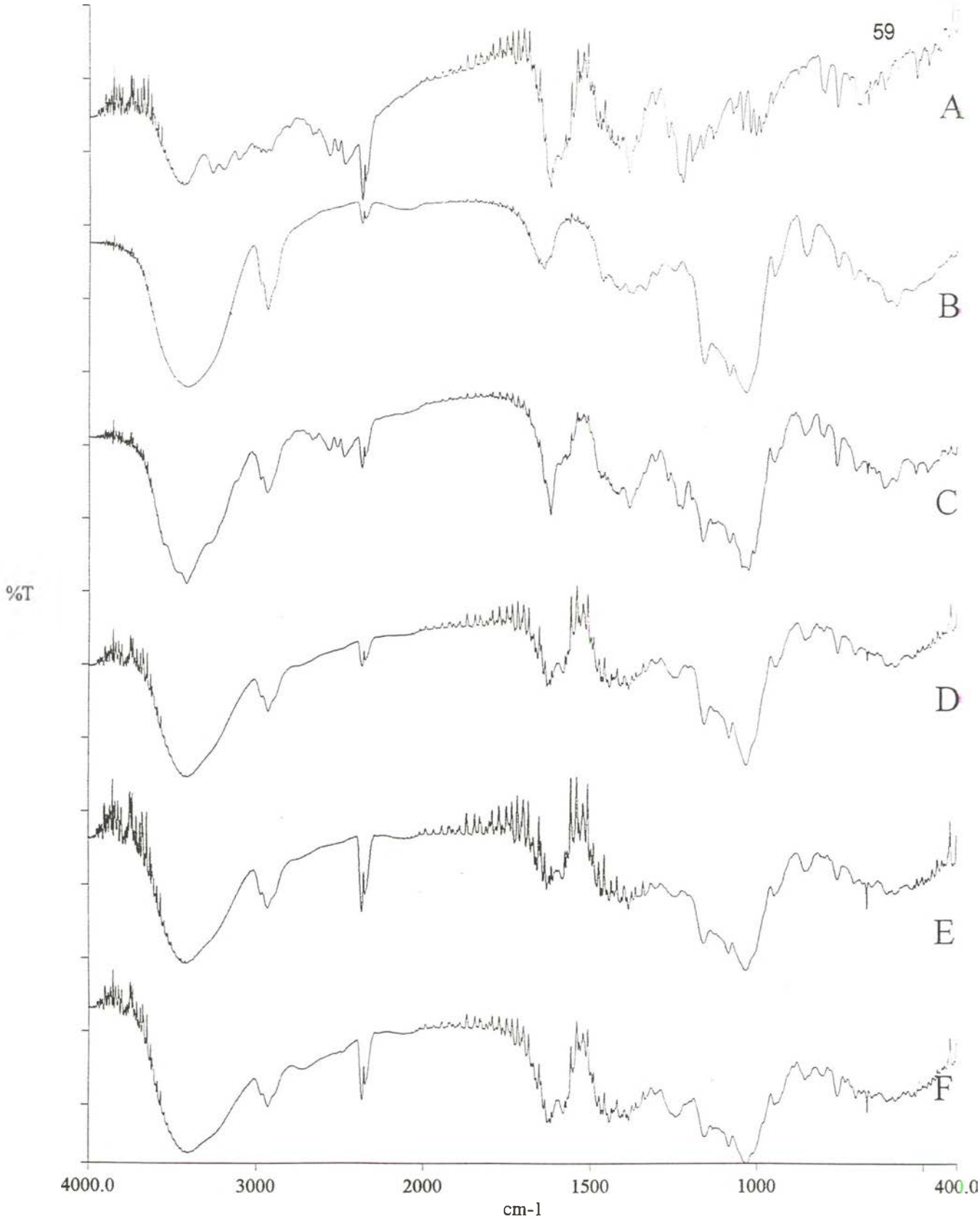

Figure 22. Infrared spectra in KBr pellet of ranitidine HCl : 2HP-β-CD products prepared by freeze-drying method. [ranitidine HCl, (A); 2HP-β-CD, (B); the physical mixture of ranitidine HCl and 2HP-β-CD molar ratio 1:1, (C); molar ratio 1:1, (D); molar ratio 1:2, (E); and molar ratio 2:1, (F)].

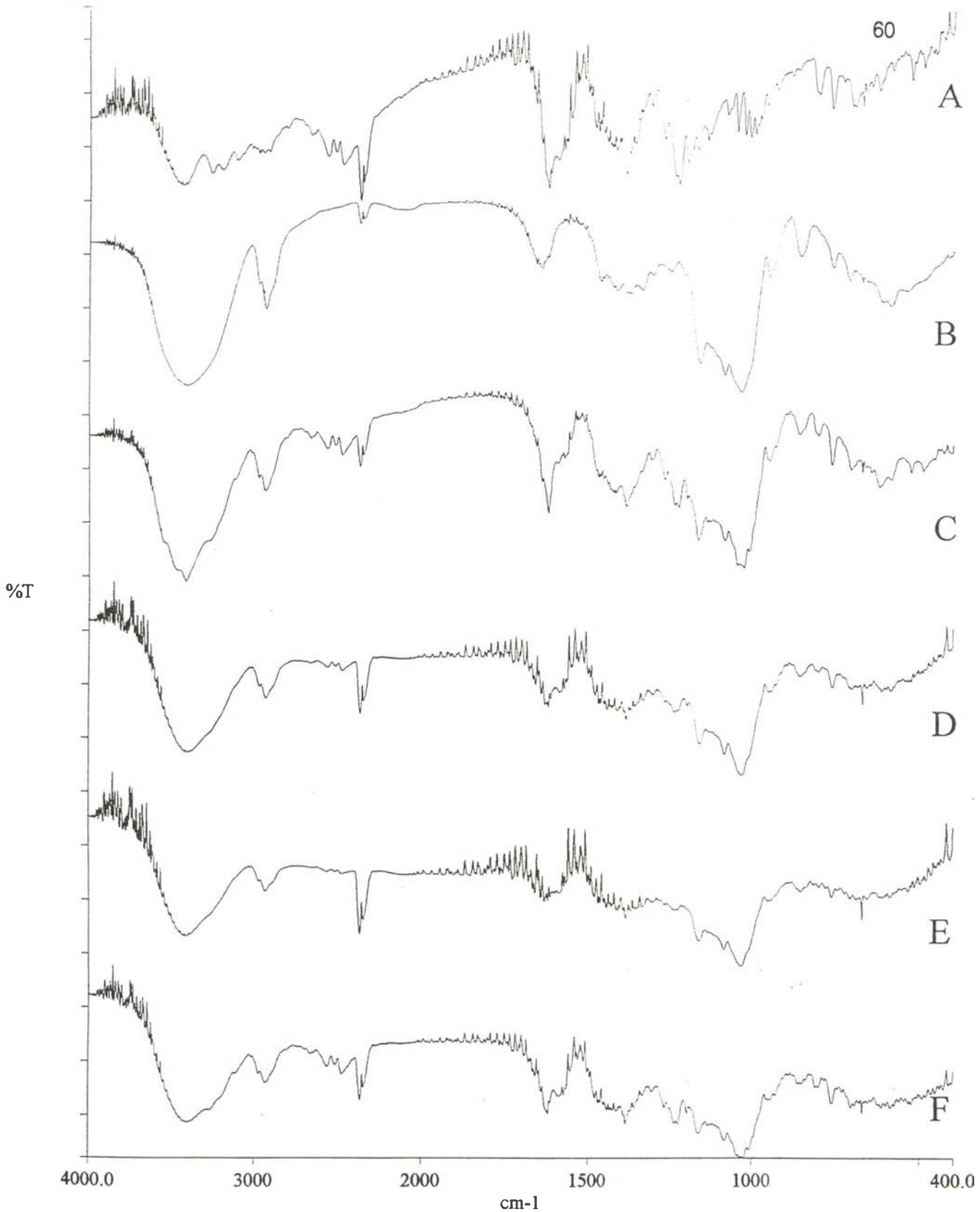

Figure 23. Infrared spectra in KBr pellet of ranitidine HCl : 2HP-β-CD products prepared by kneading method. [ranitidine HCl, (A); 2HP-β-CD, (B); the physical mixture of ranitidine HCl and 2HP-β-CD molar ratio 1:1, (C); molar ratio 1:1, (D); molar ratio 1:2, (E); and molar ratio 2:1, (F)].

co-grinding (with various grinding times), freeze-drying, and kneading methods, respectively.

The FTIR spectra of ranitidine HCl showed major peaks at 1620 and 1382 cm^{-1} which corresponded to the stretching vibration of the C=N double bond in an aci-nitro group of nitronic acid and stretching vibration of nitro group attached to a saturated carbon atom, respectively (Hohnjec et al., 1986). This C=N double bond is present in the nitronic acid tautomeric form of ranitidine HCl (Figure 24). In addition, the peaks due to the 2, 5 - disubstitued furan (1015 and 790 cm^{-1}) and the dimethyiamino group (2820 and 2780 cm^{-1}) reported by Cholerton et al. (1984) were fairly observed.

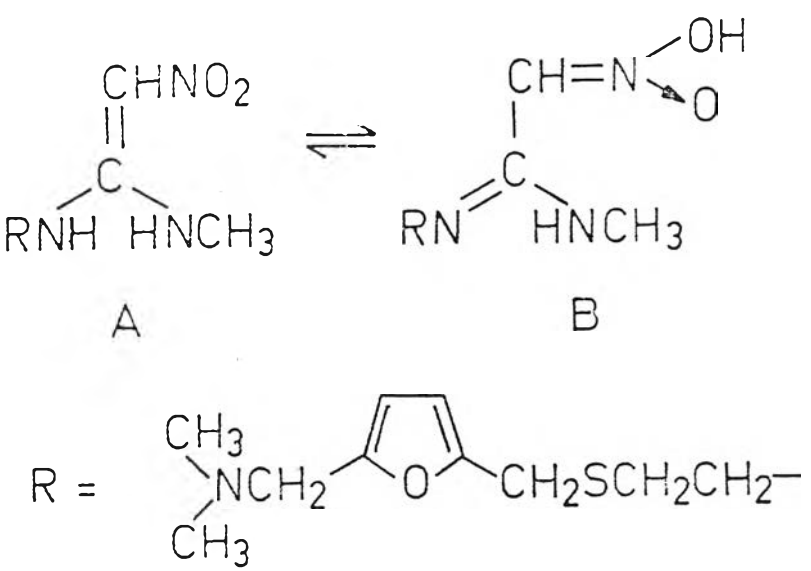

Figure 24. Nitronic acid tautomeric form of ranitidine HCl.

The FTIR spectra of β - CD and 2HP-β-CD were not significantly different. They were characterized by intense bands at 3500-3300 cm^{-1} corresponding to the absorption of hydrogen bonds produced by - OH groups of the CDs. The vibrations of the -CH and -CH_2 groups appeared in the 2950-2800 cm^{-1} region. Several sharp and intense bands at 1160-1130 cm^{-1} might be assigned to the stretching vibrations of the C-OH groups. It should be noted that the CDs contained some moisture, which is characterized by the band at 1640 cm^{-1} (Arias, Moyano, and Gines, 1997).

From the FTIR spectra of the R:CD products prepared by the co-grinding method, there was no significant shift of the major peaks of ranitidine HCl in all grinding times studied when they were compared with those of the physical mixture and pure drug (Figures 13 -15 for R:β-CD system and Figures 19 -21 for R:2HP-β-CD system).

The FTIR spectra of all the R:CD products prepared by freeze-drying and kneading were also illustrated the combination peaks of ranitidine HCl and each cyclodextrin similar to the spectra of their physical mixtures (Figures 16 -17 for R:β-CD system and Figures 22 -23 for R:2HP-β-CD system).

The results obtained by FTIR studies indicated strongly that no strong chemical interaction between ranitidine HCl and CD (β-CD, 2HP-β-CD) was formed. However, the FTIR technique alone could not be used to conclude absolutely that the product was simply a physical mixture. The major FTIR peaks of all the processed products were similar to those of the physical mixture, but the intensity was proportional to the molar ratios of ranitidine HCl : CD.

Szejtli (1988) suggested that the polarity of the guest molecule is also an important factor for the extent of the complex formation. Strongly hydrophilic molecules, strongly hydrated and ionized groups are usually unfavorable in complex formation or form a very weak complex. Ranitidine HCl could be protonated and ionized, and

therefore, the complex formation might not be favorable. In addition, there were interferences in the spectra from the CDs, and some of the changes were very subtle requiring careful interpretation of the spectra.

2.2 Differential Scanning Calorimetry

The thermal behavior of R:CD products were also studied by DSC in order to determine the formation of a solid complex. This technique can be applied if the guest molecule has a melting or boiling temperature below the temperature at which the CDs decompose, i.e., about 300°C. In this case, no energy absorption is observed at the melting temperature of the guest molecule when it is complexed. This is because the guest molecule is surrounded by the CD and not interacting with other guest molecules, and therefore there is no more crystalline guest structure to absorb energy. Additionally, if a large amount of guest molecules are not complexed, DSC can be used for estimation of the amount of non complexed guests (Hedges, 1998).

R:β-CD system: DSC thermograms of pure drug, β - CD, and the physical mixture are presented in Figure 25. DSC thermograms of the R:CD products prepared by co-grinding, freeze-drying, and kneading are shown in Figures 26 - 28, respectively.

The DSC thermogram of ranitidine HCl gave a sharp endothermic peak at 149.17°C, which was closed to its melting point, 143-144°C (Hohnjec et al., 1986). The thermogram of β-CD displayed a broad endothermic peak around 100°C. This broad endothermic peak around 100 °C in the thermogram of β-CD was confirmed by the thermogravimetric analysis (TGA) method. The TGA thermogram of β-CD (Figure 29) showed the loss of 14.57% in weight around this temperature. This might be due to the loss of water from β -CD molecule (Fini et al., 1997; Montassier, Duchêne, and Poelman,

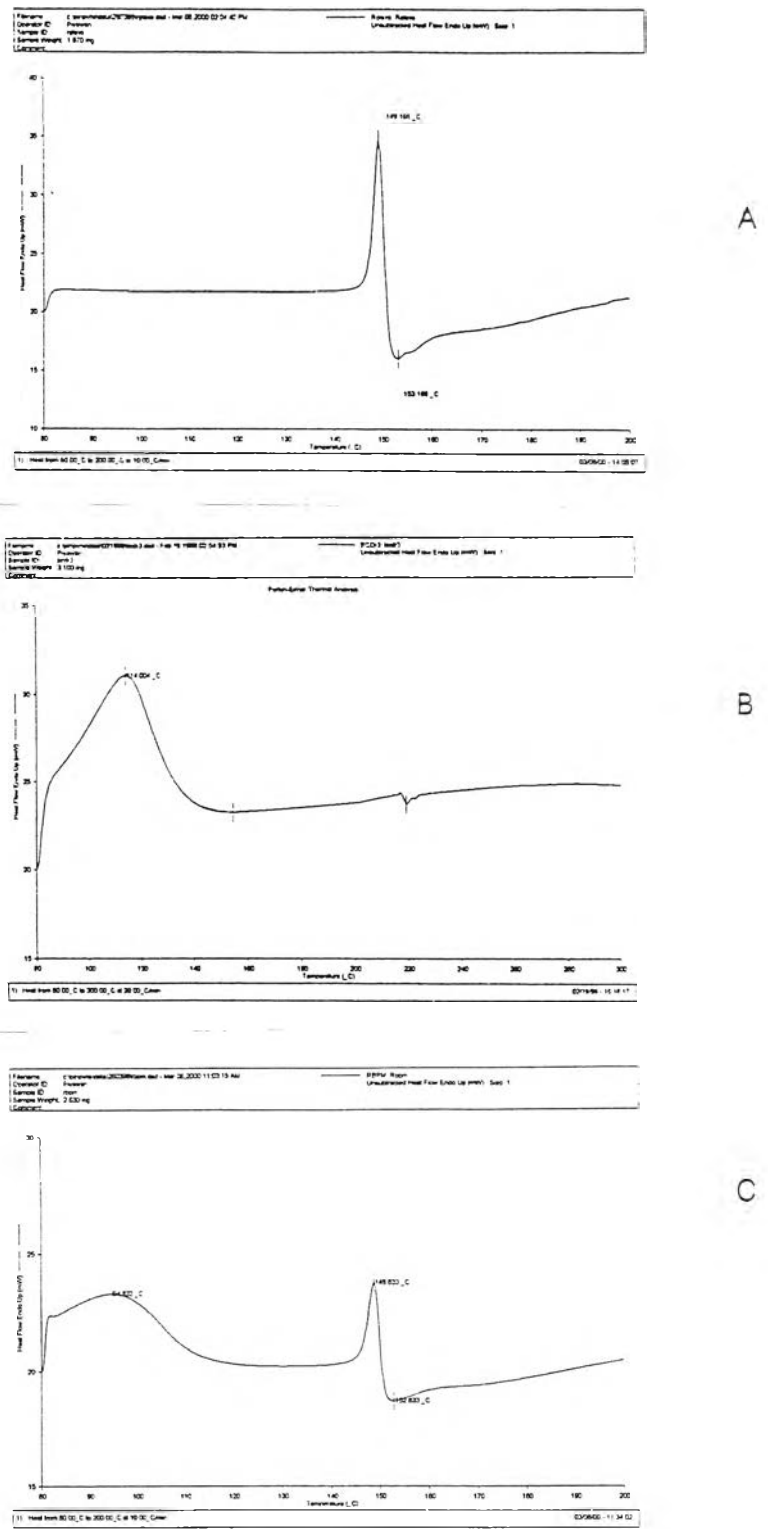

Figure 25. DSC thermograms of ranitidine HCl, (A); β - CD, (B); and the physical mixture of ranitidine HCl and β - CD molar ratio 1:1 (C).

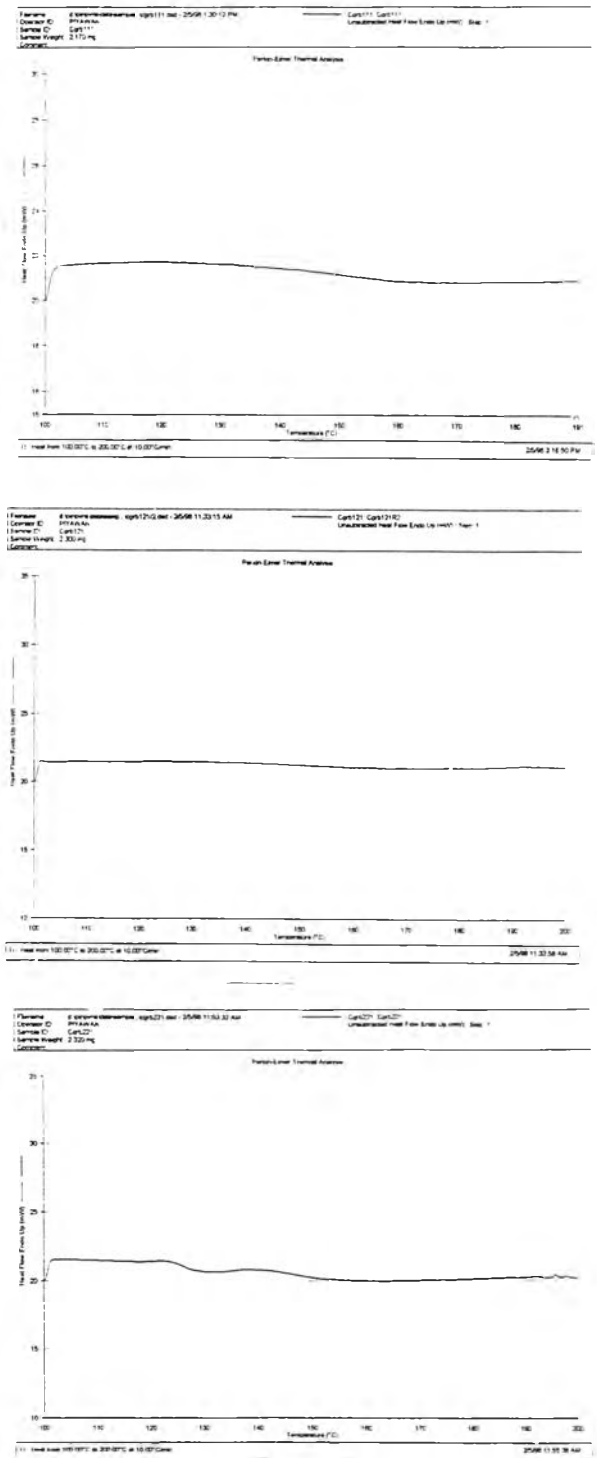

A

B

C

Figure 26. DSC thermograms of ranitidine HCl : β - CD products prepared by co-grinding method, grinding time 30 min. [molar ratio 1:1, (A); molar ratio 1:2, (B); and molar ratio 2:1, (C)].

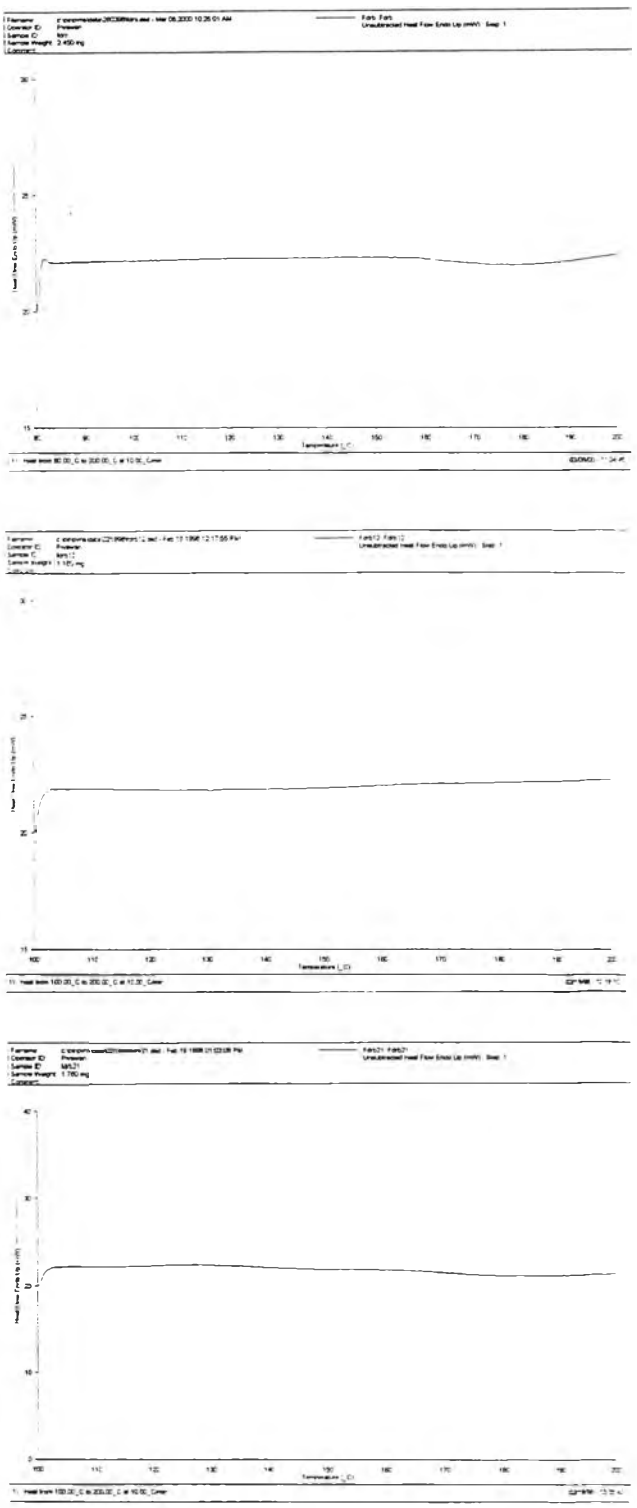

A

B

C

Figure 27. DSC thermograms of ranitidine HCl : β - CD products prepared by freeze-drying method. [molar ratio 1:1, (A); molar ratio 1:2, (B); and molar ratio 2:1, (C)].

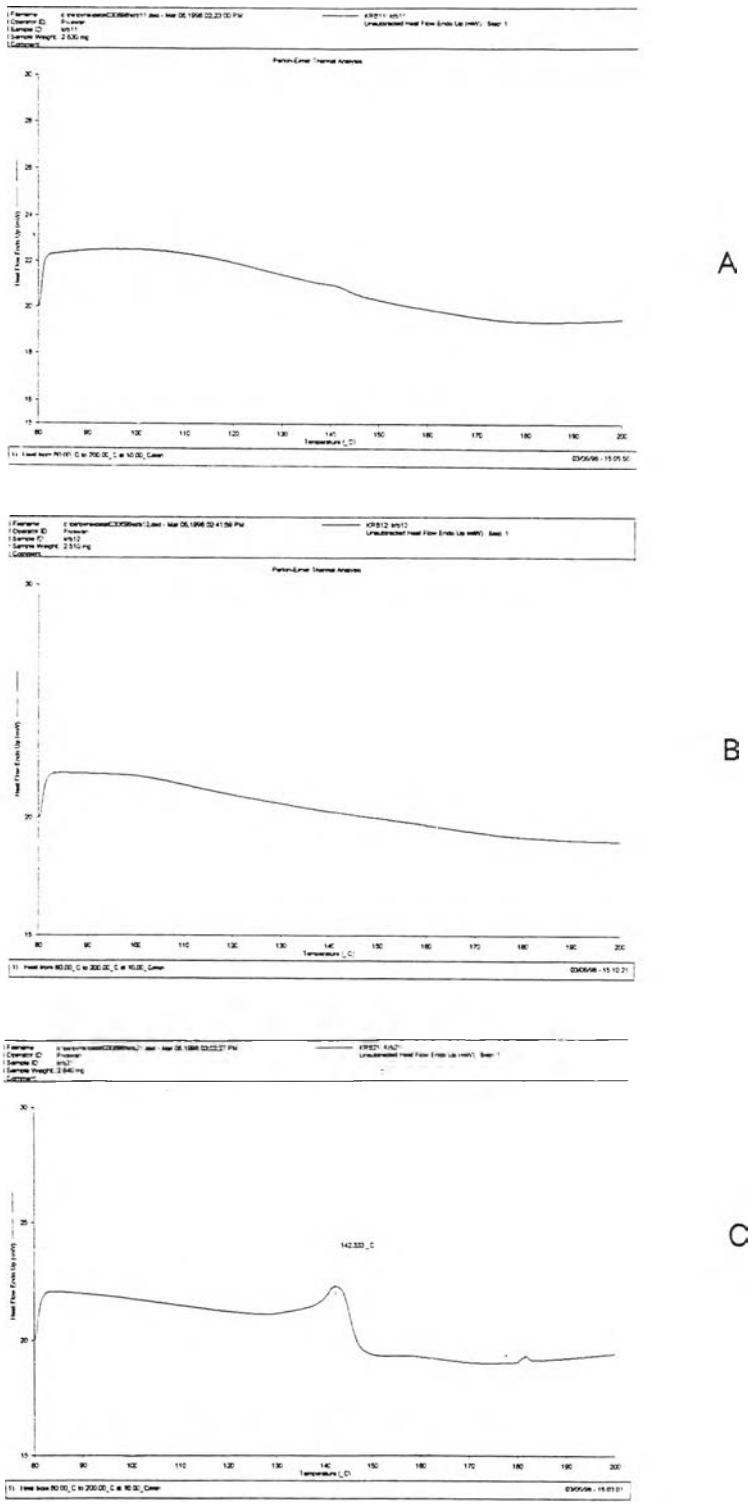

Figure 28. DSC thermograms of ranitidine HCl : β - CD products prepared by kneading method. [molar ratio 1:1, (A); molar ratio 1:2, (B); and molar ratio 2:1, (C)].

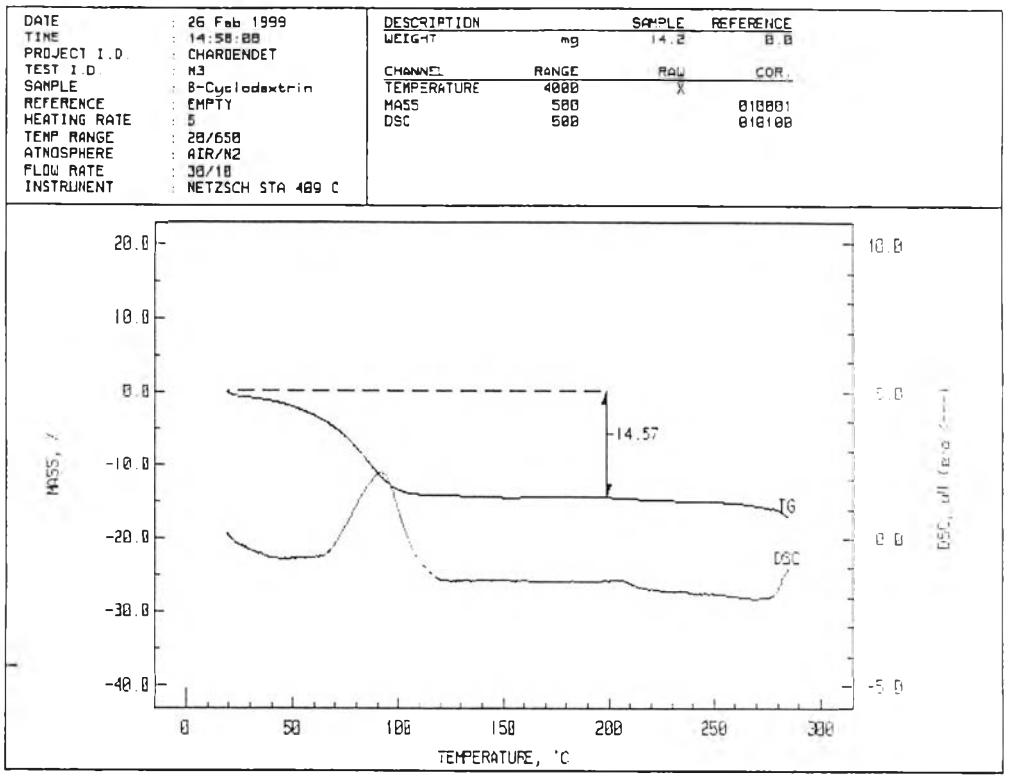

Figure 29. TGA thermogram of β - CD.

1997). Therefore, this broad endothermic peak should not due to the melting of β -CD molecule since its melting point is about 255-265 °C (Wade and Weller, 1994).

The thermogram of physical mixture showed a broad endothermic peak around 100°C and a small endothermic peak at 148.83 °C which were the combination peaks of ranitidine HCl and β - CD. On the contrary, no peak was observed within the temperature range studied (80,100 - 200 °C) for all solid R:CD products studied except for the kneaded mixture at a molar ratio of 2:1 which showed a small endothermic peak

at 142.33 °C (Figure 28, C) which suggested some non complexed ranitidine HCl molecules. In addition, the grinding times studied in the co-grinding method did not affect the characteristic of the thermograms of the R:CD products.

R:2HP-β-CD system: DSC thermograms of ranitidine HCl, 2HP-β-CD, and physical mixture are presented in Figure 30. In the case of R:CD products, DSC thermograms are demonstrated in Figures 31 -33 for co-grinded, freeze-dried, and kneaded complexes, respectively. The 2HP-β-CD did not show any peaks at the temperature range studied (80 - 300°C), while the physical mixture displayed a small endothermic peak at 143.33°C. As expected, no peak was observed within the temperature range studied (80, 100 - 200°C) for all solid R:CD products except for the product prepared by co-grinding method at a molar ratio of 2:1 which showed a little drop in the base-line of the thermogram around 140-145°C (Figure 31, C).

The DSC thermograms in Figures 25 and 30 illustrated endothermic peaks of ranitidine HCl at 149.17, 148.83, and 143.33°C for pure compound, R:β-CD physical mixture, and R:2HP-β-CD physical mixture, respectively. The peak of ranitidine HCl in the physical mixtures changed when they were compared with that of pure ranitidine HCl due to the between run variation.

Most of the DSC thermograms of obtained products presented the evidence that these products were not simple physical mixtures. This was based upon the fact that the endothermic peak due to the phase transition profile of ranitidine HCl was not observed. The disappearance of the endothermic peak might be attributed to either the formation of inclusion complexes or the molecular dispersion of ranitidine HCl and CD molecules.

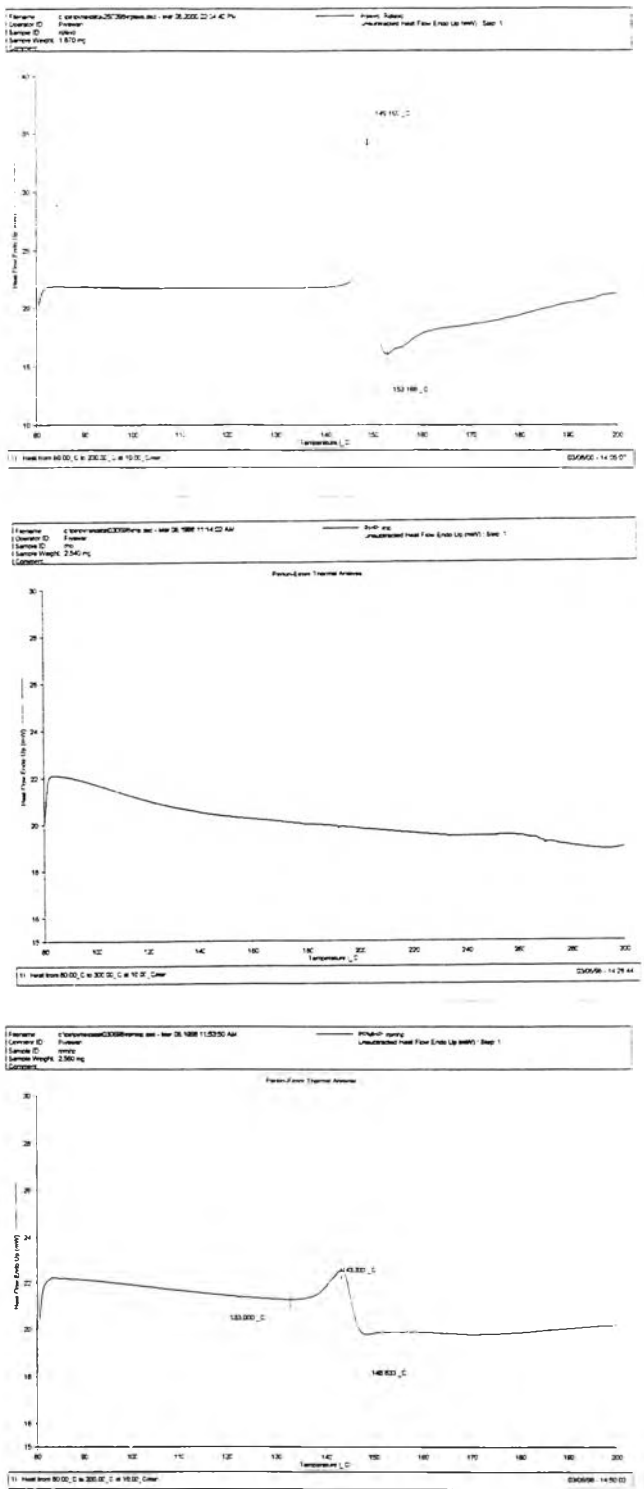

A

B

C

Figure 30. DSC thermograms of ranitidine HCl, (A); 2HP-β-CD, (B); and the physical mixture of ranitidine HCl and 2HP-β-CD molar ratio 1:1 (C).

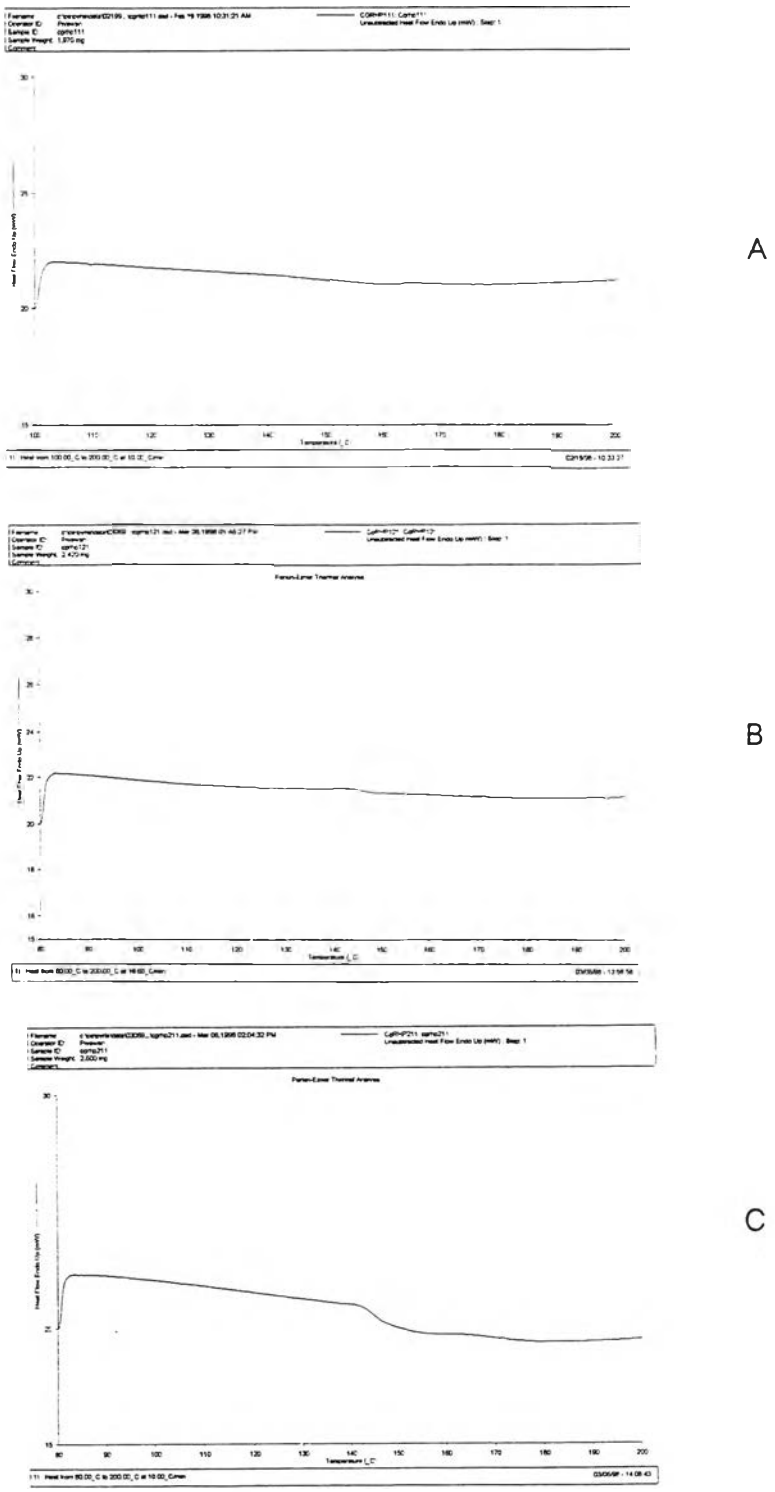

Figure 31. DSC thermograms of ranitidine HCl : 2HP-β-CD products prepared by co-grinding method, grinding time 30 min. [molar ratio 1:1, (A); molar ratio 1:2, (B); and molar ratio 2:1, (C)].

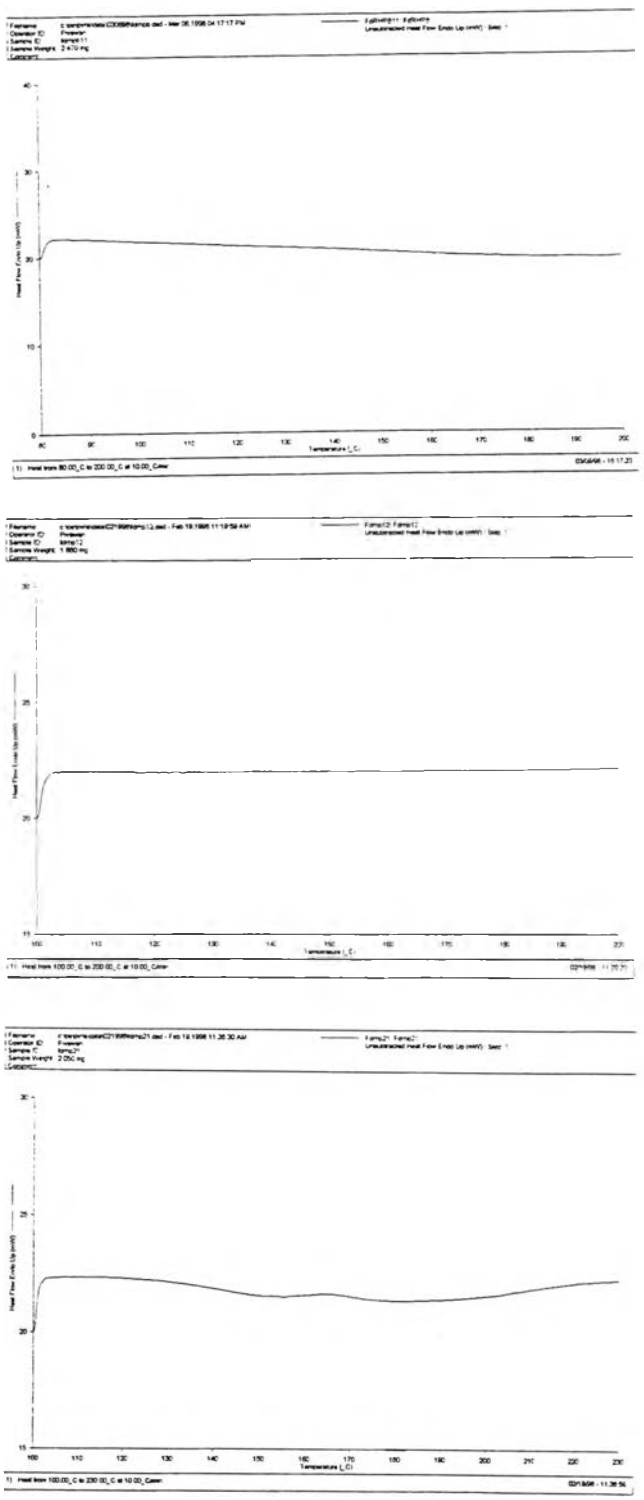

Figure 32. DSC thermograms of ranitidine HCl : 2HP-β-CD products prepared by freeze-drying method. [molar ratio 1:1, (A); molar ratio 1:2, (B); and molar ratio 2:1, (C)].

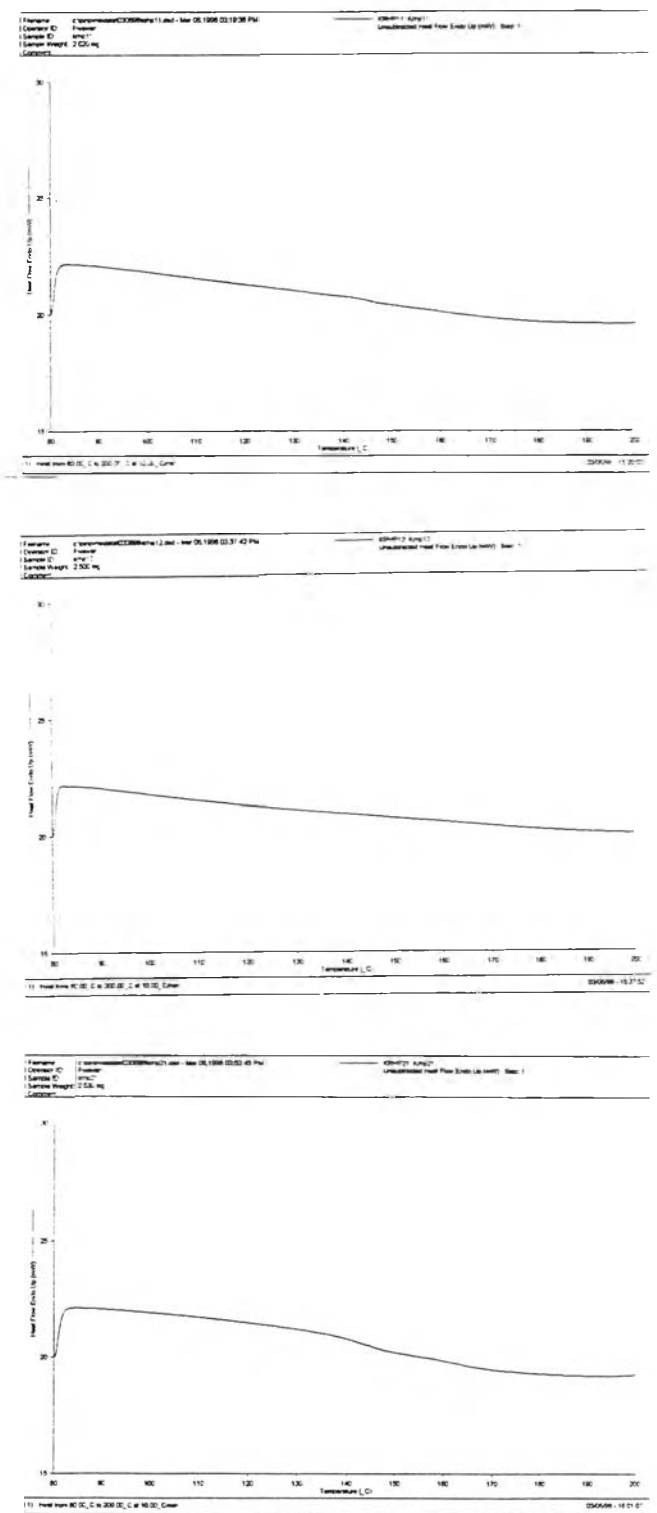

Figure 33. DSC thermograms of ranitidine HCl : 2HP-β-CD products prepared by kneading method. [molar ratio 1:1, (A); molar ratio 1:2, (B); and molar ratio 2:1, (C)].

2.3 X-ray Powder Diffractometry

X-ray powder diffractometry is widely used for the identification of solid phases since the X-ray powder pattern of every crystalline form of a compound is unique. This technique has limited utility in the identification of non-crystalline (amorphous) materials since their X-ray patterns consist of one or more broad diffuse maxima (Suryanarayanan, 1995).

R:β-CD system: Figure 34 shows the X-ray powder diffractograms of ranitidine HCl, β-CD, and the physical mixture. Major X-ray diffraction peaks at 2θ of ranitidine HCl were 8.40°, 14.56°, 15.32°, 16.44°, 18.08°, 20.24°, 20.88°, 22.84°, 23.48°, 24.08°, and 27.52°, respectively, with the highest intensity peak at 20.24° which was also reported by Carstensen and Franchini (1995). While the X-ray powder diffractogram of β-CD presented the highest intensity peak at 12.56°. X-ray powder diffractograms of 1:1 R:CD products prepared by the three methods are presented in Figure 35. The comparison of diffractograms of each component, the physical mixture, and the obtained 1:1 products are summarized in Table 7. The X-ray diffractogram of the physical mixture was simply the superposition of each component. The products prepared by co-grinding method (Figure 35, A) showed some crystalline patterns. The products obtained by the kneading method (Figure 35, C) exhibited the diffraction peaks mostly similar to the physical mixture, however decreases in intensities could be observed. This observation suggested that the grinding and kneading processes could contribute to decrease in the crystallinity of the mixture. The freeze-drying method brought the product to amorphous state which is well known. Some peaks could be observed in the diffractogram of the obtained freeze-dried product (Figure 35, B), however, the main peaks (at 8.40°, 14.56°, 16.44°, 18.08°, 20.24°, 20.88°, 22.84°, and 27.52°, respectively) that represented ranitidine HCl were completely lost. Some of the observed peaks were new peaks and the others contributed to β - CD peaks. The contribution of β - CD peaks was due to the lower water soluble β - CD when

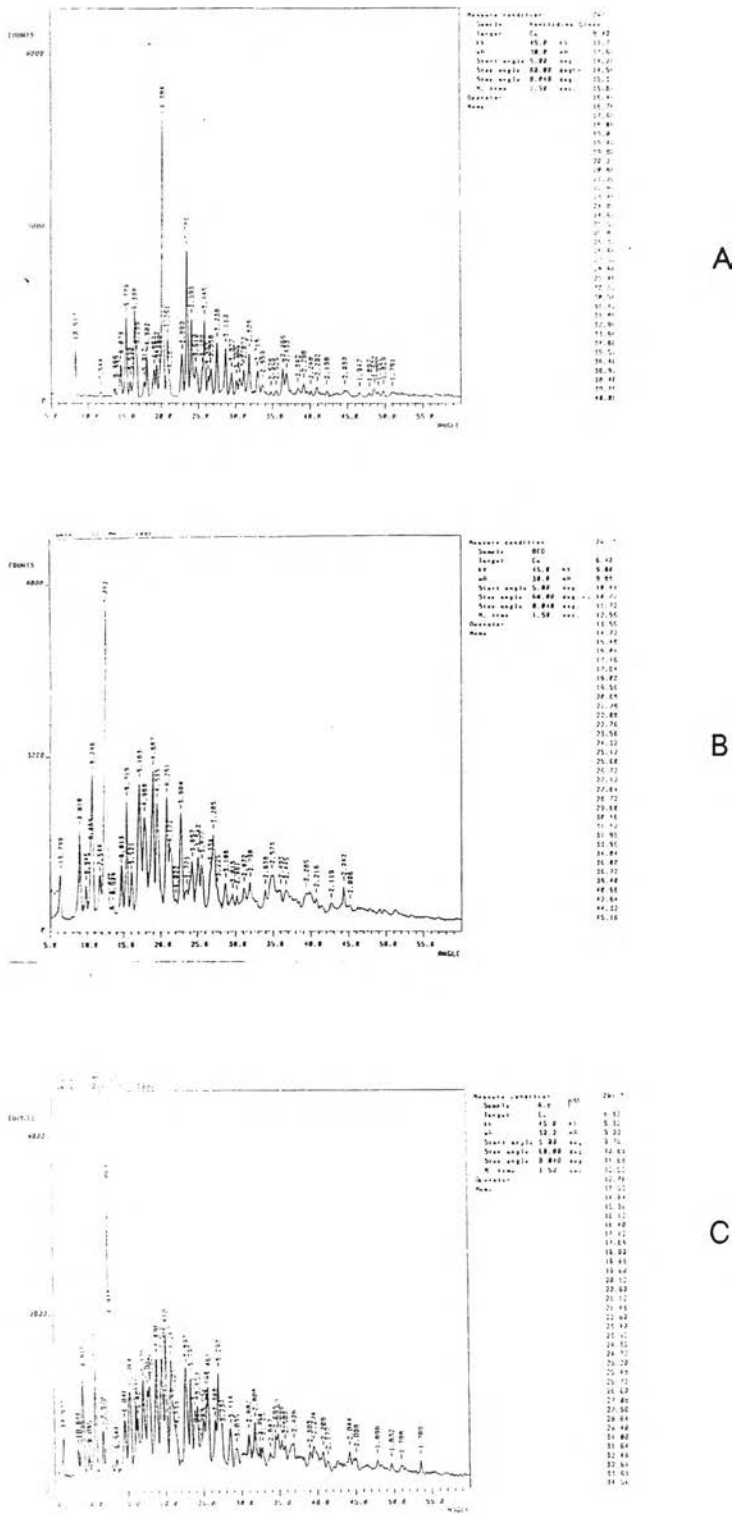

Figure 34. X-ray powder diffractograms of ranitidine HCl, (A); β - CD, (B); and the physical mixture of ranitidine HCl and β - CD molar ratio 1:1 (C).

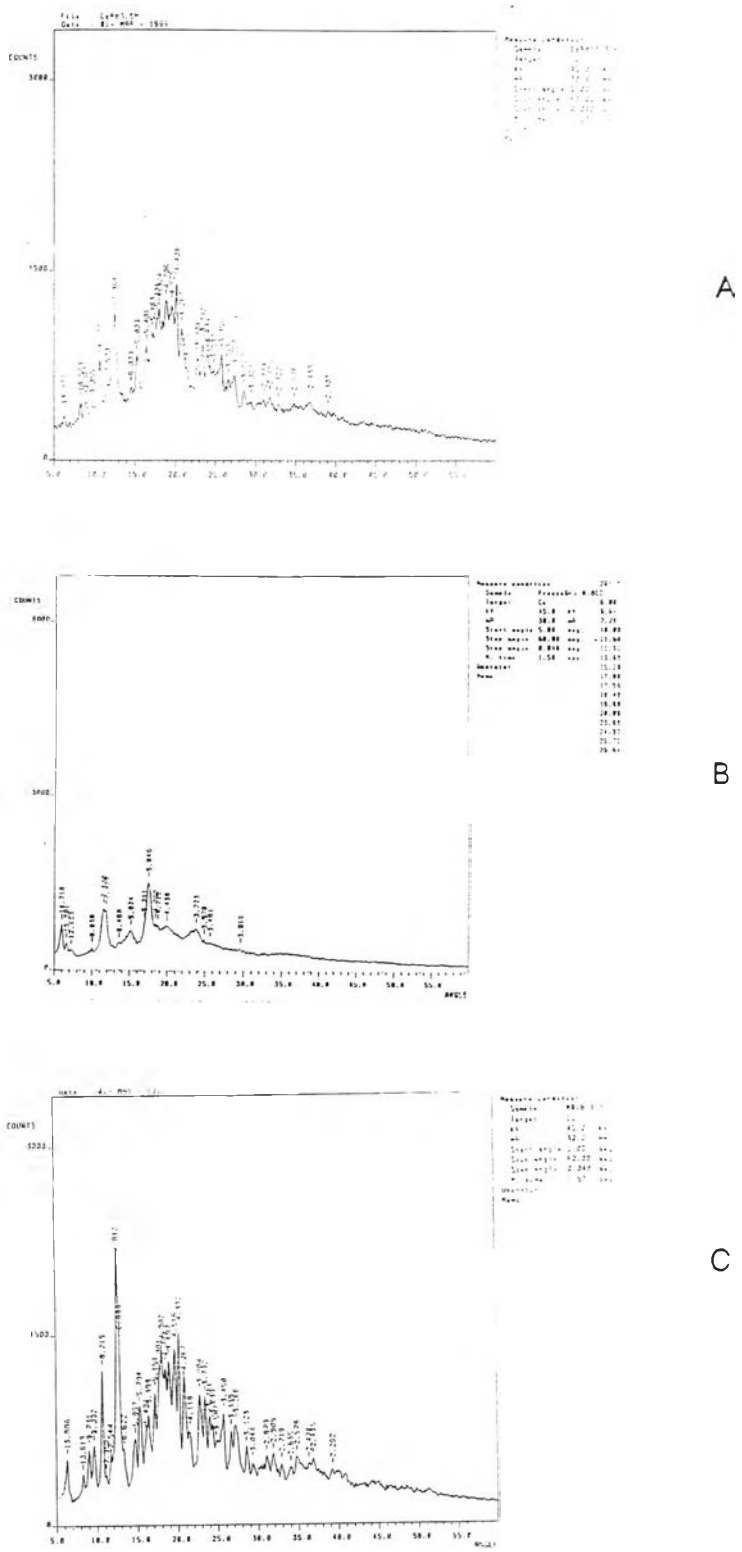

Figure 35. X-ray powder diffractograms of the 1:1 ranitidine HCl : β - CD products prepared by three methods. [co-grinding method, (A); freeze-drying method, (B); and kneading method, (C)].

Table 7. X-ray powder diffraction patterns of the R : β - CD system.

R		β - CD		physical mixture		co-grinding		freeze-drying		kneading	
2θ (°)	I*	2θ (°)	I*	2θ (°)	I*	2θ (°)	I*	2θ (°)	I*	2θ (°)	I*
								6.00	768		
		6.40	969	6.32	623	6.32	343	6.64	457	6.36	529
8.40	914			8.32	483	8.36	446			8.32	411
		9.00	1737	9.00	1282	8.96	456			9.08	602
		9.88	784	9.76	428					9.72	626
		10.72	2695	10.68	1408	10.68	781	10.00	375	10.76	1226
		11.72	969	11.68	694	11.68	594	11.60	1056	11.72	561
		12.56	5842	12.52	3317	12.52	1160	11.92	1024	12.56	2202
14.56	656	14.72	1137	14.64	806	14.56	576			14.76	698
15.32	1459	15.48	2245	15.36	1130	15.24	821	15.20	683	15.28	935
		16.04	958	16.12	979					16.12	766
16.44	1584			16.40	808	16.40	903			16.44	854
		17.16	2541	17.12	1261	17.16	1003			17.20	1048
		17.84	1976	17.68	1150	17.72	1115	17.56	1507	17.72	1181
18.08	799			18.00	1184	18.00	1195			18.08	1378
		19.00	2762	18.88	1514	18.84	1263	18.80	772	18.92	1295
		19.56	2216	19.60	1502	19.60	1215	20.00	757	19.64	1391
20.24	4895			20.12	1791	20.16	1398			20.20	1523
20.88	1098	20.88	2303	20.80	1487	20.80	1040			20.80	1132
22.84	826	22.76	2005	22.80	1384	22.76	802			22.76	1032
23.48	2618			23.40	1275	23.44	915	23.88	721	23.44	1015
24.08	1430			24.32	959	24.32	748	24.92	531	23.96	841
25.84	1414			25.72	1176	25.76	830			25.80	877
27.52	1037	27.12	1663	27.08	1132	27.36	661			27.28	795

I* diffraction intensity

temperature was decreased (Szejtli, 1988), during the freezing process, and recrystallization of β - CD might occur.

R:2HP-β-CD system: The X-ray powder diffraction patterns of ranitidine HCl, 2HP-β-CD, and the physical mixture are presented in Figure 36. The X-ray powder diffractograms of 1:1 R:CD products prepared by the three methods are shown in Figure 37. The comparison of diffractograms of each component, the physical mixture, and the obtained 1:1 R:2HP-β-CD system are summarized in Table 8. 2HP-β-CD is amorphous in nature, its diffractogram (Figure 36, B) consisted of two broad diffuse maxima. The physical mixture (Figure 36, C), co-grinded (Figure 37, A), and kneaded (Figure 37, C) products gave similar results. An amorphous structure in the product prepared by freeze-drying technique (Figure 37, B) was observed since, in the presence of an amorphous carrier, the drug was prevented from nucleating in its original crystal structure (Mura et al., 1998).

In the solid state characterization of the ranitidine HCl : CD (β - CD, 2HP-β-CD) products, DSC played an important role in determining the inclusion complexes. It clearly discriminated the thermograms of physical mixture and inclusion complexes. However, the DSC technique alone did not give a strong evidence to conclude that the inclusion complexes were formed.

2.4 Proton Nuclear Magnetic Resonance Spectroscopy

^{1}H-NMR spectroscopy was the only technique in this study for the detection of inclusion complexes in a solution state. NMR spectroscopy is an analytical procedure based on the magnetic properties of certain atom nuclei. The signals (peaks) in NMR spectrum are characterized by four parameters: resonance frequency, multiplicity, line width, and relative intensity. The analytical usefulness of the NMR technique resides in the fact that the same types of nuclei, when locate in different

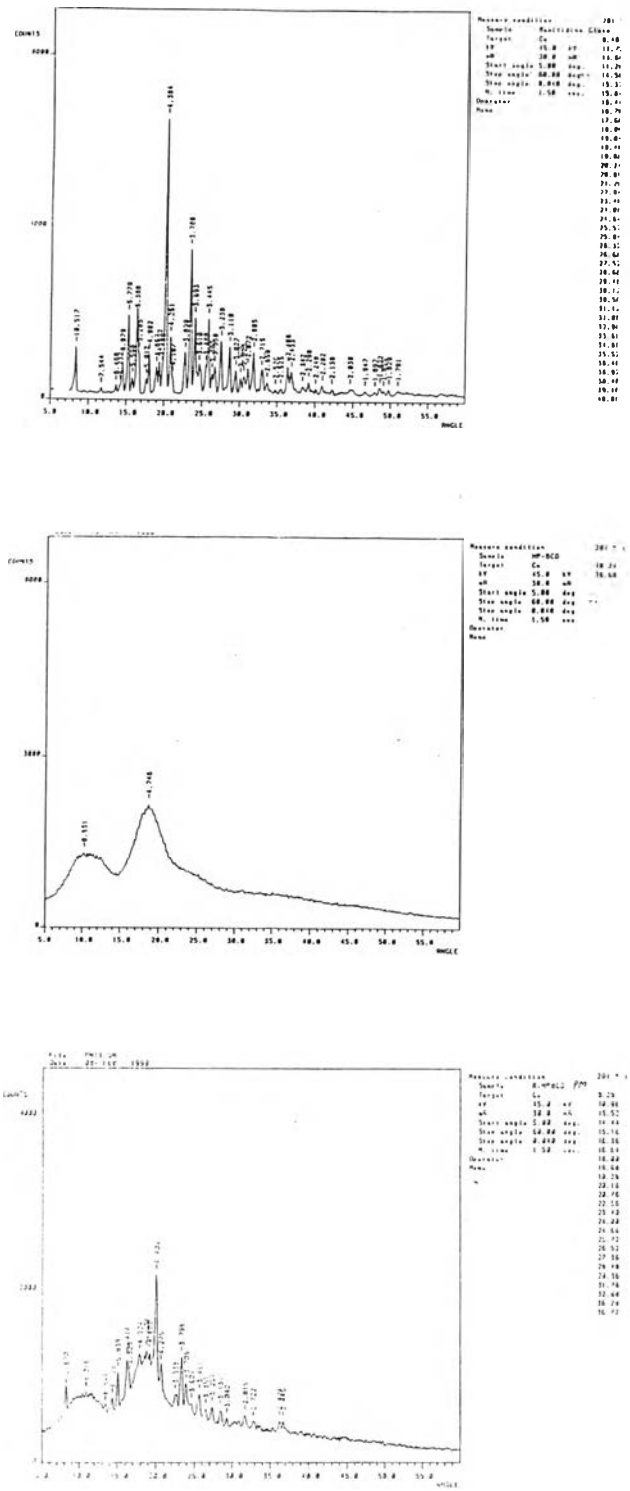

Figure 36. X-ray powder diffractograms of ranitidine HCl, (A); 2HP-β-CD, (B); and the physical mixture of ranitidine HCl and 2HP-β -CD molar ratio 1:1 (C).

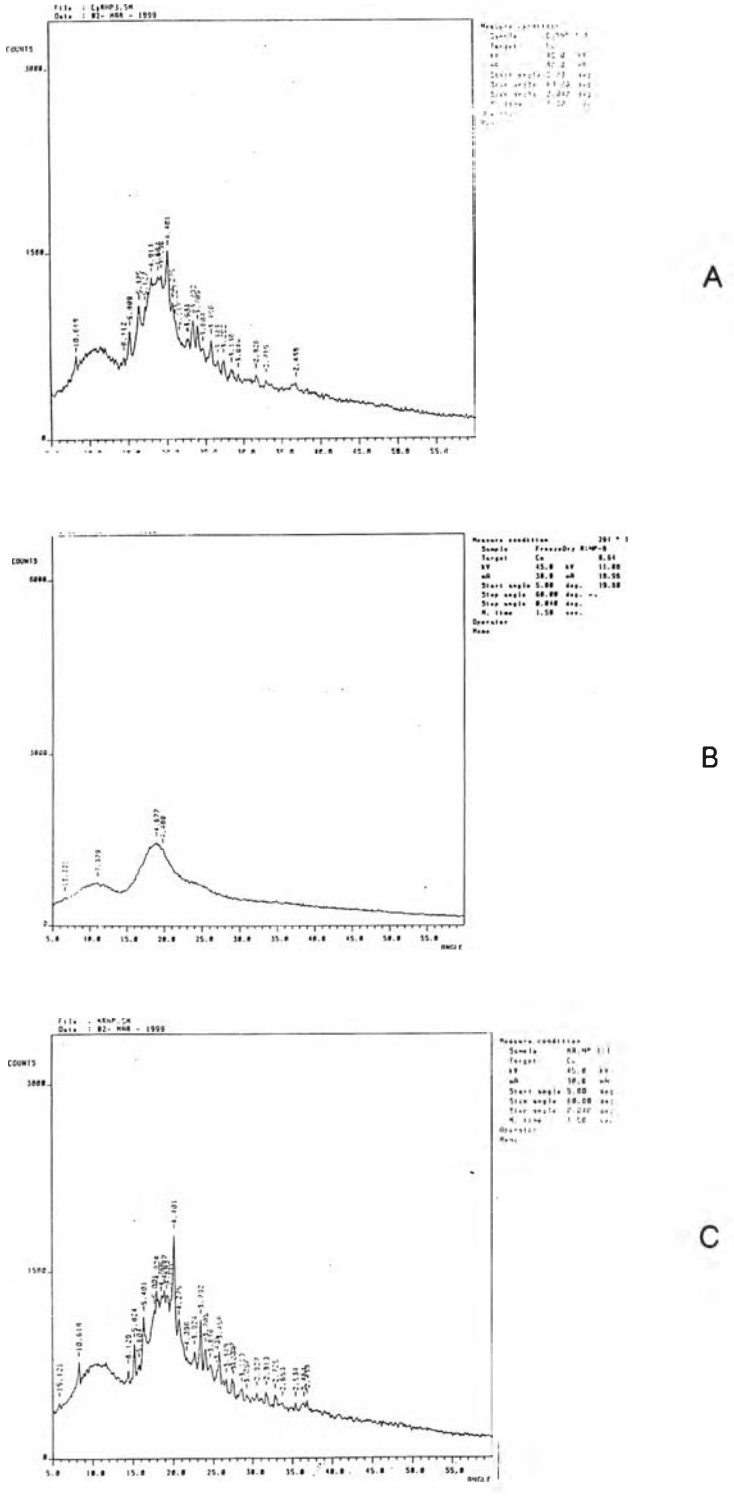

Figure 37. X-ray powder diffractograms of the 1:1 ranitidine HCl : 2HP-β-CD products prepared by three methods. [co-grinding method, (A); freeze-drying method, (B); and kneading method, (C)].

Table 8. X-ray powder diffraction patterns of the R:2HP-β-CD system.

R		β - CD		physical mixture		co-grinding		freeze-drying		kneading	
2θ (°)	I*	2θ (°)	I*	2θ (°)	I*	2θ (°)	I*	2θ (°)	I*	2θ (°)	I*
								6.64	505	5.84	449
8.40	914			8.28	890	8.32	669			8.32	781
		10.24	1330	10.96	808			11.08	765		
14.56	656			14.44	737	14.48	654			14.44	711
15.32	1459			15.16	1045	15.24	861			15.20	923
16.44	1584			16.36	1185	16.48	1067			16.40	1137
18.08	799			18.00	1247	18.04	1290			18.00	1345
		18.68	2156	18.88	1291	18.92	1302	18.96	1480	18.60	1311
20.24	4895			20.16	2162	20.16	1516			20.16	1789
20.88	1098			20.76	1150	20.76	1093			20.76	1124
22.84	826			22.56	781	22.76	792			22.64	861
23.48	2618			23.40	1221	23.44	948			23.44	1109
24.08	1403			24.00	901	24.00	903			24.00	880
25.84	1414			25.72	786	25.76	786			25.76	861
27.52	1037			27.36	634	27.40	627			27.36	644

I* diffraction intensity

molecular environments, exhibit different resonance frequencies. Therefore, NMR spectroscopy is a powerful technique for investigation of the formation of inclusion complex and results in information on the driving forces and binding modes in these non-covalent associations (Schneider, Hacket, and Rudiger, 1998).

The CD molecule has primary and secondary hydroxyl groups crowning opposite ends of its torus; H-3 and H-5 direct towards the interior, H-6 on the rim, while H-1, H-2, and H-4 on the exterior. It is expected that if the inclusion does occur, protons located within or near the cavity, such as H-3, H-5, and H-6, should be strongly shielded due to the anisotropy of the hydrophobic part of guest molecule. Whereas protons that locate on the exterior of the torus (H-1, H-2, and H-4) should be relatively unaffected. Alternatively, if associations take place on the exterior of the torus, H-1, H-2, and H-4 should be more strongly affected. It is well recognized that upfield shifts are observed in the CD protons, while downfield shifts observed in the drug protons (Demarco and Thakkar, 1970; Marques et al., 1990).

R:β-CD system: The ^{1}H-NMR spectra in D_2O of ranitidine HCl, β-CD, and the 1:1 freeze-dried products are demonstrated in Figure 38. The effect of the magnitudes of the chemical shifts induced by ranitidine HCl in the β-CD proton signals at the molar ratio of 1:1 can be seen in Table 9. It was evident that only H-3 proton of β - CD experienced a shielding effect, i.e., it moved to higher fields from its initial position. The other protons of β - CD were not significantly affected by ranitidine HCl molecule. This observation was in agreement with the shielding effect of ranitidine HCl protons (Table 10).

R:2HP-β-CD: The ^{1}H-NMR spectra in D_2O of ranitidine HCl, 2HP-β-CD, and the 1:1 freeze-dried complex are demonstrated in Figure 39. The magnitudes of the chemical shifts induced by 2HP-β-CD in the ranitidine HCl proton signals at the molar ratio of 1:1 can be seen in Table 10.

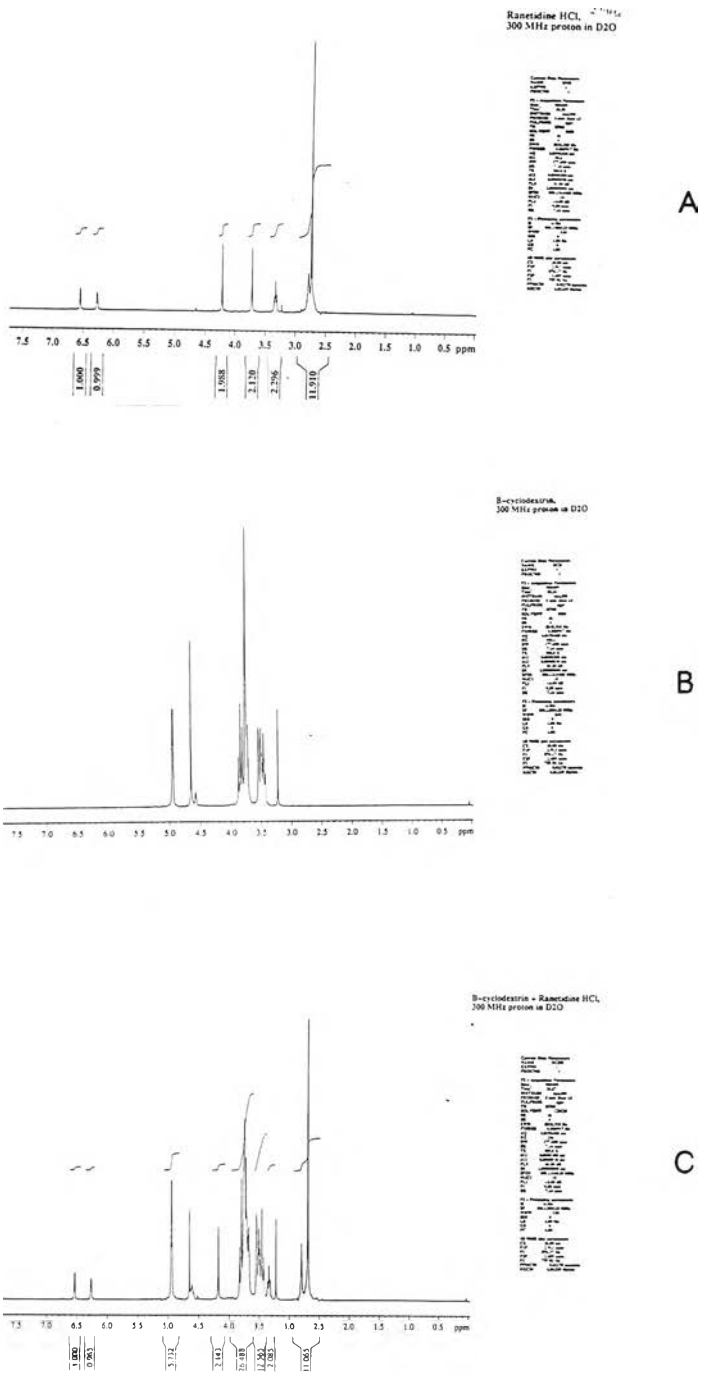

Figure 38. ^{1}H-NMR spectra in D_2O of ranitidine HCl, (A); β - CD, (B); and the 1:1 freeze-dried product of ranitidine HCl : β - CD, (C).

Table 9. ^{1}H-Chemical shifts (δ) of β-CD and its shifts in the presence of ranitidine HCl freeze-dried product (1:1 molar ratio) in D_2O.

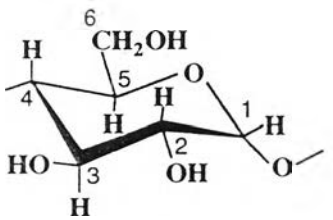

β-CD	δ_o (ppm)	$\delta_{complex}$ (ppm)	$\Delta\delta$ ($\delta_{complex}$ - δ_o) (ppm)
H - 1	4.9570	4.9567	-0.0003
H - 2	3.5519	3.5598	0.0079
H - 3	3.8451	3.8027	-0.0424
H - 4	3.4645	3.4668	0.0023
H - 5	3.7280	3.7274	-0.0006
H - 6	3.7601	3.7502	-0.0099

Table 10. ^{1}H-Chemical shifts (δ) of ranitidine HCl and its shifts in the presence of CDs (β-CD, 2HP-β-CD) freeze-dried products (1:1 molar ratio) in D_2O.

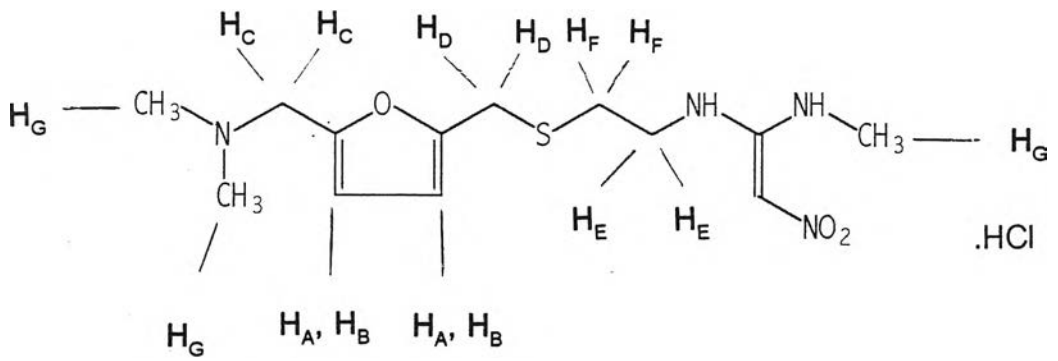

Ranitidine HCl	R:β-CD system		R:2HP-β-CD system	
δ_o (ppm)	$\delta_{complex}$ (ppm)	$\Delta\delta$ ($\delta_{complex}$ - δ_o) (ppm)	$\delta_{complex}$ (ppm)	$\Delta\delta$ ($\delta_{complex}$ - δ_o) (ppm)
A 6.5543	6.5442	-0.0101	6.5519	-0.0024
B 6.2654	6.2664	-0.0010	6.2709	0.0055
C 4.2226	4.1849	-0.0377	4.2063	-0.0163
D 3.7258	3.7157	-0.0101	3.7310*	0.0052
E 3.3364	3.3483	0.0119	3.3463	0.0099
F 2.7904	2.8058	0.0154	2.8012	0.0108
G 2.7441	2.6984	-0.0457	2.7226	-0.0215

* this peak of ranitidine HCl is fused with a broad peak of 2HP-β-CD

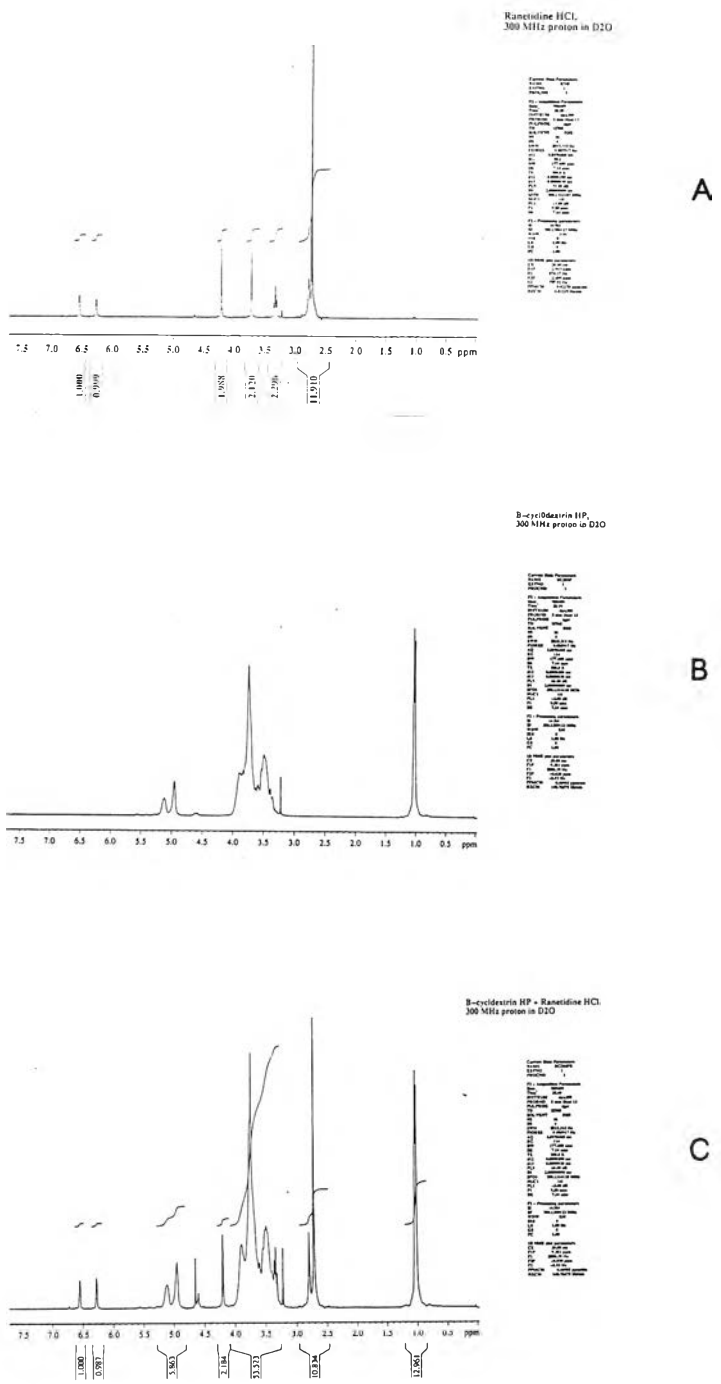

Figure 39. ^{1}H-NMR spectra in D_2O of ranitidine HCl, (A); 2HP-β-CD, (B), and the 1:1 freeze-dried product of ranitidine HCl : 2HP-β-CD, (C).

In R:β-CD system, the significant magnitude of H-3 proton upfield shifts relative to the other protons of β-CD in the 1:1 freeze-dried product informed a shallow penetration of ranitidine molecule in the β-CD cavity. This data was also in agreement with the change in chemical shifts of the methyl and methylene protons at H_G and H_C positions of ranitidine HCl molecule, respectively, in the 1:1 freeze-dried product. Consequently, the NMR technique informed the inclusion complex formation of ranitidine HCl : β-CD.

Due to unspecified substitution of 2 - hydroxypropyl group at 2 -, 3 -, or 6 - OH position in the β-CD molecule, most of signals present in ^{1}H-NMR spectra of 2HP-β-CD were overlapped and hardly characterized. Therefore, the changes in chemical shifts in R:2HP-β-CD system were detected from ranitidine HCl molecule alone. However, the results in Table 10 showed minor changes in chemical shifts of protons at H_G and H_C positions of ranitidine HCl molecule. It might imply that the inclusion of ranitidine HCl molecule in 2HP-β-CD cavity was not preferential due to the steric effect of 2-hydroxypropyl group at 2 - or 3 - OH, which located on the wider rim of 2HP-β-CD torus. In the presence of the CDs (β-CD, 2HP-β-CD), higher shifts were observed for β-CD compare with 2HP-β-CD; it was possible to suppose that ranitidine HCl preferred β-CD to 2HP-β-CD for the inclusion complex formation in the solution state.

Although many ionizable drugs are able to form CD inclusion complexes, their stability constants are much larger for the un-ionized than for the ionized forms (Loftsson and Brewster, 1996). The stability constant of 1:1 molar ratio complex of levemopamil HCl in the charge state : HP-β-CD is 30.35 ± 1.62 M^{-1}, while that in the neutral state is 1502.38 ± 15.87 M^{-1} (Mc Candless and Yalkowsky, 1998). Therefore, the stability constant of ranitidine HCl inclusion complex which was a protonated form in water should be low. For this reason, the change in chemical shifts of ranitidine HCl protons in the inclusion complex was slightly observed in ^{1}H-NMR spectra.

2.5 Scanning Electron Microscopy

The morphology changes and size changes which occurred during the co-grinding, freeze-drying, and kneading process could be revealed by scanning electron microscopy (SEM). The morphology of pure compounds and the products obtained were examined by SEM.

R:β-CD system: The SEM photomicrographs of ranitidine HCl, β-CD, and the freeze-dried β-CD are shown in Figure 40. The photomicrographs of the 1:1 inclusion complexes prepared by the three methods are demonstrated in Figure 41. Ranitidine HCl and β-CD are crystalline powder in nature. The photomicrograph of ranitidine HCl illustrates that it was small irregular-shaped crystals (Figure 40, A-B). The commercial β-CD product was large prism-shaped crystals (Figure 40, C-D). Being freeze-dried, crystallized β-CD was transformed to a mixture of amorphous and crystalline states of which the amorphous state predominate (Figure 40, E-F). The co-grinding samples showed the size reduction and the presence of agglomeration of finely crystallized powder (Figure 41, A-B). This agglomeration process occurs naturally in powders because of adhesion forces that always act between fine particles obtained by grinding (Arias et al., 1997). The freeze-dried R:CD products (Figure 41, C-D) showed similar results as the freeze-dried β-CD, i.e., a combination of irregular-sized pieces of amorphous form and finely crystalline powder. This process promoted a phase transition or disrupted the crystal lattice resulting in an amorphous state or change in the crystallinity. The kneaded products exhibited the random-sized crystals, which might be a result of small crystals of ranitidine HCl attached onto the surface of larger particles of β-CD (Figure 41, E-F). In the kneading process, both ranitidine HCl and CD (β-CD, 2HP-β-CD) were ground in a mortar with a limited amount of water. Ranitidine HCl and CDs dissolved partly which promoted the adhesion of ranitidine microcrystals to the CDs particles. This was also observed by Fini et al. (1997).

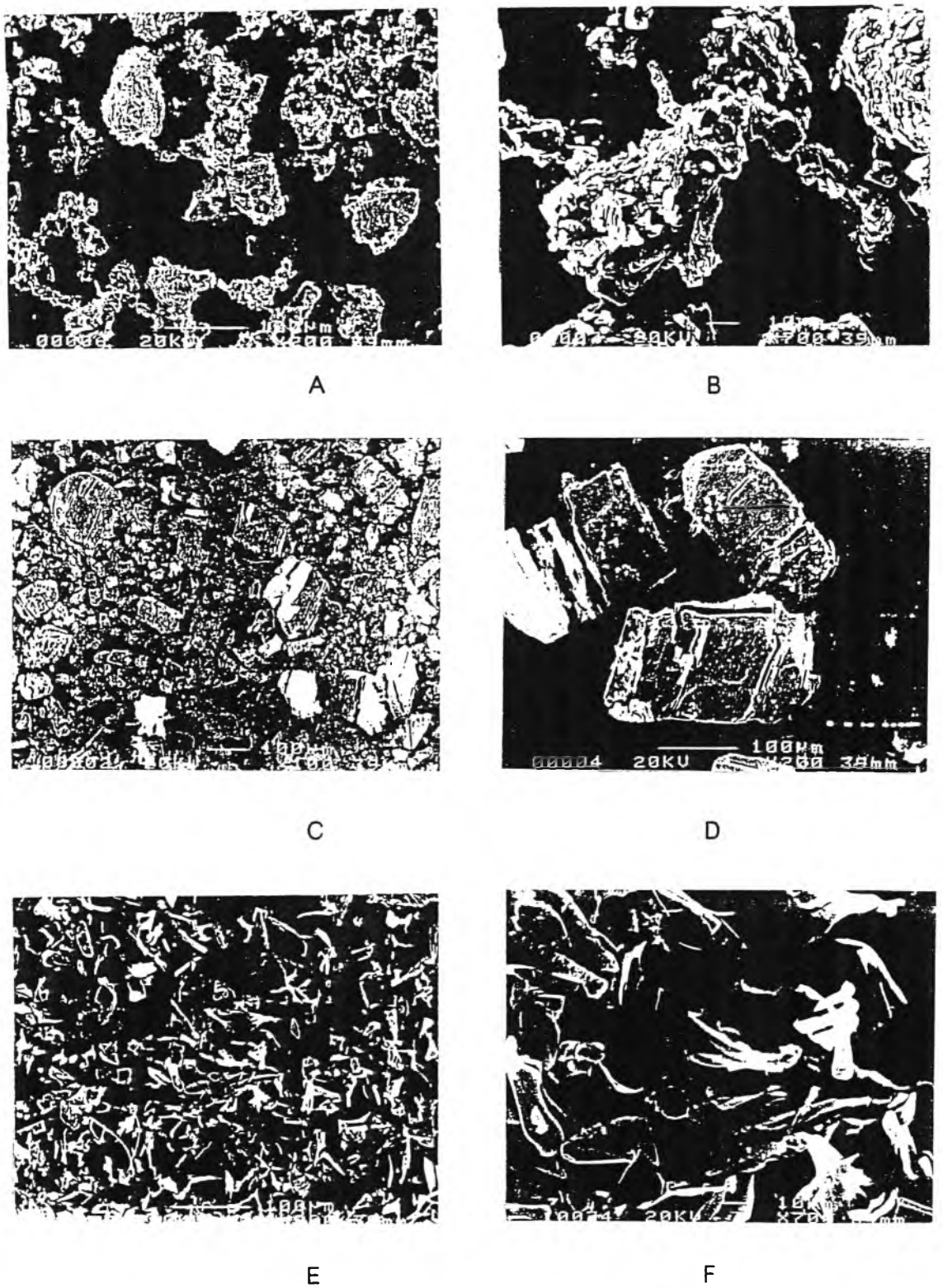

Figure 40. Scanning electron photomicrographs of ranitidine HCl (X200), (A); ranitidine HCl (X700), (B); β - CD (X200), (C); β - CD (X700), (D); the freeze-dried β -CD (X200), (E); and the freeze-dried β -CD (X700), (F).

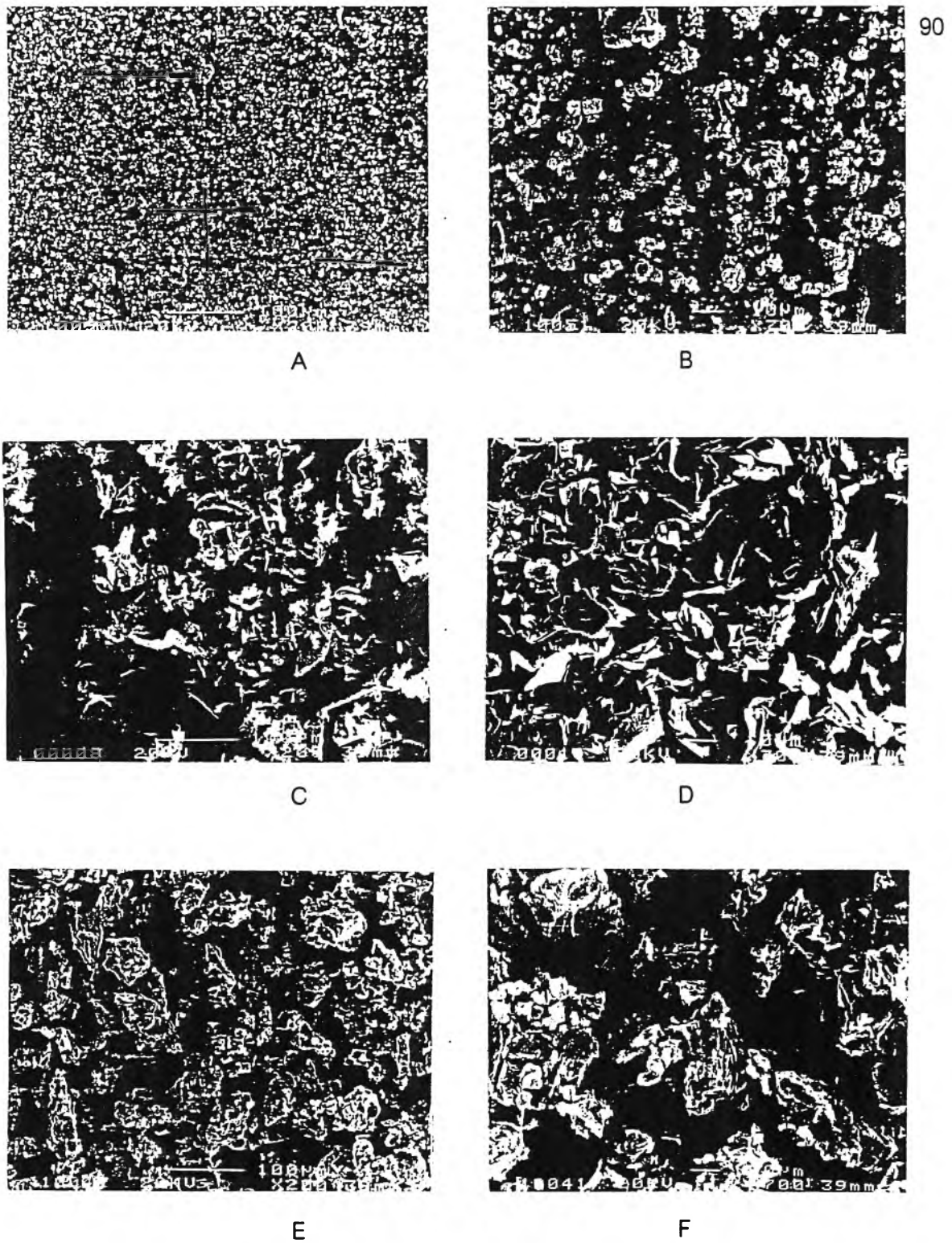

Figure 41. Scanning electron photomicrographs of the 1 : 1 ranitidine HCl : β -CD products prepared by three methods. [co-grinding (X200), (A); co-grinding (X700), (B); freeze-drying (X200), (C); freeze-drying (X700), (D), kneading (X200), (E); and kneading (X700), (F)].

R:2HP-β-CD system: The SEM photomicrographs of ranitidine HCl, 2HP-β-CD and the freeze-dried 2HP-β-CD are presented in Figure 42. The photomicrographs of the 1:1 R:CD products prepared by the three methods are demonstrated in Figure 43. 2HP-β-CD was irregular-sized pieces (Figure 42, C-D) and it was amorphous in nature. No significant change in morphology of 2HP-β-CD was observed after it had been freeze-dried (Figure 42, E-F). The morphology of the processed products by means of grinding (Figure 43, A-B) and kneading (Figure 43, E-F) were similar to those obtained in the R:β-CD system. While the freeze-dried products were irregular-sized pieces of amorphous form (Figure 43, C-D). All the morphologies of the samples detected by SEM photomicrographs were in good agreement with the results obtained from X-ray powder diffractograms.

3. Selection of Inclusion Complexes of Ranitidine HCl : Cyclodextrin (β - CD, 2HP-β-CD) for Further Studies of pH and Humidity Effects

The structures of the CD inclusion complexes in solution and in crystalline state differ significantly. In solution, the guest molecule occupies the cavity in the CD host and the entire complex is surrounded and solvated by water molecules. In crystalline state, the guest molecule can be accommodated not only in the cavity of CD molecule, but also in the intermolecular cavities formed by the crystal lattice, or sandwich-like between two complex molecules. Furthermore, some of the CD molecules remain unoccupied or may include water. This arrangement may result in the formation of non stoichiometric inclusion complexes in the solid state (Szejtli, 1988). The complex formation in the solid phase is thermodynamically spontaneous, but its stability is less than in the aqueous solution (Connors and Rosanske, 1980).

Generally, the most commonly claimed stoichiometric ratio for drug-CD complex is 1:1, and this claim is usually justified. Nevertheless, other ratios, i.e., 1:2, 2:1, and 2:2, are known; the most common of these is probable 1:2. Connors (1997) proposed a simple model relating the equilibrium in a typical CD system. The CD molecule may be

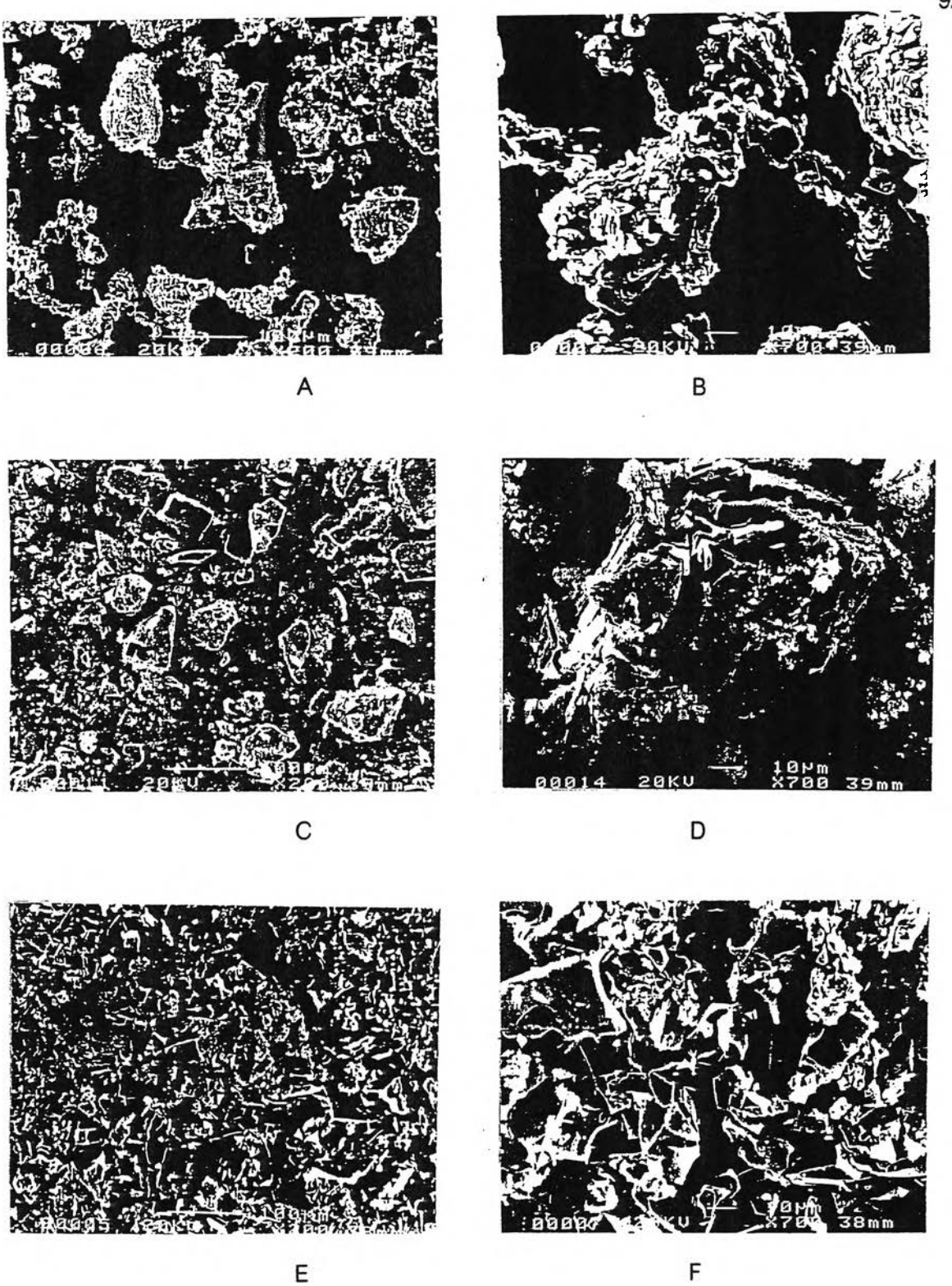

Figure 42. Scanning electron photomicrographs of ranitidine HCl (X200), (A); ranitidine HCl (X700), (B); 2HP-β-CD (X200), (C); 2HP-β-CD (X700), (D); the freeze-dried 2HP-β-CD (X200), (E); and the freeze-dried 2HP-β-CD (X700), (F).

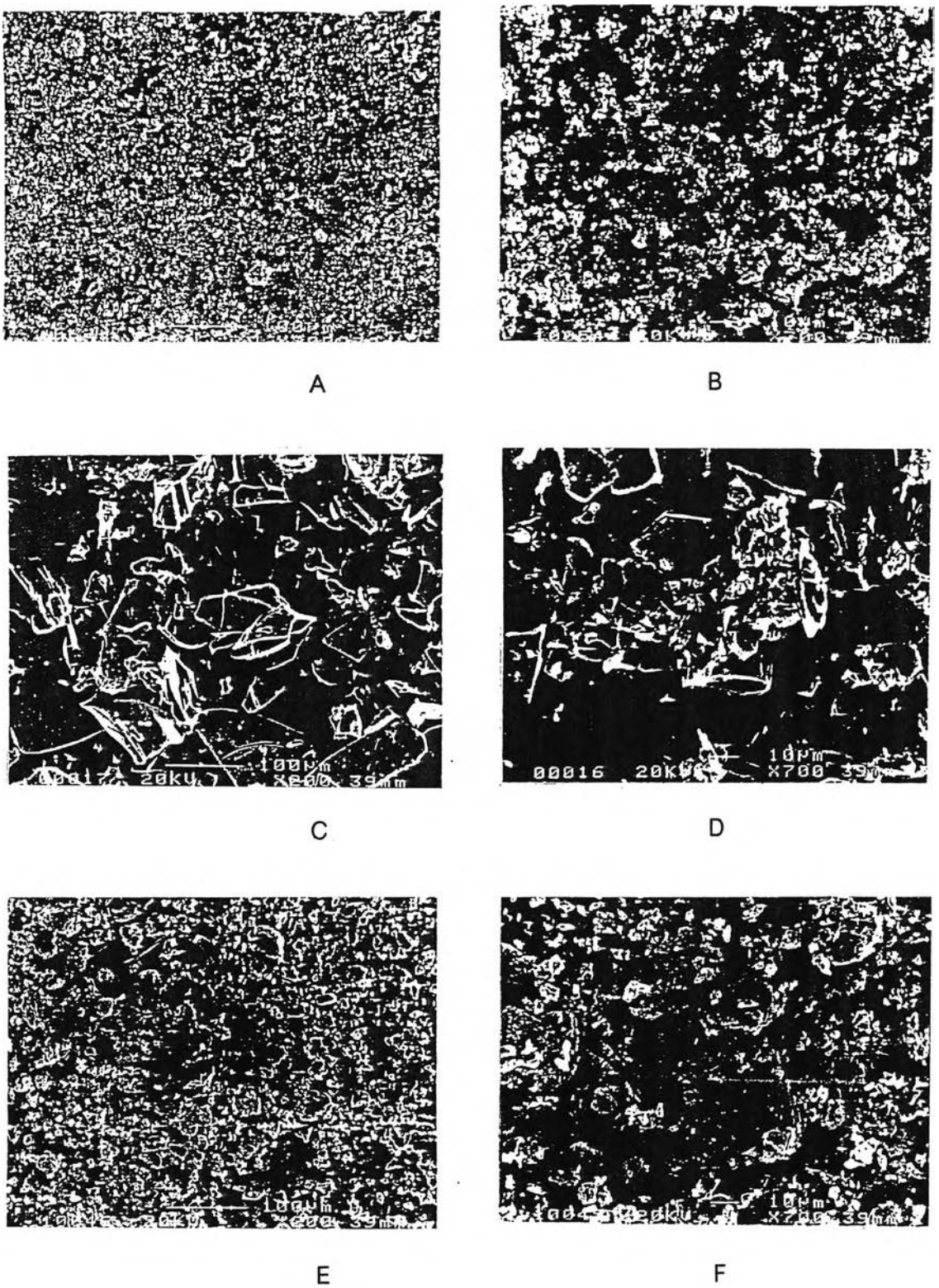

Figure 43. Scanning electron photomicrographs of the 1 : 1 ranitidine HCl : 2HP-β-CD products prepared by three methods. [co-grinding (X200), (A); co-grinding (X700), (B); freeze-drying (X200), (C); freeze-drying (X700), (D), kneading (X200), (E); and kneading (X700), (F)].

thought of as possessing two binding sites, namely the two ends of the cavity, and a guest molecule is also considered to have two potential binding sites. This description is somewhat limited. In this system, there may exist three possible stoichiometric ratios of drug : CD (1:1, 1:2, and 2:1) with four possible isomerics of each ratio. If only one end of the CD molecule can be entered, presumably a wider end, it can form only 1:1 and 1:2 complexes. This seems to be the case of α - CD but is less assured for the larger host.

Through experimental observations, the more appropriate molar ratios of ranitidine HCl : CD (β - CD, 2HP-β-CD) products may be 1:1 or 1:2. In this study, these two molar ratios illustrated no significant difference in FTIR spectra and DSC thermograms. Since the smaller amount of CDs is more preferable, and 1:1 stoichiometric ratio of the complex is the simplest and most frequently used in the essence of molecular encapsulation (Szejtli, 1988; Connors, 1997; Stella and Rajewski, 1997), then 1:1 molar ratio was chosen.

From the preparation method point of view, the kneading technique was not suitable for preparation of ranitidine HCl : CD (β - CD, 2HP-β-CD) inclusion complexes because the final products were non-uniform hard masses. In addition, this technique gave the least yield (approximately 60-70%). In the case of co-grinding method, the products were fine-uniform crystalline powder with approximately 70-80% yield. Furthermore, the solid state characterizations of the kneaded and co-grinded products could not lead strongly to conclude that they were true inclusion complexes. The most appropriate method was freeze-drying because the obtained products were homogeneous inclusion complexes with the highest yield (approximately 90-95%).

For the aforementioned reasons, the inclusion complexes of ranitidine HCl : CD (β - CD, 2HP-β-CD) were prepared by freeze-drying method at the molar ratio of 1:1 for further studies.

4. Effect of pH on the Chemical Stability of Ranitidine HCl : Cyclodextrin (β-CD, 2HP-β-CD) Inclusion complexes

The goal of chemical kinetics is to elucidate reaction mechanisms, therefore the kinetic principle is always of great importance in stability programs. Solution kinetics are most conveniently elucidated and described among these fundamental principles. Two important parameters indicating the kinetics of chemical reactions are order and rate of reactions. The order of reaction determines the shape of the concentration-time profile of drugs and drug products, while the rate constant is determined by its slope (Carstensen, 1995).

The graphic method is one of the convenient methods used to determine the order of reaction. If a plot of concentration of drug remaining in a degradation process versus time is a straight line, the reaction kinetic is said to be zero-order. The reaction kinetic is first-order when a plot of log (concentration of drug remaining) versus time gives a straight line. While the second-order is a result of the straight line of the plot of 1/ (concentration of drug remaining) versus time (Martin,1993). In this study, the graphic method and residual plots were used to determine the kinetic order of reaction. The linear regression analysis was used to examine the obtained data and to draw meaningful conclusions. Residual plots showing scattering of points also inform no deviation of assumptions including the linearity one. The residual plots of the zero-order, first-order, and second-order of all formulations studied are shown in Appendix II, and their correlation coefficients (r) are illustrated in Tables 11-13. Although the residual plots show some patterns, the degradation kinetics of ranitidine HCl might be grouped into three zones; the very low pH value (pH 1), the acid pH values (pH 3 and 5), and the neutral to basic pH values (pH 7, 9, 11, and 13), from the correlation coefficient stand point. The correlation coefficients proposed the zero-order, second-order, and first-order plots for the drug degradation at the very low pH, the acid pH values, and the neutral to basic pH values, respectively. The residual plots also showed similar results.

Table 11. Correlation coefficients (r) of regression lines of zero-order, first-order and second-order plots of ranitidine HCl degradation in pH 1-13 buffers.

pH	Conc. (M)	Correlation coefficient (r)		
		Zero-order	First-order	Second-order
1	0.10	0.9057	0.8021	0.6443
(phosphate)	0.20	0.8948	0.8351	0.7222
	0.30	0.9580	0.8886	0.7660
3	0.05	0.8810	0.9634	0.9953
(phosphate)	0.10	0.6454	0.8654	0.9874
	0.20	0.5442	0.7539	0.9407
5	0.10	0.8299	0.9507	0.9978
(acetate)	0.20	0.7724	0.8983	0.9803
	0.30	0.8288	0.9252	0.9863
7	0.05	0.9454	0.9890	0.9291
(phosphate)	0.10	0.9437	0.9910	0.9246
	0.20	0.8996	0.9916	0.9398
9	0.10	0.8924	0.9943	0.9514
(glycine-NaOH)	0.20	0.8671	0.9880	0.9469
	0.30	0.8275	0.9786	0.9547
11	0.10	0.8157	0.9832	0.9671
(glycine-NaOH)	0.20	0.8223	0.9822	0.9569
	0.30	0.8702	0.9889	0.9459
13	0.03	0.9216	0.9884	0.8603
(phosphate)	0.05	0.9430	0.9965	0.8888
	0.08	0.9542	0.9918	0.8866

Table 12. Correlation coefficients (r) of regression lines of zero-order, first-order and second-order plots of ranitidine HCl degradation in R : β-CD complex at pH 1-13 buffers.

pH	Conc. (M)	Correlation coefficient (r)		
		Zero-order	First-order	Second-order
1	0.10	0.9328	0.8513	0.7253
(phosphate)	0.20	0.9137	0.7486	0.5320
	0.30	0.9487	0.8366	0.6545
3	0.05	0.8844	0.9532	0.9877
(phosphate)	0.10	0.6873	0.9010	0.9924
	0.20	0.5482	0.7972	0.9625
5	0.10	0.8419	0.9595	0.9988
(acetate)	0.20	0.7790	0.9152	0.9919
	0.30	0.8111	0.9180	0.9846
7	0.05	0.8938	0.9829	0.9621
(phosphate)	0.10	0.8803	0.9888	0.9642
	0.20	0.8153	0.9775	0.9767
9	0.10	0.8974	0.9942	0.9508
(glycine-NaOH)	0.20	0.9044	0.9942	0.9560
	0.30	0.8653	0.9870	0.9620
11	0.10	0.8310	0.9842	0.9645
(glycine-NaOH)	0.20	0.8188	0.9823	0.9653
	0.30	0.8714	0.9922	0.9387
13	0.03	0.9342	0.9944	0.8858
(phosphate)	0.05	0.9452	0.9979	0.9142
	0.08	0.9378	0.9959	0.9004

Table 13. Correlation coefficients (r) of regression lines of zero-order, first-order and second-order plots of ranitidine HCl degradation in R : 2HP-β-CD complex at pH 1-13 buffers.

pH	Conc. (M)	Correlation coefficient (r)		
		Zero order	First order	Second order
1	0.10	0.9269	0.8629	0.7733
(phosphate)	0.20	0.9277	0.8459	0.7244
	0.30	0.9428	0.8843	0.7955
3	0.05	0.8701	0.9430	0.9830
(phosphate)	0.10	0.7053	0.9032	0.9902
	0.20	0.5871	0.8304	0.9618
5	0.10	0.8910	0.9776	0.9953
(acetate)	0.20	0.8300	0.9316	0.9861
	0.30	0.8683	0.9479	0.9896
7	0.05	0.9275	0.9911	0.9448
(phosphate)	0.10	0.9161	0.9937	0.9449
	0.20	0.8165	0.9754	0.9728
9	0.10	0.9059	0.9942	0.9658
(glycine-NaOH)	0.20	0.9006	0.9908	0.9582
	0.30	0.8726	0.9860	0.9588
11	0.10	0.8417	0.9791	0.9747
(glycine-NaOH)	0.20	0.8017	0.9851	0.9387
	0.30	0.8484	0.9877	0.9276
13	0.03	0.9298	0.9946	0.8869
(phosphate)	0.05	0.9498	0.9980	0.9278
	0.08	0.9534	0.9957	0.9142

This was not surprising since Haywood et al. (1987) also reported that two different hydrolytic pathways of ranitidine HCl are operative under acid and alkaline conditions. At intermediate pH values both pathways are operative with the basic pathway predominating over the acid pathway whilst at very low pH values ranitidine HCl is resistant to hydrolytic cleavage. Their final pH values are illustrated in Tables 14 - 16.

The rate of reaction can be expressed as a decrease in concentration per unit of time of any of the reacting substances. Thus, a slope of the straight line plot which best fit to the order of that reaction can be used to determine the observed degradation rate constant (k_{obs}) of the reaction (Carstensen, 1995). All of the best fitted reaction orders and their rate constants in solutions having various pH values studied are concluded in Tables 17-23.

The kinetics of ranitidine HCl degradation both in its free form and in the inclusion complexes with CDs (β-CD, 2HP-β-CD) in pH 1-13 buffer solutions were similar. Both CDs had similar effects on degradation rate of ranitidine HCl; their effects depended on the pH values of solutions. A modified t -test was used to compare the differences in degradation rate constant values under the null hypothesis that a pair of degradation rate values was not different from each other against an alternative hypothesis that one rate constant value is either more or less than the other. The five percent significant level ($\alpha = 0.05$) is normally used as the priori cut-off for significance. The derivation of this modified t -test are shown in Appendix III.

From the acid/base catalysis point of view, the observed rate constants, k_{obs}, could be expressed as:

$$k_{obs} = k_o + k_{H^+}[H^+] + k_{OH^-}[OH^-] + k_{buffer}[buffer] \qquad (4)$$

Table 14. pH values and buffer capacities of ranitidine HCl in buffered solutions.

Buffer conc. (M)	pH of buffer solutions	Buffer capacity (β)	Initial pH of drug solutions	Final pH of drug solutions*
0.10	1.14	0.0149	1.41	1.64
0.20	0.98	0.298	1.11	1.41
0.30	1.08	0.4478	1.19	1.24
0.05	2.90	0.0138	3.33	5.69
0.10	2.93	0.0276	3.21	5.37
0.20	2.86	0.0552	3.02	4.98
0.10	5.08	0.0532	5.08	6.15
0.20	5.07	0.1064	5.08	5.80
0.30	5.08	0.1596	5.08	5.51
0.05	6.91	0.0271	6.90	7.01
0.10	6.95	0.0543	6.82	7.01
0.20	7.08	0.1085	7.07	7.08
0.10	8.94	0.0286	8.33	8.46
0.20	8.97	0.0571	8.67	8.55
0.30	9.98	0.0857	8.77	8.60
0.10	10.91	0.0121	10.23	9.27
0.20	11.04	0.0242	10.57	9.73
0.30	11.06	0.0363	10.67	9.98
0.03	12.82	0.0150	12.66	12.34
0.05	12.89	0.0250	12.74	12.30
0.08	12.87	0.0400	12.73	12.23

* measured at last day of storage.

Table 15. pH values and buffer capacities of R: β-CD in buffered solutions.

Buffer conc. (M)	pH of buffer solutions	Buffer capacity (β)	Initial pH of drug solutions	Final pH of drug solutions*
0.10	1.14	0.0149	1.42	1.73
0.20	0.98	0.298	1.12	1.45
0.30	1.08	0.4478	1.18	1.27
0.05	2.90	0.0138	3.31	5.72
0.10	2.93	0.0276	3.20	5.39
0.20	2.86	0.0552	3.01	5.01
0.10	5.08	0.0532	5.08	6.07
0.20	5.07	0.1064	5.07	5.74
0.30	5.08	0.1596	5.08	5.54
0.05	6.91	0.0271	6.75	6.78
0.10	6.95	0.0543	6.93	6.82
0.20	7.08	0.1085	6.99	6.90
0.10	8.94	0.0286	7.56	7.98
0.20	8.97	0.0571	8.24	8.32
0.30	8.98	0.0857	8.52	8.46
0.10	10.91	0.0121	10.14	9.15
0.20	11.04	0.0242	10.51	9.60
0.30	11.06	0.0363	10.57	9.89
0.03	12.82	0.0150	12.42	11.98
0.05	12.89	0.0250	12.47	11.87
0.08	12.87	0.0400	12.47	11.90

* measured at the last day of storage.

Table 16. pH values and buffer capacities of R: 2HP-β-CD in buffered solutions.

Buffer conc. (M)	pH of buffer solutions	Buffer capacity (β)	Initial pH of drug solutions	Final pH of drug solutions*
0.10	1.14	0.0149	1.43	1.70
0.20	0.98	0.298	1.11	1.46
0.30	1.08	0.4478	1.21	1.28
0.05	2.90	0.0138	3.33	5.73
0.10	2.93	0.0276	3.20	5.42
0.20	2.86	0.0552	3.03	5.01
0.10	5.08	0.0532	5.11	6.31
0.20	5.07	0.1064	5.11	5.82
0.30	5.08	0.1596	5.12	5.53
0.05	6.91	0.0271	6.80	6.80
0.10	6.95	0.0543	6.88	6.87
0.20	7.08	0.1085	7.03	6.92
0.10	8.94	0.0286	7.83	8.08
0.20	8.97	0.0571	8.41	8.38
0.30	8.98	0.0857	8.64	8.49
0.10	10.91	0.0121	10.17	9.16
0.20	11.04	0.0242	10.53	9.63
0.30	11.06	0.0363	10.58	9.91
0.03	12.82	0.0150	12.52	12.08
0.05	12.89	0.0250	12.62	11.99
0.08	12.87	0.0400	12.55	11.99

* measured at last day of storage.

Table 17. Observed zero-order rate constants of ranitidine HCl degradation in pH 1 phosphate buffer with various buffer concentrations (ionic strength = 0.5).

pH of buffer solutions	Buffer conc. (M)	Formula	$f_{H_3PO_4}$*		$f_{H_2PO_4^-}$ *		k_{obs}
			At initial pH of drug solutions	At final pH of drug solutions	At initial pH of drug solutions	At final pH of drug solutions	($mg.mL^{-1}.hr^{-1}$)
1.14	0.10	R	0.84	0.75	0.16	0.25	0.3592
		R:β-CD	0.83	0.71	0.17	0.29	0.6436
		R:2HP-β-CD	0.83	0.72	0.17	0.28	0.4217
0.98	0.20	R	0.91	0.84	0.09	0.16	0.2693
		R:β-CD	0.91	0.82	0.09	0.18	0.5563
		R:2HP-β-CD	0.91	0.82	0.09	0.18	0.3916
1.08	0.30	R	0.89	0.88	0.11	0.12	0.2739
		R:β-CD	0.90	0.88	0.10	0.12	0.4907
		R:2HP-β-CD	0.89	0.87	0.11	0.13	0.2848

*calculated from:

$$pH = pK_a + \log \frac{[Salt]}{[Acid]}$$

Table 18. Observed second-order rate constants of ranitidine HCl degradation in pH 3 phosphate buffer with various buffer concentrations (ionic strength = 0.5).

pH of buffer solutions	Buffer conc. (M)	Formula	$f_{H_3PO_4}$ *		$f_{H_2PO_4^-}$ *		$k_{obs} \times 10^3$ ($mg^{-1}.mL.hr^{-1}$)
			At initial pH of drug solutions	At final pH of drug solutions	At initial pH of drug solutions	At final pH of drug solutions	
2.90	0.05	R	0.06	0.00	0.94	1.00	1.2305
		R:β-CD	0.06	0.00	0.94	1.00	0.7260
		R:2HP-β-CD	0.06	0.00	0.94	1.00	0.6780
2.93	0.10	R	0.08	0.00	0.92	1.00	1.3286
		R:β-CD	0.08	0.00	0.92	1.00	1.1249
		R:2HP-β-CD	0.08	0.00	0.92	1.00	1.0377
2.86	0.20	R	0.11	0.00	0.89	1.00	3.0936
		R:β-CD	0.11	0.00	0.89	1.00	2.4492
		R:2HP-β-CD	0.11	0.00	0.89	1.00	3.2527

*calculated from:

$$pH = pK_a + \log \frac{[Salt]}{[Acid]}$$

Table 19. Observed second-order rate constants of ranitidine HCl degradation in pH 5 acetate buffer with various buffer concentrations (ionic strength = 0.5).

pH of buffer solutions	Buffer conc. (M)	Formula	f_{CH_3COOH} *		$f_{CH_3COO^-}$ *		$k_{obs} \times 10^3$ ($mg^{-1}.mL.hr^{-1}$)
			At initial pH of drug solutions	At final pH of drug solutions	At initial pH of drug solutions	At final pH of drug solutions	
5.08	0.10	R	0.32	0.04	0.68	0.96	1.0290
		R:β-CD	0.32	0.05	0.68	0.95	0.8196
		R:2HP-β-CD	0.31	0.03	0.69	0.97	0.5863
5.07	0.20	R	0.32	0.08	0.68	0.92	1.0325
		R:β-CD	0.33	0.09	0.67	0.91	0.8987
		R:2HP-β-CD	0.31	0.08	0.69	0.92	0.6495
5.08	0.30	R	0.32	0.15	0.68	0.85	1.1793
		R:β-CD	0.32	0.14	0.68	0.86	0.9296
		R:2HP-β-CD	0.30	0.15	0.70	0.85	0.7043

*calculated from:

$$pH = pK_a + \log \frac{[Salt]}{[Acid]}$$

Table 20. Observed first-order rate constants of ranitidine HCl degradation in pH 7 phosphate buffer with various buffer concentrations (ionic strength = 0.5).

pH of buffer solutions	Buffer conc. (M)	Formula	$f_{H_2PO_4^-}$ *		$f_{HPO_4^{2-}}$ *		$k_{obs} \times 10^3$ (hr^{-1})
			At initial pH of drug solutions	At final pH of drug solutions	At initial pH of drug solutions	At final pH of drug solutions	
6.91	0.05	R	0.67	0.61	0.33	0.39	1.0427
		R:β-CD	0.74	0.73	0.26	0.27	1.1448
		R:2HP-β-CD	0.72	0.72	0.28	0.28	1.1518
6.95	0.10	R	0.71	0.61	0.29	0.39	1.0481
		R:β-CD	0.66	0.71	0.34	0.29	1.1435
		R:2HP-β-CD	0.68	0.69	0.32	0.31	1.1416
7.08	0.20	R	0.58	0.57	0.42	0.43	1.2397
		R:β-CD	0.62	0.67	0.38	0.33	1.2558
		R:2HP-β-CD	0.60	0.66	0.40	0.34	1.2601

*calculated from:

$$pH = pK_a + \log \frac{[Salt]}{[Acid]}$$

Table 21. Observed first-order rate constants of ranitidine HCl degradation in pH 9 glycine-NaOH buffer with various buffer concentrations (ionic strength = 0.5).

pH of buffer solutions	Buffer conc. (M)	Formula	$f\ ^{+}NH_3CH_2COO^-$ *		$f\ NH_2CH_2COO^-$ *		$k_{obs} \times 10^3$ (hr^{-1})
			At initial pH of drug solutions	At final pH of drug solutions	At initial pH of drug solutions	At final pH of drug solutions	
8.94	0.10	R	0.97	0.95	0.03	0.05	1.4648
		R:β-CD	0.99	0.98	0.01	0.02	1.4031
		R:2HP-β-CD	0.99	0.98	0.01	0.02	1.3278
8.97	0.20	R	0.93	0.94	0.07	0.06	2.3201
		R:β-CD	0.97	0.97	0.03	0.03	1.7371
		R:2HP-β-CD	0.96	0.96	0.04	0.04	1.6268
8.98	0.30	R	0.91	0.94	0.09	0.06	2.6074
		R:β-CD	0.95	0.95	0.05	0.05	1.8855
		R:2HP-β-CD	0.93	0.95	0.07	0.05	1.7468

*calculated from:

$$pH = pK_a + \log \frac{[Salt]}{[Acid]}$$

Table 22. Observed first-order rate constants of ranitidine HCl degradation in pH 11 glycine-NaOH buffer with various buffer concentrations (ionic strength = 0.5).

pH of buffer solutions	Buffer conc. (M)	Formula	$f\ ^{+}NH_3CH_2COO^{-}$ *		$f\ NH_2CH_2COO^{-}$ *		$k_{obs} \times 10^3$
			At initial pH of drug solutions	At final pH of drug solutions	At initial pH of drug solutions	At final pH of drug solutions	(hr^{-1})
10.91	0.10	R	0.26	0.76	0.74	0.24	2.5093
		R:β-CD	0.30	0.81	0.70	0.19	2.2391
		R:2HP-β-CD	0.29	0.81	0.71	0.19	1.9616
11.04	0.20	R	0.14	0.53	0.86	0.47	5.3246
		R:β-CD	0.16	0.60	0.84	0.40	4.8779
		R:2HP-β-CD	0.15	0.59	0.85	0.41	3.9369
11.06	0.30	R	0.11	0.39	0.89	0.61	8.7427
		R:β-CD	0.14	0.44	0.86	0.56	8.4533
		R:2HP-β-CD	0.14	0.43	0.86	0.57	6.7812

*calculated from:

$$pH = pK_a + \log \frac{[Salt]}{[Acid]}$$

Table 23. Observed first-order rate constants of ranitidine HCl degradation in pH 13 phosphate buffer with various buffer concentrations (ionic strength = 0.5).

pH of buffer solutions	Buffer conc. (M)	Formula	$f_{HPO_4^{2-}}$ *		$f_{PO_4^{3-}}$ *		k_{obs} (hr^{-1})
			At initial pH of drug solutions	At final pH of drug solutions	At initial pH of drug solutions	At final pH of drug solutions	
12.82	0.03	R	0.51	0.68	0.49	0.32	0.5787
		R:β-CD	0.64	0.83	0.36	0.17	0.4358
		R:2HP-β-CD	0.59	0.80	0.41	0.20	0.4465
12.89	0.05	R	0.51	0.70	0.49	0.30	0.5489
		R:β-CD	0.61	0.86	0.39	0.14	0.4107
		R:2HP-β-CD	0.53	0.83	0.47	0.17	0.4224
12.87	0.08	R	0.47	0.73	0.53	0.27	0.5541
		R:β-CD	0.61	0.85	0.39	0.15	0.4717
		R:2HP-β-CD	0.57	0.83	0.43	0.17	0.4476

*calculated from:

$$pH = pK_a + \log \frac{[Salt]}{[Acid]}$$

where k_o, k_{H^+}, and k_{OH^-} were the rate constants of solvent, hydronium ion, and hydroxide ion catalyzed degradation, respectively, and k_{buffer} was the sum of the rate constants for the degradation catalyzed by each of the buffer components. From this equation, a plot of k_{obs} versus total buffer concentration would give a slope and intercept that were k_{buffer} and $k_o + k_{H^+}[H^+] + k_{OH^-}[OH^-]$ (the sum of the degradation rate constants at zero buffer concentration), respectively.

Ranitidine HCl degradation in pH 1 phosphate buffer solutions: The plot of ranitidine HCl concentration remaining versus time gave the greatest correlation coefficient values; therefore, the degradation reaction of ranitidine HCl at pH 1 was concluded to be apparent zero-order. Bar charts representing degradation rate constants of ranitidine HCl in pH1 phosphate buffer at various buffer concentrations are shown in Figure 44. β-CD increased the rate constants significantly in all buffer concentrations. 2HP-β-CD did not increased the rate constants significantly except for the 0.20 M buffer concentration. Plots of k_{obs} versus total buffer concentrations are presented in Figure 45. The slopes of these plots, which were k_{buffer}, were -0.4266, -0.7644, and -0.6846 for ranitidine HCl (R), R:β-CD, and R:2HP-β-CD complexes, respectively. Due to the first ionization constant of phosphoric acid, $pK_1 = 2.12$ (Martin, 1993), H_3PO_4 was the dominant species (fraction of H_3PO_4 = 0.83 - 0.91) when drug solutions were prepared initially. Then k_{buffer} was likely to be k_{H3PO4} and they were all negative values. These negative values of k_{H3PO4} assured that H_3PO_4 was not a catalytic species but seemed to stabilize the drug. The intercepts of the k_{obs} versus total buffer concentration plot, which were the rate constants at zero buffer concentration, were 0.3862, 0.7164, and 0.5030 $mg.mL^{-1}.\ hr^{-1}$ for R, R:β-CD, and R:2HP-β-CD complexes, respectively. The rate constants at zero buffer concentration should represent $k_{H^+}[H^+]$ term since the solutions were very acidic. However, the specific acid catalysis could not be proposed because the degradation kinetics at other acidic solutions were different and therefore the pH-rate profile could not be established. The rank order of the rate constant at zero buffer concentration were R:β-CD > R: 2HP-β-CD > R. This meant that

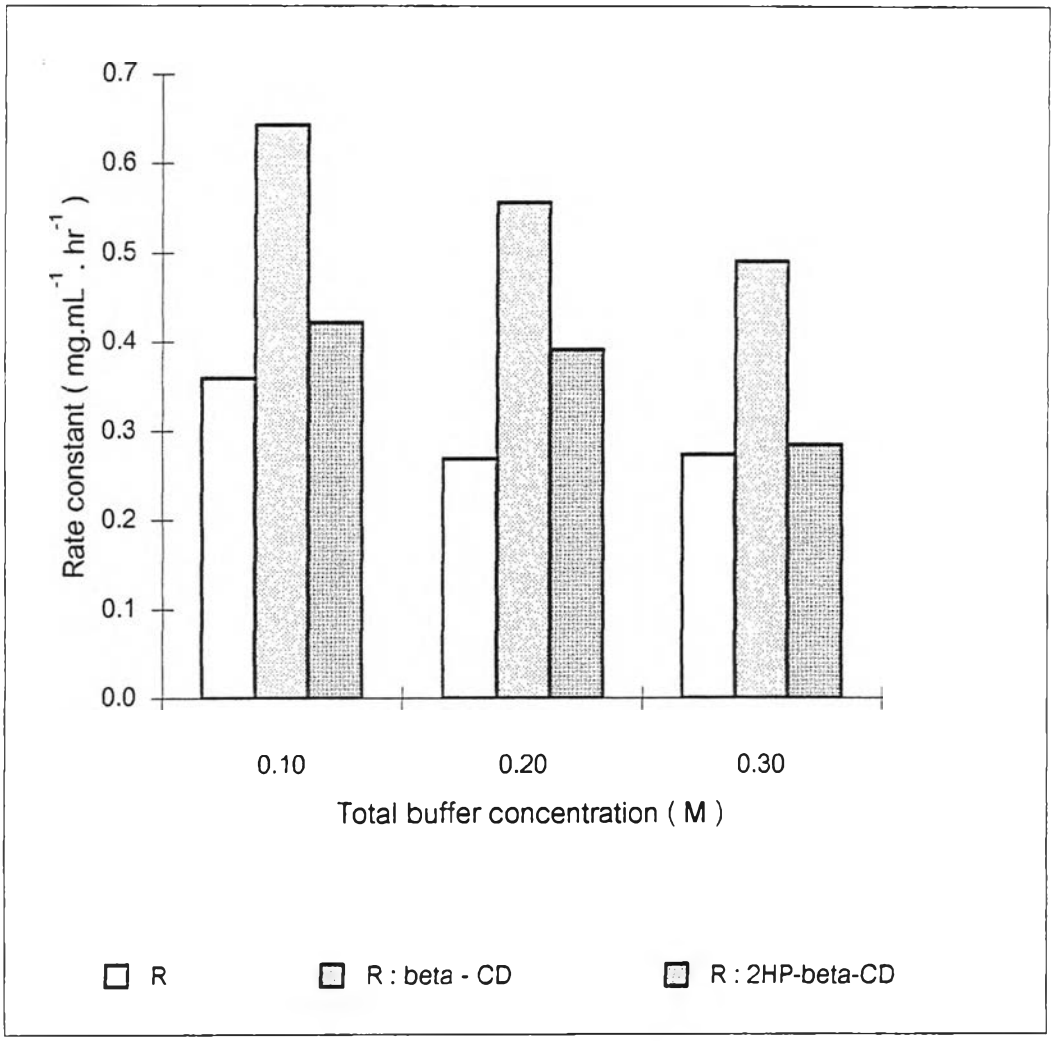

0.10 M ; R : β - CD > R : 2HP-β-CD ≈ R at $\alpha = 0.05$

0.20 M ; R : β - CD > R : 2HP-β-CD > R at $\alpha = 0.05$

0.30 M ; R : β - CD > R : 2HP-β-CD ≈ R at $\alpha = 0.05$

Figure 44. Bar charts presenting the apparent zero order rate constants at pH 1.

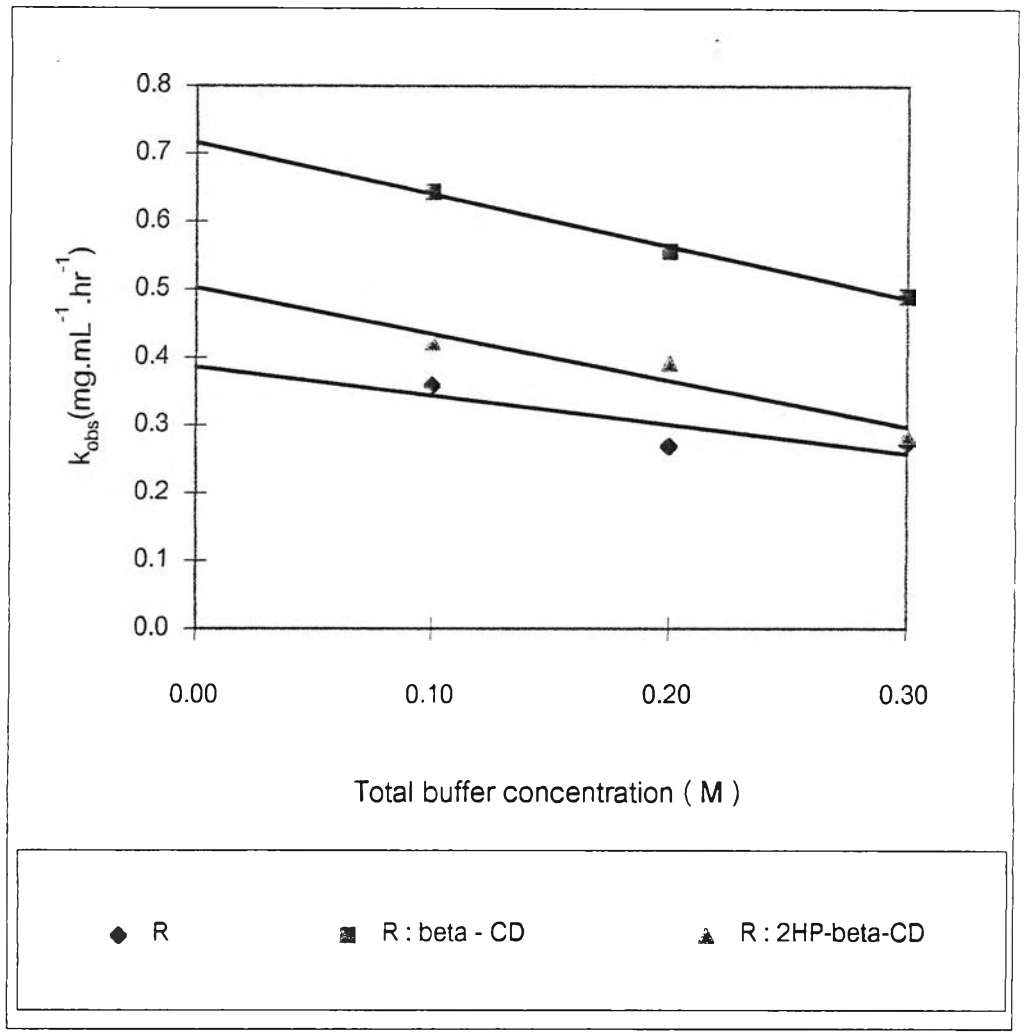

R ; Y = 0.3862 - 0.4266 X, r = -0.8425, SE = 0.0386

R : β - CD ; Y = 0.7164 - 0.7644 X, r = -0.9966, SE = 0.0089

R : 2HP-β-CD ; Y = 0.5030 - 0.6846 X, r = -0.9515, SE = 0.0313

Figure 45. Zero-order plots of ranitidine HCl degradation in pH 1 solutions.

the CDs did not stabilized the drug but, in stead, they made the drug degrade faster, especially β-CD increased the degradation rate constants significantly. The slight increase in the final pH values of drug solutions suggested that the degradation products at this condition did not affect the pH of drug solutions.

Ranitidine HCl degradation in pH 3 phosphate buffer solutions: The greatest correlation coefficient values were obtained from 1/(ranitidine HCl concentration remaining) versus time plots at this pH; therefore, the kinetics of ranitidine HCl degradation was said to be apparent second-order. The rate limiting step should be the interaction between a proton-induced degradation involving the nitro group and double bond shift intermediate (Figure 8) and nitroso form of the free base of the compound (2), or between this intermediate and the drug. The reaction between this intermediate and water should not be the rate limiting step since the amount of water was excess and the kinetics would, therefore, reduce to pseudo-first order. In addition, if the attack of H^+ was the rate limiting step, then the kinetics should be reduced to pseudo-first order since the solution pH was fixed. Bar charts of degradation rate constants of ranitidine HCl in pH 3 phosphate buffer at various buffer concentrations are shown in Figure 46. The inclusion of ranitidine HCl in CDs' cavities resulted in decreases in the degradation rate constants of ranitidine HCl. At low buffer concentrations, 2HP-β-CD could stabilize the drug. However, it did not affect the degradation rate significantly at the buffer concentration of 0.20 M. Plots of k_{obs} versus total buffer concentrations are presented in Figure 47. The slopes of these plots, which were k_{buffer}, were 0.0132, 0.0117, and 0.0179 for ranitidine HCl (R), R:β-CD, and R:2HP-β-CD complexes, respectively. In a solution of phosphate buffer having a pH of 3, which is between its pK_1 (2.12) and pK_2 (7.21) (Martin, 1993), $[H_2PO_4^-]$ was dominant and its fraction was 0.89 - 0.94 when the drug solutions were initially prepared. Then k_{buffer} was dominated by k_{H2PO4^-} and they were all positive values. These suggested that $H_2PO_4^-$ was a catalytic species which corresponded with that reported by Kanokwan Thiengthawat (1994). Since all k_{buffer} values were comparable, both CDs should not affect the rate acceleration by $H_2PO_4^-$.

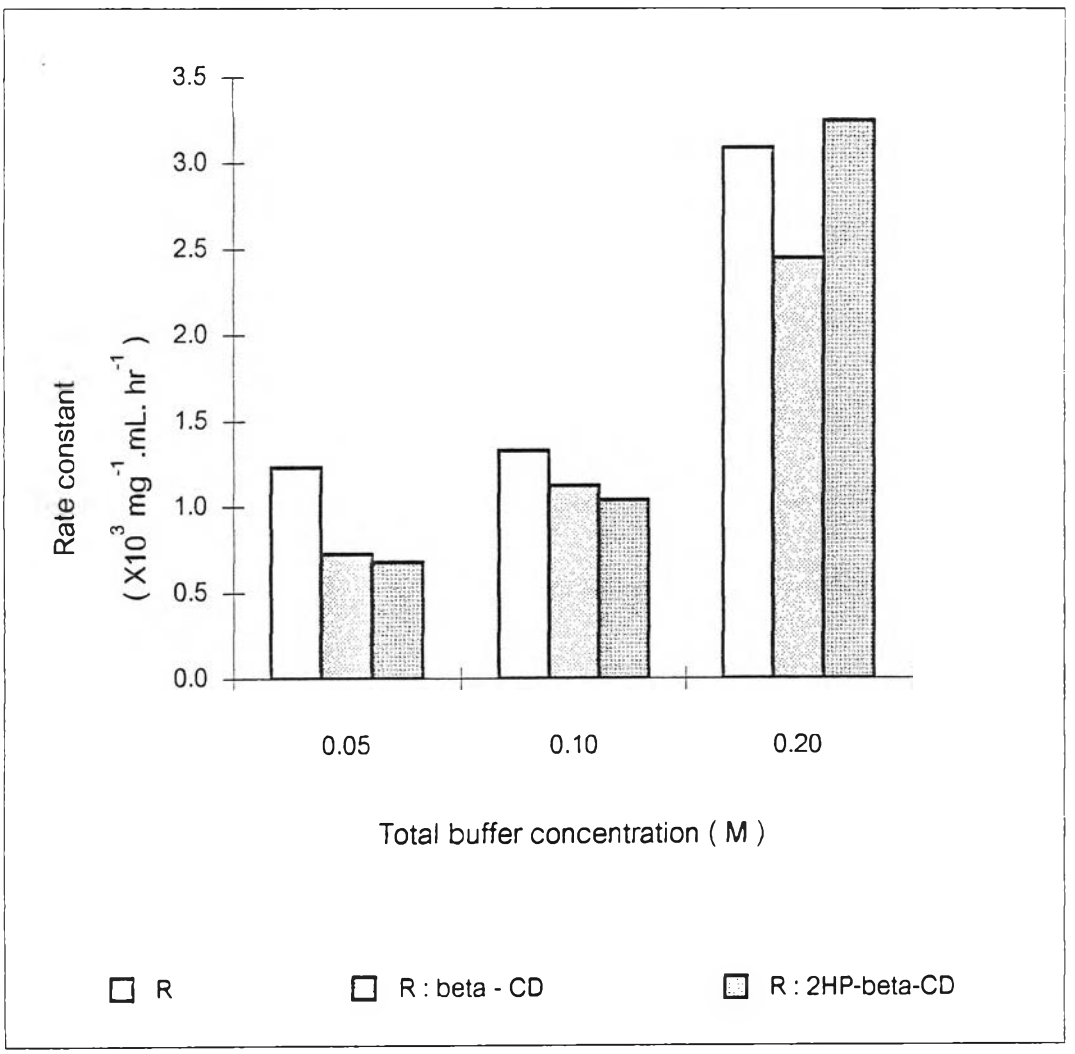

0.05 M ;	R	>	R : β - CD	≈	R : 2HP-β-CD	at	$\alpha = 0.05$
0.10 M ;	R	>	R : β - CD	>	R : 2HP-β-CD	at	$\alpha = 0.05$
0.20 M ;	R	≈	R : 2HP-β-CD	>	R : β - CD	at	$\alpha = 0.05$

Figure 46. Bar charts presenting the apparent second order rate constants at pH 3.

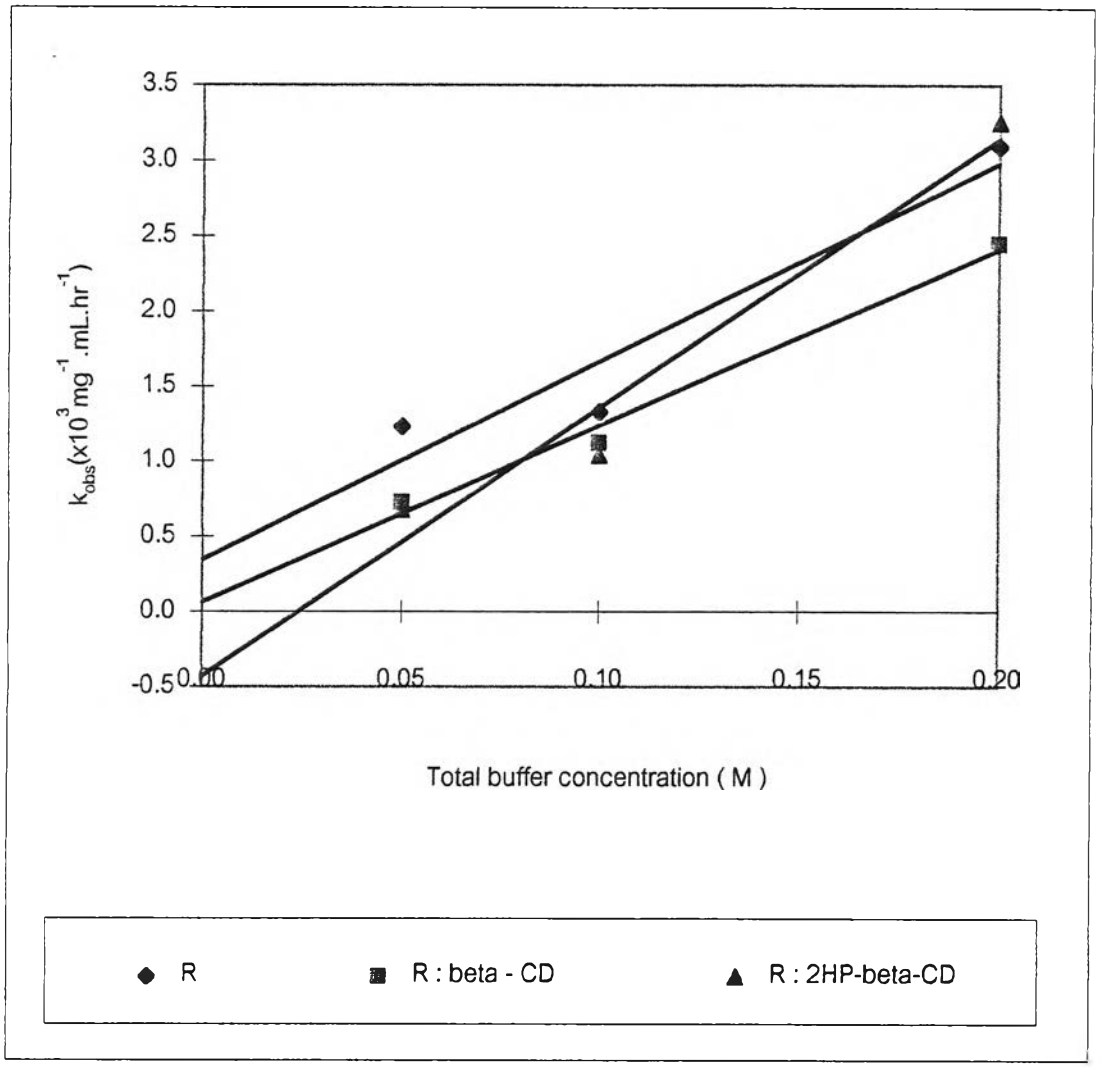

R ; $Y = 3.48 \times 10^{-4} + 0.0132\ X$, $r = 0.9592$, $SE = 3.48 \times 10^{-4}$

R : β - CD ; $Y = 6.38 \times 10^{-5} + 0.0117\ X$, $r = 0.9939$, $SE = 1.41 \times 10^{-4}$

R : 2HP-β-CD; $Y = -4.30 \times 10^{-4} + 0.0179\ X$, $r = 0.9792$, $SE = 4.00 \times 10^{-4}$

Figure 47. Second-order plots of ranitidine HCl degradation in pH 3 solutions.

The intercepts of the k_{obs} versus total buffer concentration plots, which were the rate constants at zero buffer concentration, were 3.48 $x10^{-4}$, 6.38 $x10^{-5}$, and -4.30 $x10^{-4}$ mg^{-1}. $mL.hr^{-1}$ for R, R:β-CD, and R:2HP-β-CD complexes, respectively. Since the values of the rate constants at zero buffer ccncentration were nearly zero, $k_o + k_{H^+}[H^+] + k_{OH^-}[OH^-]$ were negligible, especially $k_{H^+}[H^+]$ which was dominant at this pH. This confirmed that the rate limiting step of reaction at this pH did not involve H^+. The only significant increases in the final pH values of drug solutions at this pH (see Tables 14-16) suggested that OH^- might be one of the degradation products; this supported the reaction between a proton-induced degradation involving the nitro group and double bond shift intermediate and nitroso form of the free base of the compound (2), or between this intermediate and water, or between this intermediate and the drug since the reactions yielded OH^- as a product.

Ranitidine HCl degradation in pH 5 acetate buffer solutions: Results at this pH were similar to those at pH 3. The kinetics of ranitidine HCl degradation at pH 5 was also apparent second-order. Bar charts of degradation rate constants of ranitidine HCl in pH 5 acetate buffer at various buffer concentrations are shown in Figure 48. The rank order of k_{obs} in all total buffer concentrations were R > R:β-CD > R: 2HP-β-CD. Steric hindrances of CDs, especially 2HP-β-CD, should hinder the degradation rate acceleration. Plots of k_{obs} versus total buffer concentrations are presented in Figure 49. The slopes of these plots, which were k_{buffer}, were 7.52 x 10^{-4}, 5.50 x 10^{-4}, and 5.90 x 10^{-4} for ranitidine HCl (R), R:β-CD, and R:2HP-β-CD complexes, respectively. Due to the ionization constant of acetic acid. pK_a = 4.76 (Martin, 1993), CH_3COO^- was the dominant species (fraction of CH_3COO^- = 0.67 - 0.70) when the drug solutions were initially prepared. However, k_{buffer} in this case could be either $k_{CH3COOH}$ or $k_{CH3COO-}$, and their values were negligible. Therefore, both CH_3COOH and CH_3COO^- should not act as general acid and base catalyses. The intercepts of the k_{obs} versus total buffer concentration plots, which were the rate constants at zero buffer concentration, were 9.30 x 10^{-4}, 7.73 x 10^{-4}, and 5.29 x 10^{-4} $mg^{-1}.mL.hr^{-1}$ for R, R:β-CD, and R:2HP-β-CD

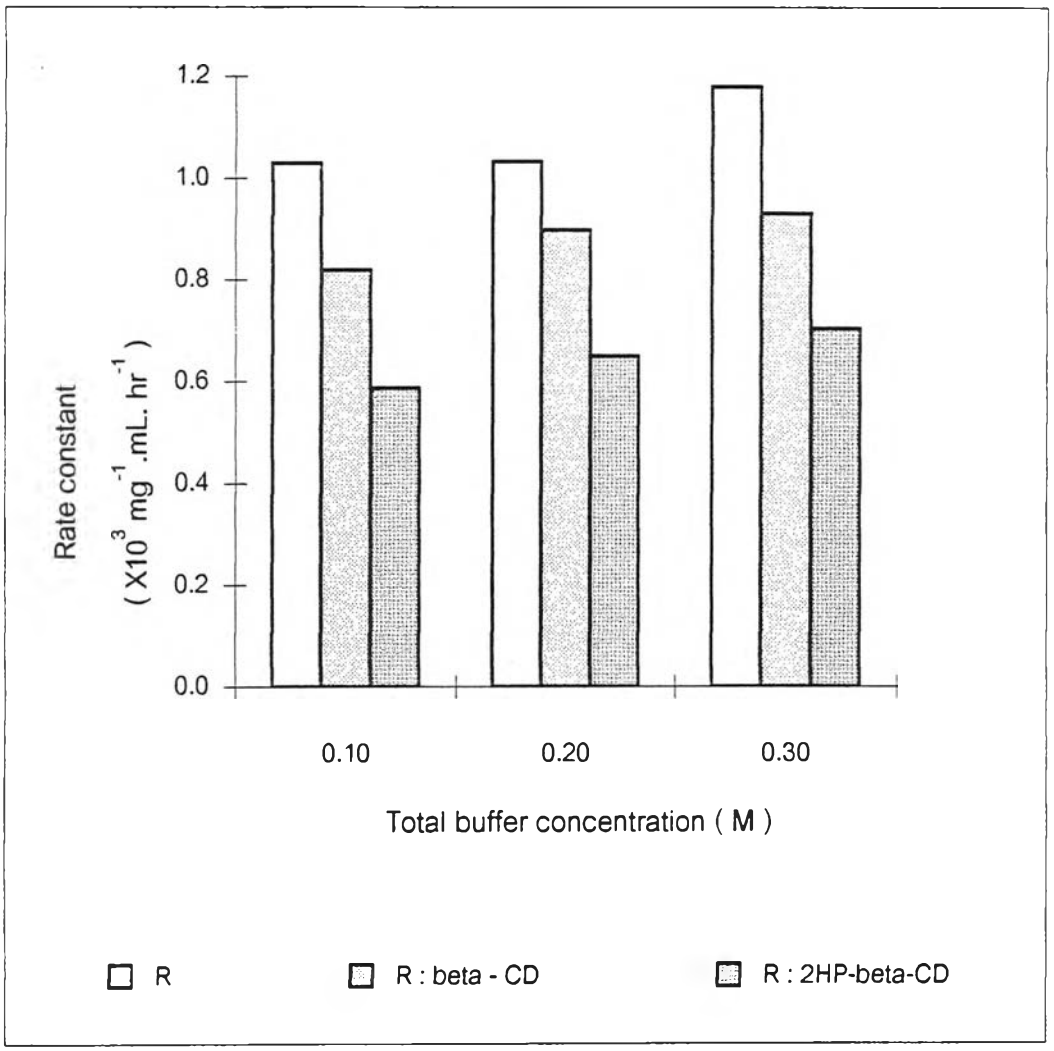

0.10 M ;	R	>	R : β - CD	>	R : 2HP-β-CD	at $\alpha = 0.05$
0.20 M ;	R	>	R : β - CD	>	R : 2HP-β-CD	at $\alpha = 0.05$
0.30 M ;	R	>	R : β - CD	>	R : 2HP-β-CD	at $\alpha = 0.05$

Figure 48. Bar charts presenting the apparent second order rate constants at pH 5.

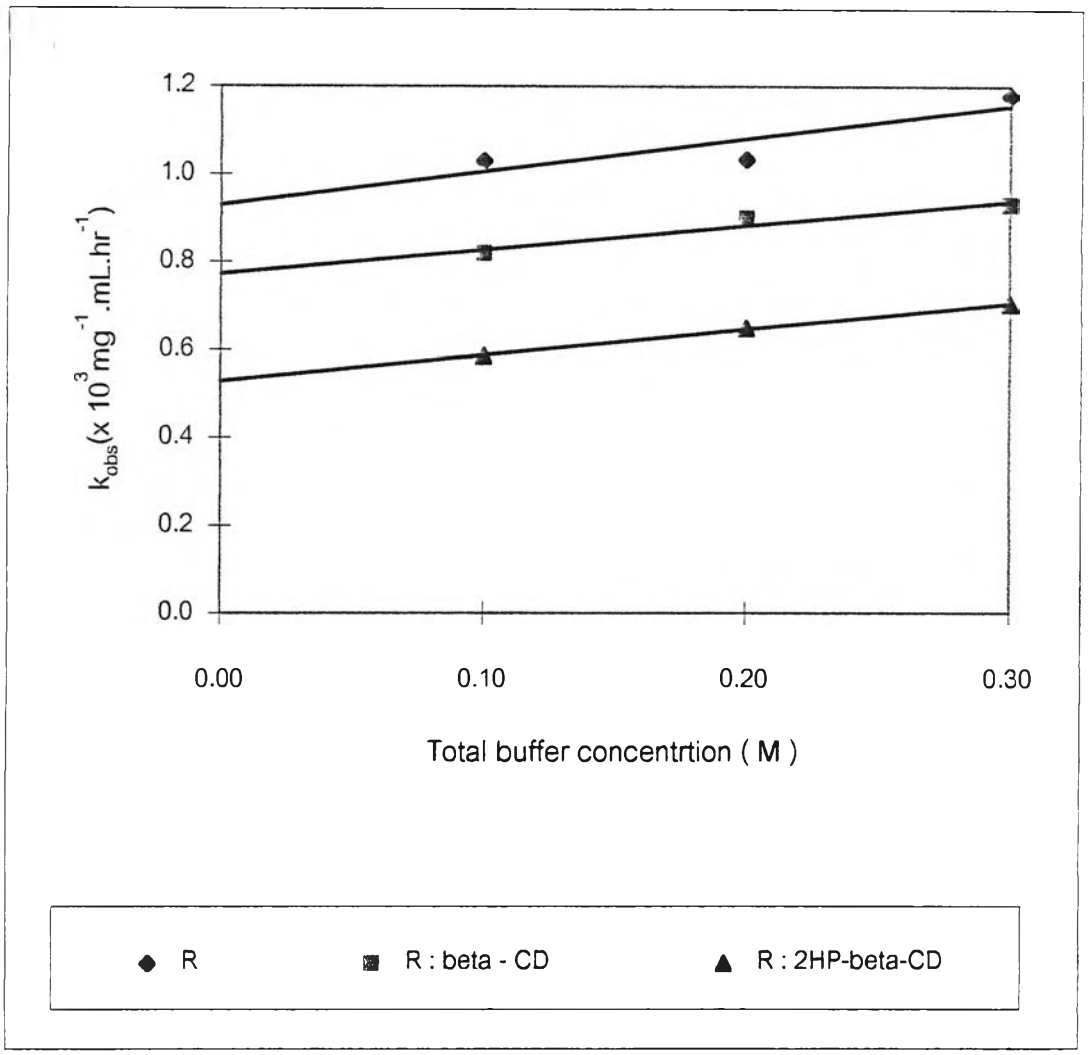

R ; $Y = 9.30 \times 10^{-4} + 7.52 \times 10^{-4} X$, $r = 0.8760$, $SE = 5.85 \times 10^{-5}$

R : β - CD ; $Y = 7.73 \times 10^{-4} + 5.50 \times 10^{-4} X$, $r = 0.9696$, $SE = 1.96 \times 10^{-5}$

R : 2HP-β-CD; $Y = 5.29 \times 10^{-4} + 5.90 \times 10^{-4} X$, $r = 0.9992$, $SE = 3.41 \times 10^{-6}$

Figure 49. Second-order plots of ranitidine HCl degradation in pH 5 solutions.

complexes, respectively. These negligible rate constant values informed the absence of specific acid/base catalyses. This also confirmed the absence of general acid/base catalyses. Since the proposed mechanism at this pH was similar to that occurred at pH 3, the small increases in the final pH values of drug solutions suggested the small amount of degradation products of which OH^- was the one.

Ranitidine HCl degradation in pH 7 phosphate buffer solutions: Since the greatest correlation coefficient values were obtained from ln(ranitidine HCl concentration remaining) versus time plots, the kinetics of ranitidine HCl degradation at pH 7 was proposed to be first-order. It was reported previously that the mechanism at neutral pH values can be those occur both in the acidic and basic pH values with those in the basic side being dominant. Figure 10 shows the hydrolysis mechanism at pH > 9 proposed by Haywood (1987). In this mechanism, both OH^- and H_2O can act as catalyses. Either OH^- or H_2O could involve in the rate limiting step and thus yield the pseudo-first order kinetics since OH^- could be held constant and H_2O was in excess amount. Bar charts of degradation rate constants of ranitidine HCl in pH 7 phosphate buffer at various buffer concentrations are shown in Figure 50. Both CDs increased the rate constants indifferently from the statistical stand point. The increases in rates were statistically significant at buffer concentrations of 0.05 and 0.10 M. Plots of k_{obs} versus total buffer concentrations are presented in Figure 51. The slopes of plots, which were k_{buffer}, were 1.40×10^{-3}, 7.95×10^{-4}, and 7.88×10^{-4} for ranitidine HCl (R), R:β-CD, and R:2HP-β-CD complexes, respectively. In a solution of phosphate buffer having the pH of 7, which is between its pK_1 (2.12) and pK_2 (7.21) (Martin, 1993), $[H_2PO_4^-]$ was dominant, fraction of $H_2PO_4^-$ = 0.58 - 0.74 when the drug solutions were initially prepared. Then k_{buffer} should be the summation of k_{H2PO4^-} and $k_{HPO4^{2-}}$. Since the slope values were nearly zero, both $H_2PO_4^-$ and HPO_4^{2-} should not act as general acid and base catalyses. The intercepts of the k_{obs} versus total buffer concentration plots, which were the rate constants at zero buffer concentration, were 9.47×10^{-4}, 1.09×10^{-3}, and

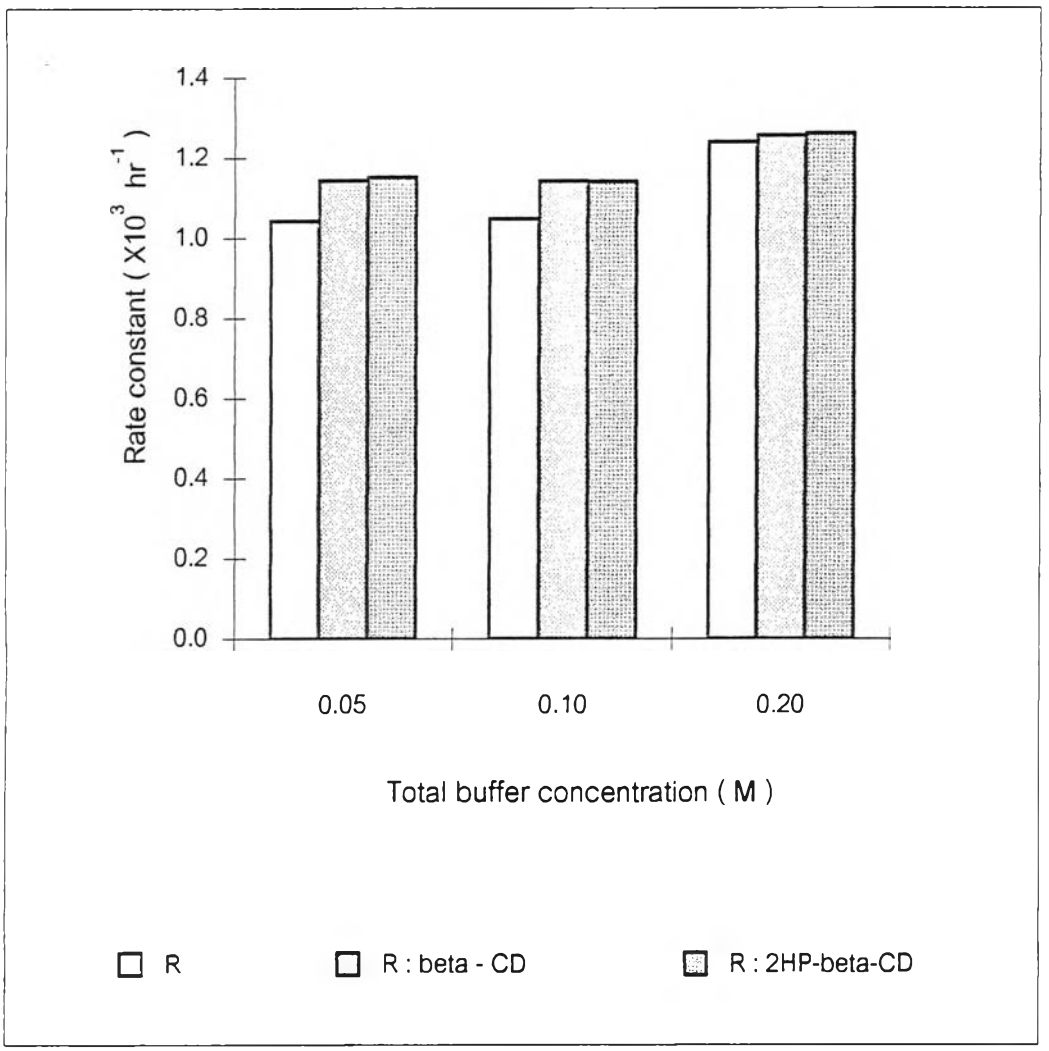

0.05 M ; R : β - CD ≈ R : 2HP-β-CD > R at $\alpha = 0.05$

0.10 M ; R : β - CD ≈ R : 2HP-b-CD > R at $\alpha = 0.05$

0.20 M ; R ≈ R : β - CD ≈ R : 2HP-β-CD at $\alpha = 0.05$

Figure 50. Bar charts presenting the apparent first order rate constants at pH 7.

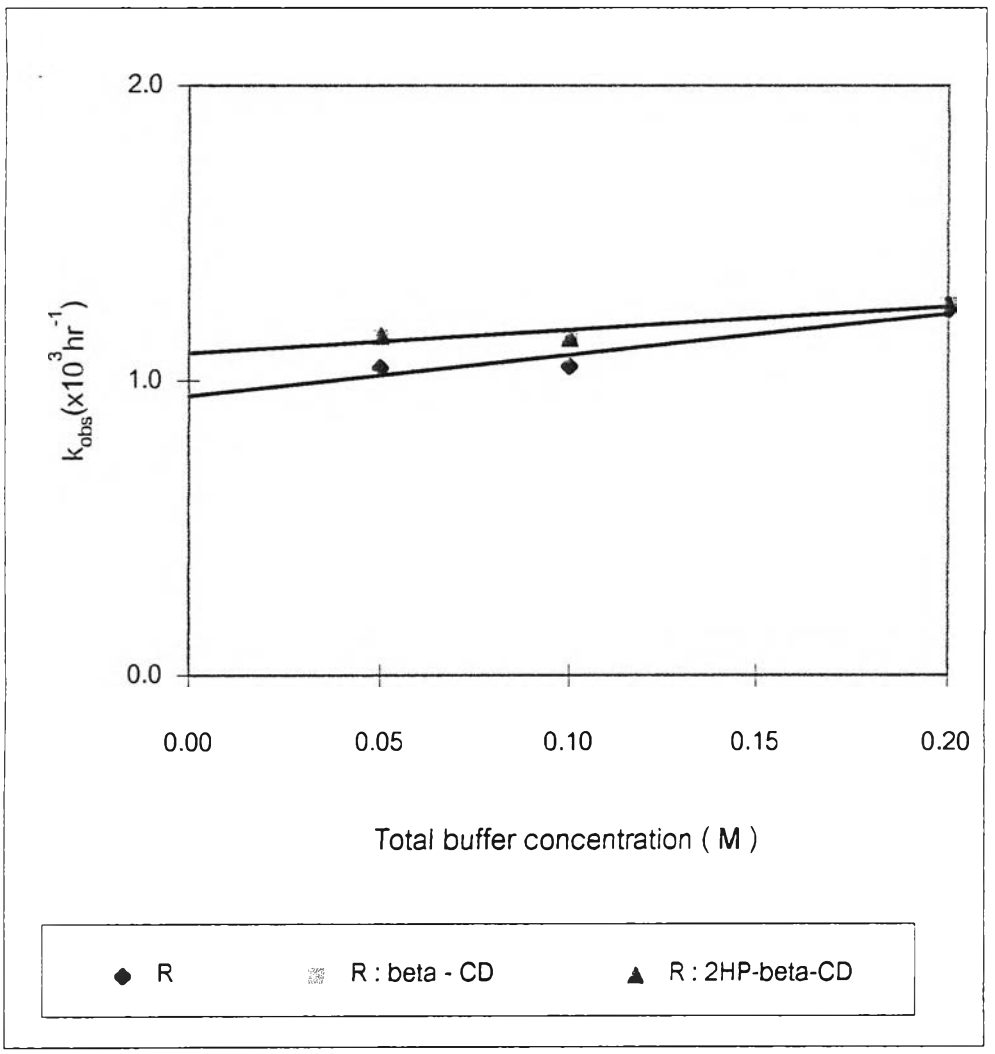

R ; $Y = 9.47x10^{-4} + 1.40x10^{-3} X$, $r = 0.9525$, $SE = 4.83x10^{-5}$

R : β - CD ; $Y = 1.09x10^{-3} + 7.95x10^{-4} X$, $r = 0.9416$, $SE = 3.07x10^{-5}$

R : 2HP-β-CD; $Y = 1.09x10^{-3} + 7.88x10^{-4} X$, $r = 0.9166$, $SE = 3.71x10^{-5}$

Figure 51. First-order plots of ranitidine HCl degradation in pH 7 solutions.

1.09×10^{-3} hr^{-1} for R, R:β-CD, and R:2HP-β-CD complexes, respectively. These values were nearly zero suggesting the solvent catalysis.

Ranitidine HCl degradation in pH 9 glycine-NaOH buffer solutions: Since the plots of ln(ranitidine HCl concentration remaining) versus time gave the greatest correlation coefficient values, the kinetics of ranitidine HCl degradation at pH 9 was concluded to be first-order. As it was presented previously, either OH^- or H_2O could be catalytic species at the rate limiting step. Bar charts of degradation rate constants of ranitidine HCl in pH 9 glycine-NaOH buffer at various buffer concentrations are shown in Figure 52. The inclusion of ranitidine HCl in CDs' cavities resulted in decreases of the degradation rate constant values of ranitidine HCl. 2HP-β-CD stabilized the drug more than β-CD did. Plots of k_{obs} versus total buffer concentrations are presented in Figure 53. The slopes of these plots, which were k_{buffer}, were 5.71×10^{-3}, 2.41×10^{-3}, and 2.10×10^{-3} for ranitidine HCl (R), R:β-CD, and R:2HP-β-CD complexes, respectively. In a solution of glycine-NaOH buffer having the pH of 9, which is between its pK_1 (2.35) and pK_2 (9.78) (Martin, 1993), the zwitter ion [$^+NH_3CH_2COO^-$] was dominant, fraction of $^+NH_3CH_2COO^-$ = 0.91 - 0.99 when the drug solutions were initially prepared. Therefore, $k_{^+NH3CH2COO^-}$ was dominant, although k_{buffer} was the summation of $k_{^+NH3CH2COO^-}$ and $k_{NH2CH2COO^-}$. Since the slope values were small, the general acid/base catalyses were also small. The rank order of the k_{buffer} were R > R:β-CD > R: 2HP-β-CD. Thus, CDs, especially 2HP-β-CD, retarded the catalytic effect of buffer. The intercepts of the k_{obs} versus total buffer concentration plots, which were the rate constants at zero buffer concentration, were 9.88×10^{-4}, 1.19×10^{-3}, and 1.15×10^{-3} hr^{-1} for R, R:β-CD, and R:2HP-β-CD complexes, respectively. These rate constant values were nearly zero suggesting the solvent catalysis.

Ranitidine HCl degradation in pH 11 glycine-NaOH buffer solutions: Results at this pH were similar to those at pH 9. Since the greatest correlation coefficient values were obtained from ln(ranitidine HCl concentration remaining) versus time plots, the

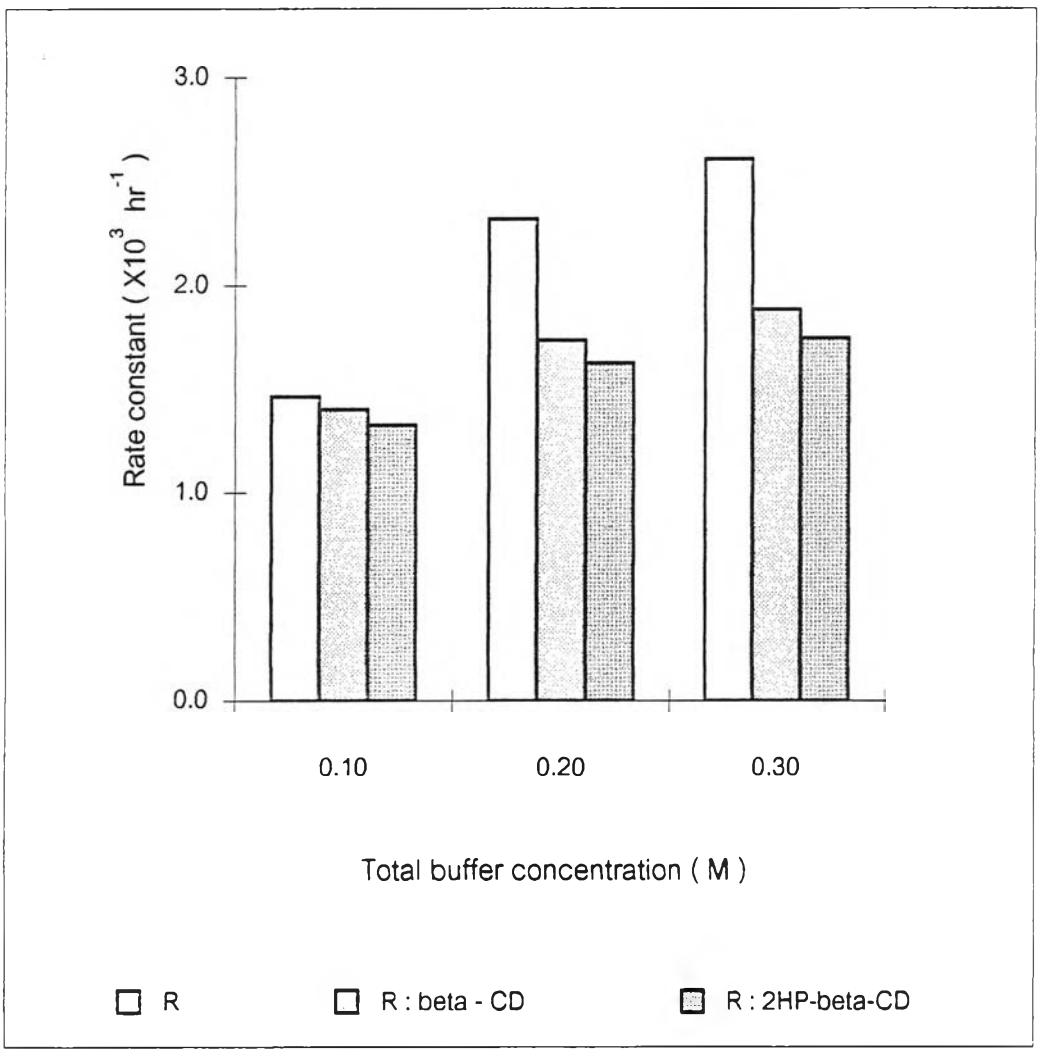

0.10 M ;	R	≈	R : β - CD	>	R : 2HP-β-CD	at α = 0.05
0.20 M ;	R	>	R : β - CD	>	R : 2HP-β-CD	at α = 0.05
0.30 M ;	R	>	R : β - CD	>	R : 2HP-β-CD	at α = 0.05

Figure 52. Bar charts presenting the apparent first order rate constants at pH 9.

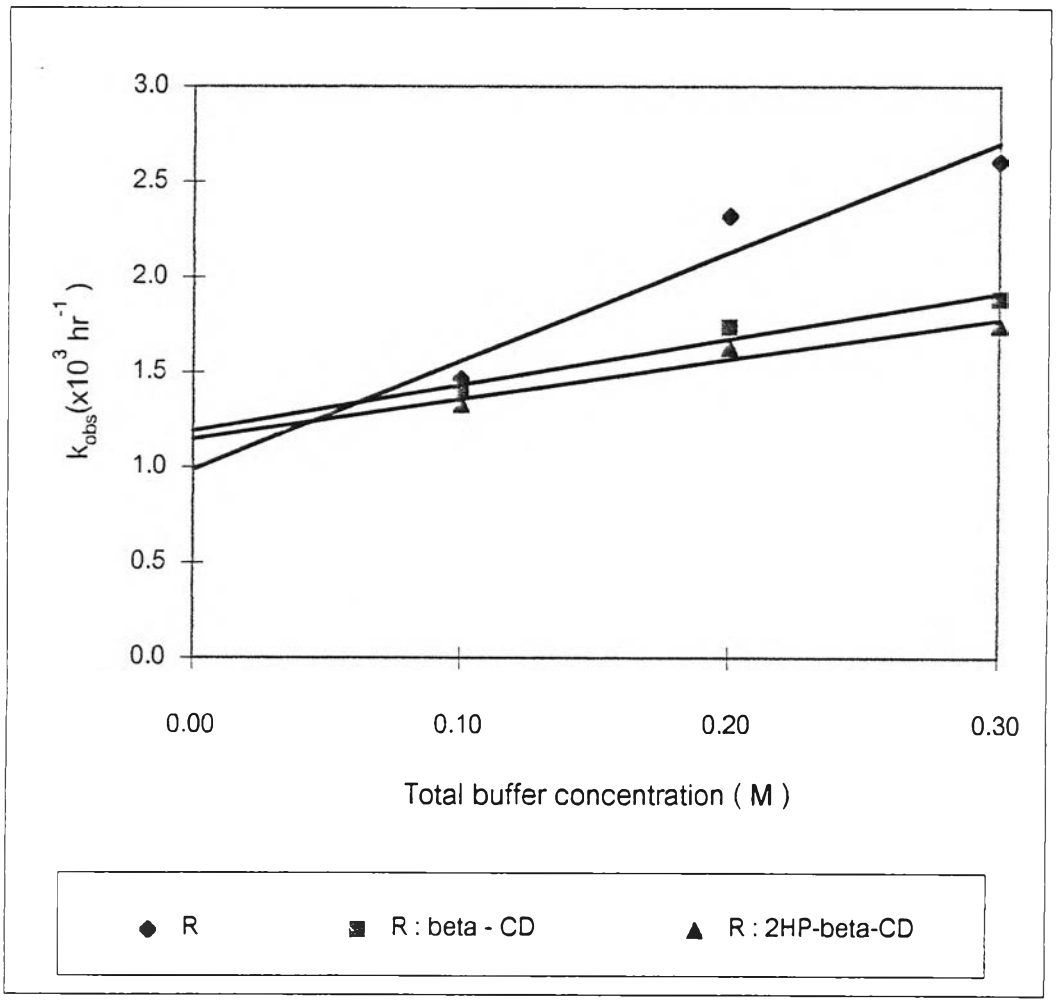

R ; $Y = 9.88x10^{-4} + 5.71x10^{-3} X$, $r = 0.9612$, $SE = 2.32x10^{-4}$

R : β - CD ; $Y = 1.19x10^{-3} + 2.41x10^{-3} X$, $r = 0.9762$, $SE = 7.58x10^{-5}$

R : 2HP-β-CD; $Y = 1.15x10^{-3} + 2.10x10^{-3} X$, $r = 0.9709$, $SE = 7.31x10^{-5}$

Figure 53. First-order plots of ranitidine HCl degradation in pH 9 solutions.

kinetics of ranitidine HCl degradation at pH 11 was proposed to be first-order. Bar charts of degradation rate constants of ranitidine HCl in pH 11 glycine-NaOH buffer at various buffer concentrations are shown in Figure 54. The rank order of k_{obs} in all buffer concentrations were R > R:β-CD > R: 2HP-β-CD. The inclusion of ranitidine HCl in CDs' cavities resulted in decreases of the degradation rate constant values, especially in the case of 2HP-β-CD. Plots of k_{obs} versus total buffer concentrations are presented in Figure 55. The slopes of these plots, which were k_{buffer}, were 0.0312, 0.0311, and 0.0241 for ranitidine HCl (R), R:β-CD, and R:2HP-β-CD complexes, respectively. In a solution of glycine-NaOH buffer having the pH of 11, which is over its pK_2 (9.78) value (Martin, 1993), [$NH_2CH_2COO^-$] was dominant and the fraction of $NH_2CH_2COO^-$ was 0.70 - 0.89 when the drug solutions were initially prepared. Therefore k_{buffer} at this pH was dominated by $k_{NH2CH2COO^-}$. The significant amount of k_{buffer} values suggested that $NH_2CH_2COO^-$ could act as a general base. At pH 9; the fraction of $NH_2CH_2COO^-$ was relatively small, and therefore the $k_{NH2CH2COO^-}$ values were small. The rank order of the k_{buffer} were R ≈ R:β-CD > R: 2HP-β-CD. 2HP-β-CD had more steric effect than β-CD did. The intercepts of the k_{obs} versus total buffer concentration plots, were -7.08×10^{-4}, -1.02×10^{-3}, and -5.93×10^{-4} hr^{-1} for R, R:β-CD, and R:2HP-β-CD complexes, respectively. These rate constant values were negative values and nearly zero suggesting the solvent catalysis as well.

Ranitidine HCl degradation in pH 13 phosphate buffers: The plots of ln (ranitidine HCl concentration remaining) versus time yielding the greatest correlation coefficient values suggested the apparent first-order kinetics. Bar charts of degradation rate constants of ranitidine HCl in pH 13 phosphate buffer at various buffer concentrations are shown in Figure 56. The inclusion of ranitidine HCl in CDs' cavities also resulted in decreases of the degradation rate constant values. Plots of k_{obs} versus total buffer concentrations are presented in Figure 57. The slopes of these plots were -0.4404, 0.8222, and 0.0879 for ranitidine HCl (R), R:β-CD, and R:2HP-β-CD complexes, respectively. In a solution of phosphate buffer having the pH of 13, which

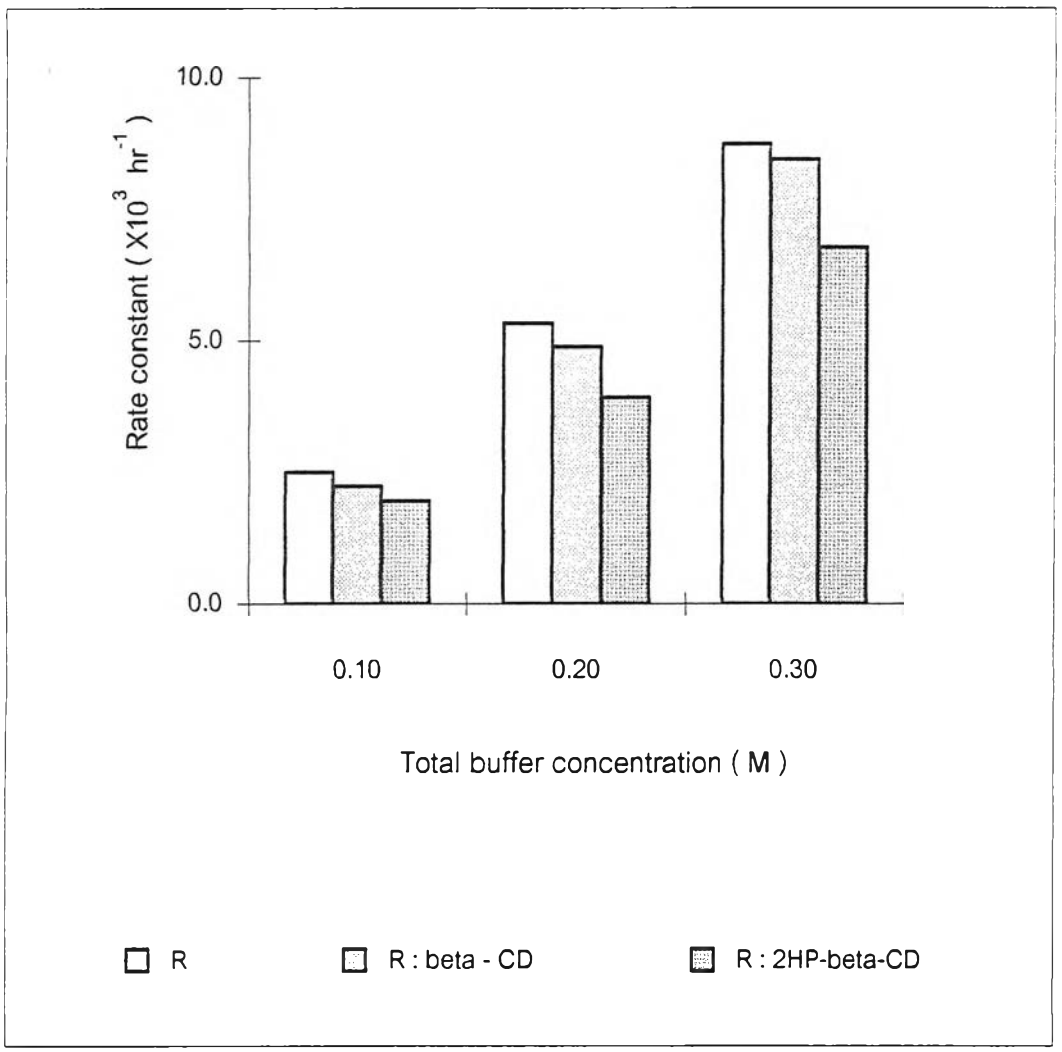

0.10 M ;	R	>	R : β - CD	>	R : 2HP-β-CD	at $\alpha = 0.05$
0.20 M ;	R	>	R : β - CD	>	R : 2HP-β-CD	at $\alpha = 0.05$
0.30 M ;	R	≈	R : β - CD	>	R : 2HP-β-CD	at $\alpha = 0.05$

Figure 54. Bar charts presenting the apparent first order rate constants at pH 11.

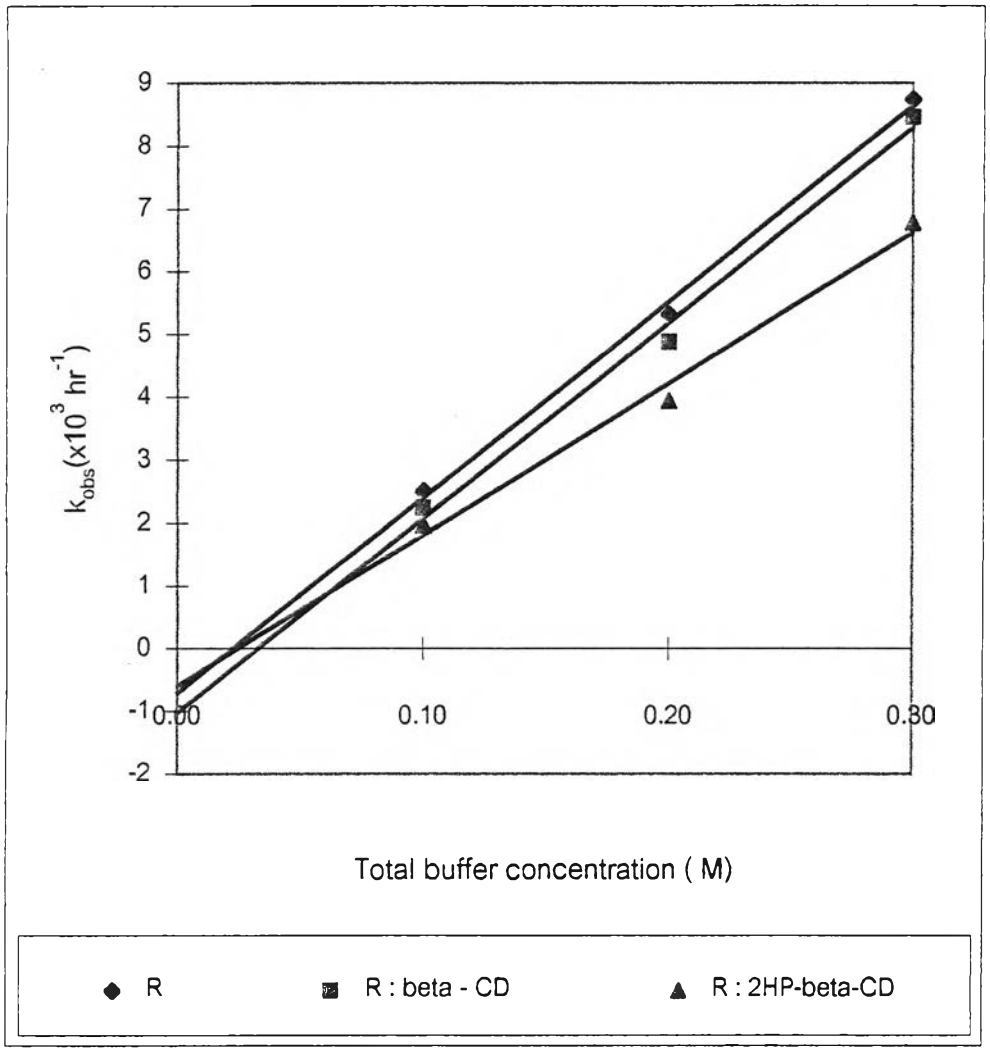

R ; $Y = -7.08x10^{-4} + 0.0312\ X$, $r = 0.9984$, $SE = 2.46x10^{-4}$

R : β - CD ; $Y = -1.02x10^{-3} + 0.0311\ X$, $r = 0.9962$, $SE = 3.82x10^{-4}$

R : 2HP-β-CD; $Y = -5.93x10^{-4} + 0.0241\ X$, $r = 0.9946$, $SE = 3.55x10^{-4}$

Figure 55. First-order plots of ranitidine HCl degradation in pH 11 solutions.

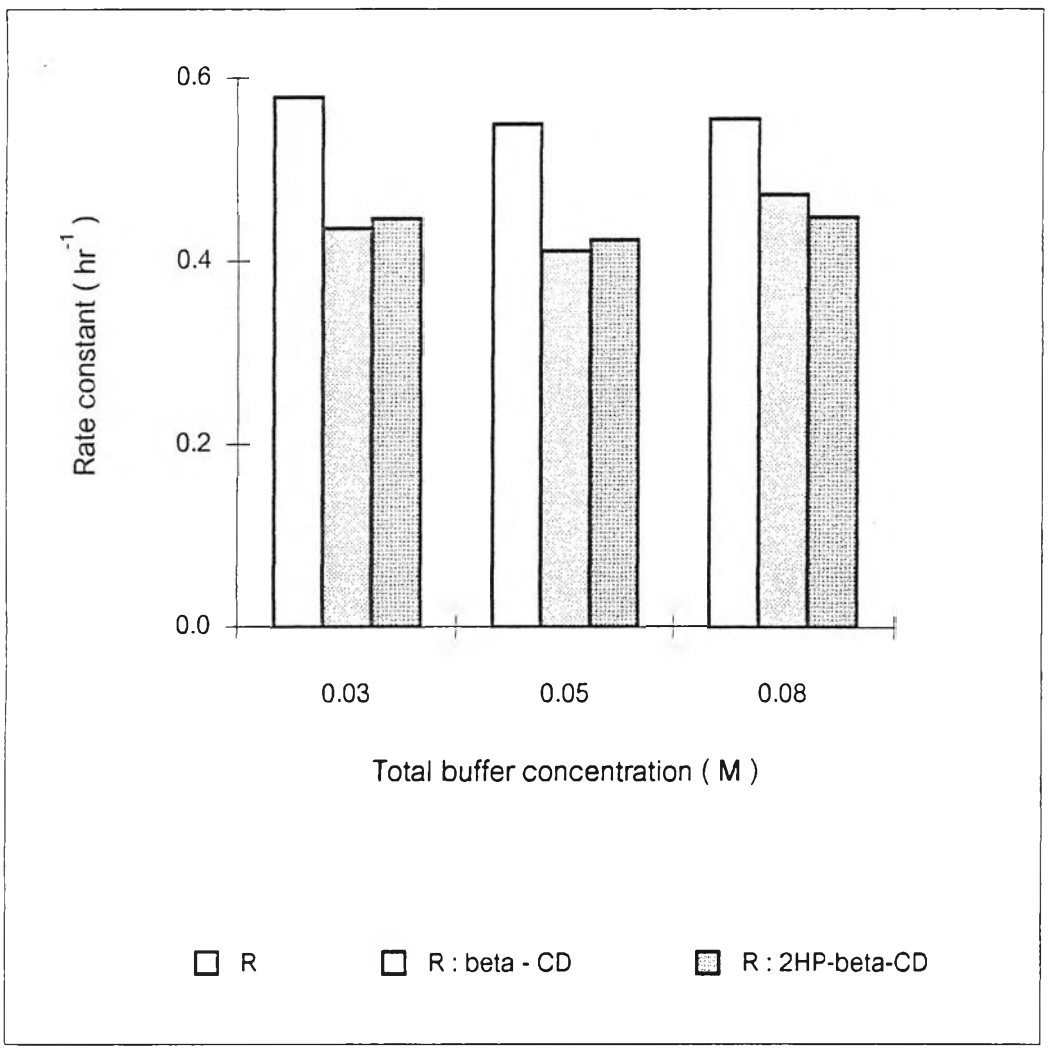

0.03 M ;	R	>	R : β - CD	≈	R : 2HP-β-CD	at $\alpha = 0.05$
0.05 M ;	R	>	R : β - CD	≈	R : 2HP-β-CD	at $\alpha = 0.05$
0.08 M ;	R	>	R : β - CD	>	R : 2HP-β-CD	at $\alpha = 0.05$

Figure 56. Bar charts presenting the apparent first order rate constants at pH 13.

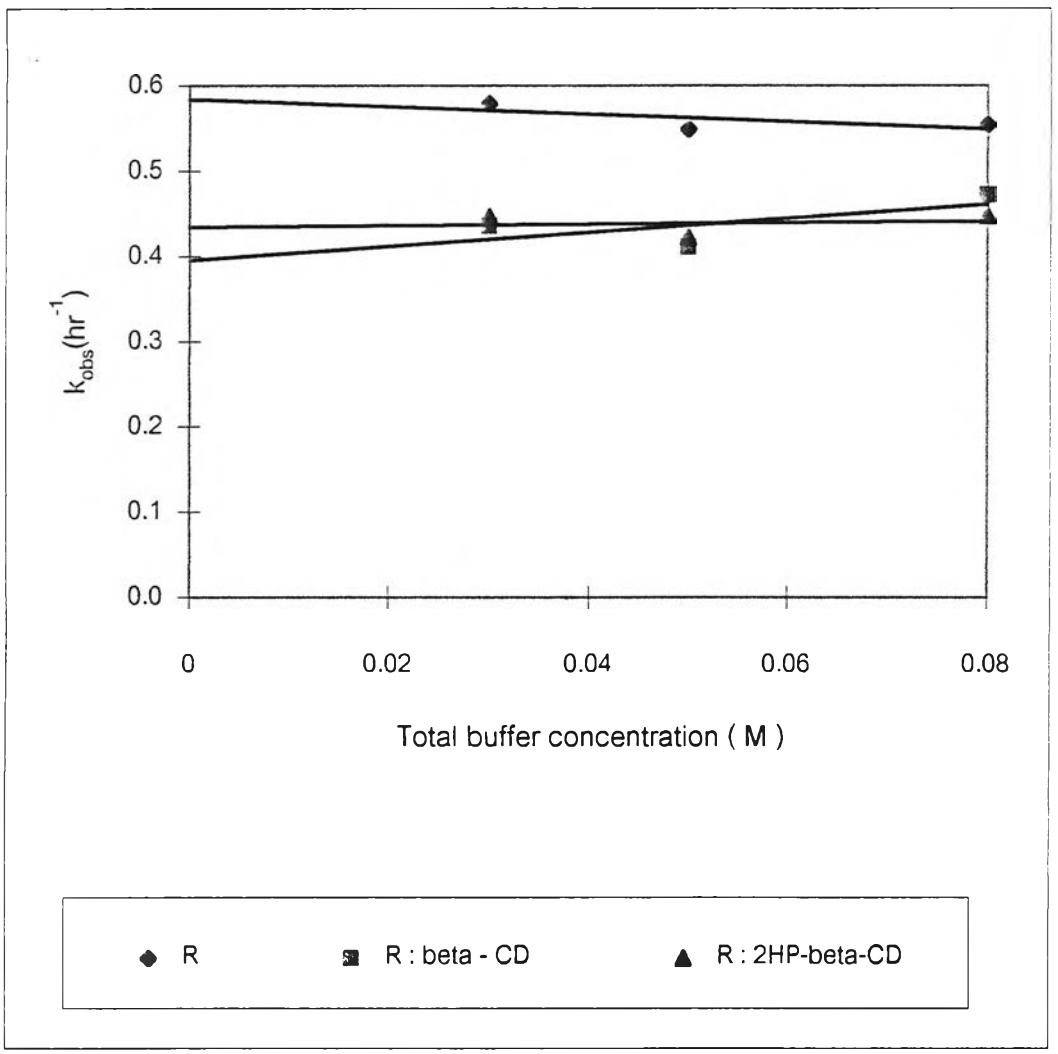

R	;	Y = 0.5841 - 0.4404 X,	r = -0.6962,	SE = 0.0162
R : β - CD	;	Y = 0.3955 + 0.8222 X,	r = 0.6755,	SE = 0.0319
R : 2HP-β-CD;		Y = 0.4341 + 0.0879 X,	r = 0.1554,	SE = 0.0199

Figure 57. First-order plots of ranitidine HCl degradation in pH 13 solutions.

is over its pK_3 (12.67) (Martin, 1993), $[PO_4^{3-}]$ should be dominant, but almost all drug solutions prepared had the pH values of less than 12.67 and, therefore, almost all the fraction of PO_4^{3-} were less than 0.50. The k_{buffer} values was the summation of $k_{HPO4^{2-}}$ and $k_{PO4^{3-}}$. The rank order of the k_{buffer} were R:β-CD > R: 2HP-β-CD > R, and therefore the buffer catalysis on ranitidine HCl was more dominant in the inclusion complexes, especially in R:β-CD. The intercepts of the k_{obs} versus total buffer concentration plots, were 0.5841, 0.3955, and 0.4341 hr^{-1} for R, R:β-CD, and R:2HP-β-CD complexes, respectively. These significant values suggested the catalysis by OH^-. Unlike the general base catalysis, the catalysis by OH^- were retarded by the CDs, especially β-CD.

When a guest is complexed with a CD, a portion of the guest is inside of the CD and not available to come into contact with other molecules because of the finite space in the cavity. Portions of the guest which project out of the cavity are available for reaction with other molecules. Because of the hydroxyl groups or other groups which might be substituted onto the hydroxyl groups of the CD molecule, some steric hindrances can occur to prevent reactions from occurring readily. The interaction of the active groups of the guest molecule with the hydroxyl groups of the CD or other groups substituted on the hydroxyl groups can also have an effect on the reactivity of the guest molecule. Depending upon the group on the guest molecule, this can result in catalysis of the reaction or prevention of chemical reactions. For labile guests, accelerated stability tests can be done on the complexes to determine if decomposition of the guest is prevented or is within the expected range for a complex (Hedges, 1998).

Through experimental observations, CDs could accelerate or retard the degradation rate of ranitidine HCl. However, they did not alter the reaction rate in some instances. The stabilizing effect might be attributed to the engulf of the preferred moieties of ranitidine HCl molecule into the CDs' cavities and thus protecting the active part of drug molecule from the catalytic environment. Cholerton et al. (1984) reported the ionization constants (pK_a) of ranitidine HCl to be 2.3 and 8.2. The pK_a at 2.3 is

reported to be C-protonation at dialkylaminonitroethene moiety as showed in Figure 6. The other pK_a at 8.2 refers to the protonation at the dimethylamino moiety. Hohnjec et al. (1986) reported only one ionization constant (pK_a) at 2.19. Teraoka et al. (1993) also reported only one pK_a value at 8.38. Therefore, in the pH range studied, ranitidine HCl could be in the forms RH_2^{2+}, RH^+, and R at pH < pK_1, pK_1 < pH < pK_2, and pH > pK_2, respectively. These observations were also corresponded with the report of Dumanovic et al. (1997) who also reported the forms of ranitidine as RH_2^{2+}, RH^+, R and ROH^- at optimal acidities of Hammett acidity function (H_o) = -1.0 to pH = 0.0, pH = 4.0 to 6.0, pH = 10.3 to 11.5, and J_ function = 15.2 to 15.4, respectively.

At pH < pK_1, ranitidine HCl was fully protonated. Therefore, both ends of ranitidine HCl with cationic nature were not likely to enter the CDs' cavities. Nagai et al. (1984) proposed that β-CD is in the molecular form at pH 1. However, Szejtli (1988) reported that the α-1,4 glycosidic bonds of CDs are fairly stable in alkaline solutions, while they are hydrolytically cleaved by strong acids to give a series of linear maltosaccharides. Miyazawa et al. (1995) reported the apparent acid-catalyzed hydrolysis rate constant of β-CD in 1N HCl at 60°C as 0.13 hr^{-1}. This might result in the unprotecting effect of CDs at the very low pH value (pH 1), but result in the protecting effect at the higher pH solutions.

At pK_1 < pH < pK_2, ranitidine HCl was unprotonated at dialkylaminonitroethene moiety. The dialkylaminonitroethene end, therefore, preferred to enter the CDs' cavities to the dimethylamino moiety. Consequently, the reacting carbon at dialkylaminonitroethene moiety was shielded and less drug degradation rates of the inclusion complexes were observed. Only free drug could undergo degradation. However, small increases in rate constants of drug degradation of R : CDs were still unexplainable.

At pH > pK_2, both ends of ranitidine HCl were unprotonated and could enter the CD' cavities. Therefore, the degradation rates of drug in the presence of CDs were decreased, especially at higher concentrations of buffer.

5. Effect of Relative Humidities on the Chemical Stability of Inclusion Complexes of Ranitidine HCl : Cyclodextrin (β-CD, 2HP-β-CD)

The stability of drugs in solid state is also important since solid dosage forms are more commonly used than other dosage forms. The most general type of interaction in the solid state is actually between water and drug. The effect of moisture on solid state stability is, in its simplest form, visualized by moisture being sorbed on the drug particles. In this sense, the sorbed water would behave like a solution, a bulk layer, and it is assumed to be saturated with drug. Additionally, solid can occur either in a crystalline form or as an amorphous form. The chemical stability of the solid crystalline form will differ from the same entity in the amorphous form. In most cases the crystalline form, under the same conditions, will be more stable than the comparable amorphous (metastable) form, but there are some limitations (Carstensen, 1995).

Hygroscopicity is the potential for moisture uptake that a solid will exert in combination with the rate which this will happen. Hygroscopicity is an important characteristic of a powder. It can be shown for a fairly soluble compound that the hygroscopicity is related to the heat of solution and its solubility. A hygroscopicity experiment is carried out easily by exposing the drug substance to an atmosphere of a known relative humidity, e.g., storing it over saturated salt solutions in desiccators. Each salt solution gives a certain relative humidity (RH). The powder is then weighed from time to time and the amount of moisture (weight gained) is determined. Since the relative humidity is dependent on the number of dissolved species, it is essential that the saturation be attained prior to beginning of experimentation (Kontny and Zografi, 1995; Carstensen, 1995). The actual relative humidities obtained from various saturated

salt solutions in desiccators at 37°C are presented in Table 24. The actual relative humidities obtained were not close to the theoretical values. One reason was the loss of equilibrium when the desiccators were opened for measuring of the RH values; the digital hygrometer used needed time to reach a constant RH value for each run. Therefore, due to the experimental error, the relative humidities of the systems having lower RH values than the ambient atmosphere tended to be greater than their theoretical values, while the relative humidity of the system having a higher RH value than the ambient atmosphere tended to be less than the expected value.

Table 24. Actual relative humidities obtained from various saturated salt solutions in desiccators at 37°C.

Saturated salt solutions	%RH at 37°C (theory)	%RH at 37°C (actual)
Potassium carbonate (K_2CO_3)	41	59.26
Magnesium nitrate (MgN_2O_6)	51	64.18
Sodium nitrite ($NaNO_2$)	62	72.70
Sodium chloride (NaCl)	75	76.35
Potassium nitrate (KNO_3)	91	88.34

Figure 58. illustrates important steps of the uptake of water vapor by crystalline water soluble solid. At low relative humidities in the atmosphere (RH_l), water is adsorbed onto the particle surface (Figure 58 A). As the relative humidity is increased (Figure 58 B), a tendency of multilayer sorption is expected. At a certain relative humidity characteristic for a given substance, the solid begins to dissolve into the sorbed film of water. A saturated solution of solute exists, and this will cause the vapor pressure over the sorbed film of water to be depressed relative to pure water and to be constant and equal to that above a saturated solution for the substance. This vapor

pressure may be expressed as the critical relative humidity (CRH) and the reaction mechanism may change at this point. If the relative humidity in the atmosphere is greater than the CRH, water will spontaneously condense on the aqueous film (Figure 58 C). This will dilute the film and allow more solid to dissolve, which in turn, will maintain the pressure gradient. The process of water vapor uptake will continue until all the solid has dissolved and further solution dilution has occurred. Only when the relative humidity above the solution is elevated to that of the atmosphere will this process terminate. Percentages of weight gained and drug remaining of ranitidine HCl, selected R:β-CD, and selected R:2HP-β-CD powder after they had been stored for 14 days in various relative humidities at 37°C are shown in Table 25. Ranitidine HCl is a water soluble crystalline solid capable of moisture sorption. At the relative humidity below 65%, its appearance did not change and its potency did not drop significantly because the small amount of water adsorbed on its particle surface. At 73% RH, the powder color changed from white to red-brown and its potency was reduced

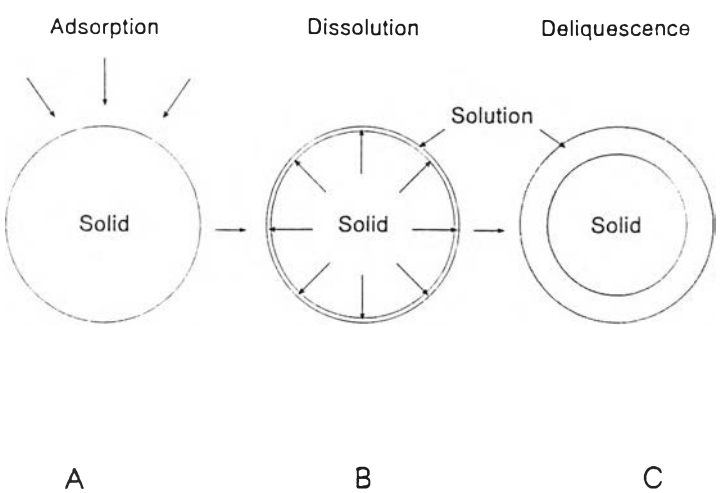

Figure 58. Water vapor adsorption of a water soluble solid. [atmospheric relative humidity, RH_i < CRH, (A); RH_i = CRH, (B); and RH_i > CRH, (C)].

Table 25. Stability data of ranitidine HCl, R:β-CD, and R:2HP-β-CD upon 14-day storage in various humidities at 37°C.

%RH	Formula	% Weight gained (SD)	%Drug remaining (SD)	Descriptions
59.26	R	0.05 ($2x10^{-4}$)	100.73 (0.64)	white powder
	R:β-CD	0.39 ($2x10^{-4}$)	106.74 (0.27)	white fluffy powder
	R:2HP-β-CD	0.42 ($8x10^{-5}$)	107.19 (0.27)	white powder
64.18	R	0.04 ($6x10^{-5}$)	98.12 (1.52)	white powder
	R:β-CD	0.49 ($4x10^{-4}$)	108.93 (0.27)	white powder
	R:2HP-β-CD	0.57 ($4x10^{-4}$)	110.58 (0.14)	pale yellow powder
72.70	R	0.35 ($2x10^{-4}$)	89.42 (1.30)	red-brown powder
	R:β-CD	0.92 ($2x10^{-4}$)	46.94 (0.15)	red-brown powder
	R:2HP-β-CD	0.89 ($3x10^{-4}$)	97.99 (0.19)	clear-brown, a sheet of hard solid
76.35	R	2.97 ($1x10^{-1}$)	78.56 (0.64)	clear-brown, sticky liquid
	R:β-CD	1.11 ($3x10^{-4}$)	83.42 (0.04)	red-brown, tight mass
	R:2HP-β-CD	1.46 ($2x10^{-4}$)	105.56 (0.17)	clear-brown, sticky liquid
88.34	R	6.20 ($6x10^{-4}$)	62.83 (0.54)	clear-brown, sticky liquid
	R:β-CD	6.20 ($6x10^{-4}$)	74.72 (0.22)	red-brown, tight mass
	R:2HP-β-CD	3.28 ($2x10^{-4}$)	83.45 (0.06)	clear-brown, sticky liquid

significantly. While at 76%RH, it became the clear-brown, sticky liquid informing that ranitidine HCl powder dissolved completely in the sorbed water. Therefore, its practical CRH in this study should be around 73 -76%RH. Teraoka et al. (1993) reported the CRH of bulk ranitidine HCl powder of about 67%RH and it is unstable mostly around this relative humidity. In this study, more water was absorbed at %RH above the CRH for further dilution of this sticky liquid and the drug potency also further reduced. In conclusion, ranitidine HCl was stable below the CRH, whereas it was less stable due to more water sorption above the CRH.

Drug-CD complexation can be regarded as molecular encapsulation, i.e., encapsulation of the drug at the molecular level. The CD molecule shields, at least partly, the drug molecule from attacks by various reactive molecules. That is, the CD can insulate a labile compound from a potentially corrosive environment and, in this way, reduce or even prevent drug hydrolysis, oxidation, racemization, and other forms of isomerization of drugs. CDs (β-CD, 2HP-β-CD) reduced the crystallinity of ranitidine HCl in the freeze-dried inclusion complexes, especially the amorphous R:2HP-β-CD. The amount of moisture sorbed by amorphous solids is typically much greater than that sorbed by nonhydrating crystalline substances below their CRH (Kontny and Zografi, 1995). This was in good agreement with more % weight gained by amorphous R:2HP-β-CD than by partially crystalline R:β-CD observed at %RH below CRH. The color of R:2HP-β-CD powder changed from white to pale yellow but its potency was not lost. At 73%RH, the color of R:β-CD powder changed from white to red-brown and the complex lost about 50% of its potency while R:2HP-β-CD complex dissolved completely in its small amount of sorbed water and became a sheet of hard solid, but its potency reduced slightly. At 88 %RH which was above the CRH, R:β-CD complex was still in the solid form though its % weight gained was relatively high and the magnitude of potency loss was less than that at 73%RH. However, R:2HP-β-CD complex became a sticky liquid, and the least amount of sorbed water and potency loss were observed. These two CDs showed different effects on the ranitidine HCl stability in various %RH's

because of their nature differences. β-CD has an ability to sorb moisture more than 2HP-β-CD does (Yoshida et al., 1988). Due to the less solubility of the parent β-CD, its inclusion complex also possessed less water solubility; the complex did not dissolve completely even when the amount of water sorbed was the greatest. Furthermore, it was unstable around the CRH. The inclusion complex of 2HP-β-CD, which is the highly water soluble derivative of β-CD, was completely soluble in the limited amount of sorbed water. However, 2HP-β-CD stabilized the drug in all % RH's studied which was not surprising since it could decrease the degradation of drug in solutions as discussed previously.

Degradation kinetics in the solid state are, in general, more complicated and progress more slowly than in the aqueous solution. In this study, the kinetic data could not be obtained properly because of too few data points.

6. HPLC Method Validation

The validation of an analytical method is the process by which performance characteristics of the method are established to meet the requirements for the intended analytical applications. The performance characteristics are expressed in terms of analytical parameters. For HPLC assay validation, these include specificity, precision, accuracy, and linearity.

6.1 Specificity

The specificity of an analytical method is its ability to measure the analyte accurately and specifically in the presence of expected components in the sample matrix.

6.1.1 In the Presence of CDs and Buffer Compositions

Peaks of all blank buffer solutions did not appear in the chromatograms (Figure 59). It might be due to the lack of absorption of all buffer compositions at this wavelength. Figure 60 shows typical chromatograms of ranitidine HCl standard solutions. Ranitidine HCl and procaine HCl were eluted at 5.00-6.00 min and 7.00-8.00 min, respectively. The resolution values, which were calculated from a mean of six replicated injections, of ranitidine HCl and its internal standard, procaine HCl, are presented in Table 26. All resolution values between ranitidine and procaine HCl peaks were more than 1.0. USP XXIII stated that two peaks are completely resoluted if their resolution values are more than 1.0. Therefore, these two peaks were completely separated from each other. Furthermore, the retention times of ranitidine HCl and procaine HCl peaks in the buffer solutions (Figure 61) did not change and were similar to the peaks that obtained from the R:CD inclusion complexes (Figures 62-63). These results suggested that CDs did not affect the peaks of ranitidine HCl in the inclusion complexes. Consequently, this method had high specificity for analysis of ranitidine HCl both in its free form and inclusion complexes with CDs. However, the retention times of these two peaks in the final phase of analysis were more closely than in the early runs; their resolution values were still more than 1.0.

6.1.2 In the Presence of Degradation Products of Ranitidine HCl

A stability indicating assay is an important methodology to ensure that the method used in the stability studies is capable of separating the parent drug from its degradation products. The chromatograms of decomposed buffer solutions showed no degradation peaks at the wavelength studied (Figure 64). The chromatograms of decomposed drug solutions in 0.30 M pH 1 phosphate buffer are presented in Figure 65. All chromatograms were similar; peaks of decomposition products were eluted before that of ranitidine HCl which obviously disappeared. The presence of CDs did not affect the chromatograms. In the case of decomposed drug solutions in 0.08 M pH 13

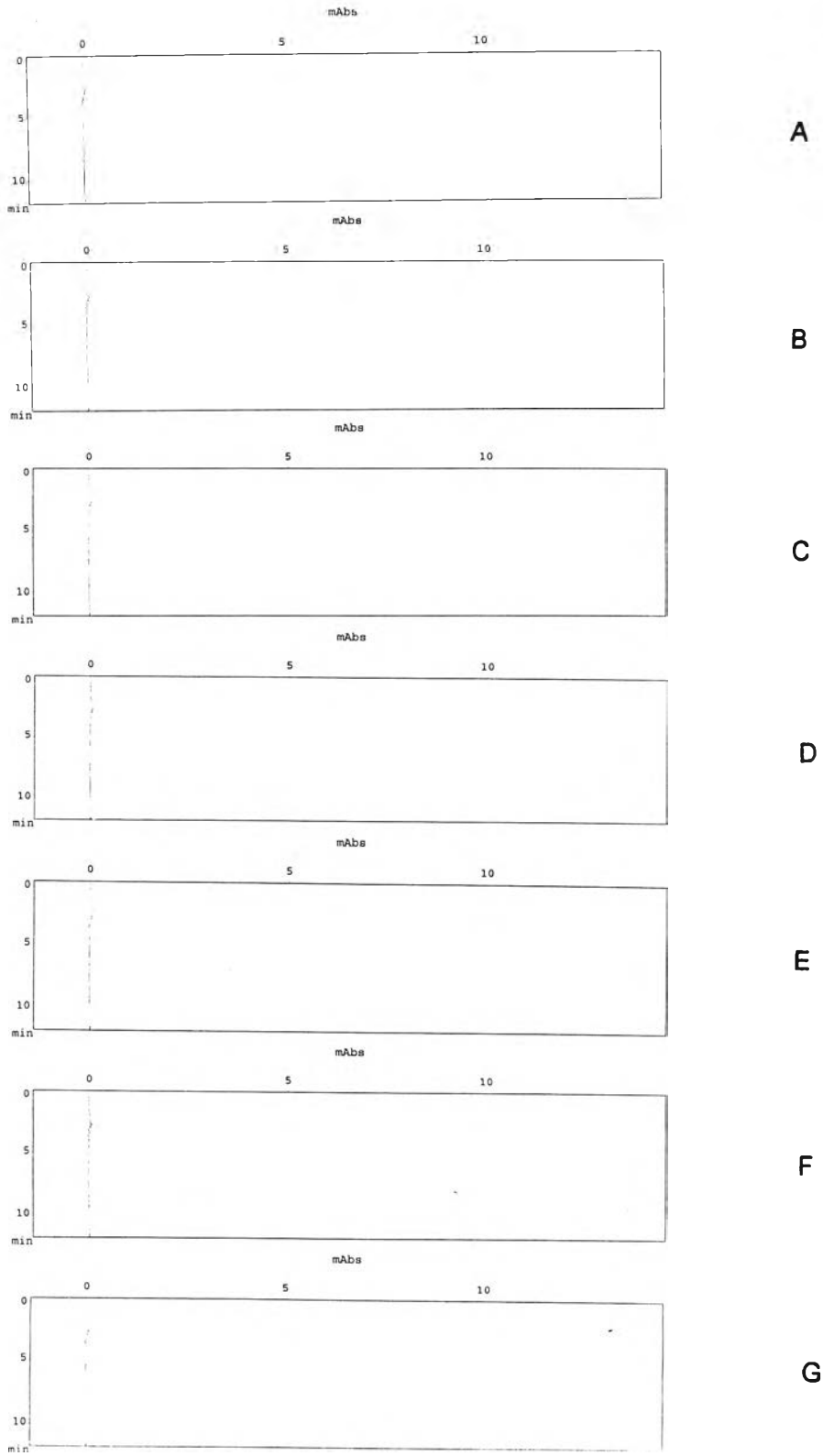

Figure 59. HPLC chromatograms of blank buffer solutions pH 1- 13. [0.30 M phosphate buffer pH 1, (A); 0.20 M phosphate buffer pH 3, (B); 0.30 M acetate buffer pH 5, (C); 0.20 M phosphate buffer pH 7, (D); 0.30 M glycine-NaOH buffer pH 9, (E); 0.30 M glycine-NaOH buffer pH11, (F); and 0.08 M phosphate buffer pH 13, (G)].

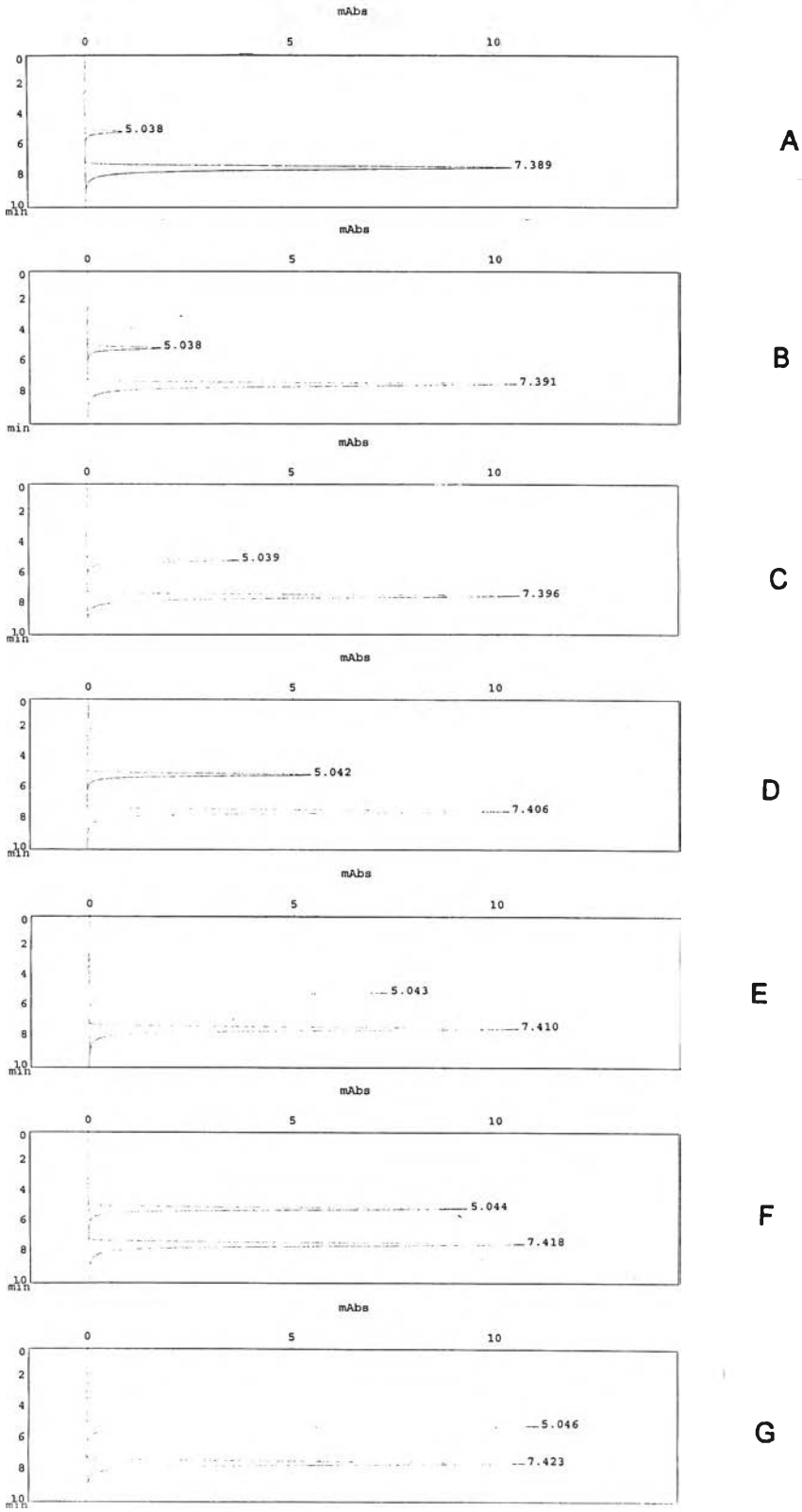

Figure 60. HPLC chromatograms of standard solutions of ranitidine HCl. [2.00 µg/mL, (A); 4.00 µg/mL, (B); 8.00 µg/mL, (C); 12.00 µg/mL, (D); 16.00 µg/mL, (E); 20.00 µg/mL, (F); and 24.00 µg/mL, (G); retention time of ranitidine HCl and procaine HCl are at 5.00-6.00 and 7.00-8.00 min, respectively].

Table 26. Resolution values of ranitidine HCl and procaine HCl peaks.

Ranitidine HCl concentrations (µg/mL)	Resolution values
2.00	4.45
4.00	4.40
8.00	4.48
12.00	4.44
16.00	4.52
20.00	4.36
24.00	4.40

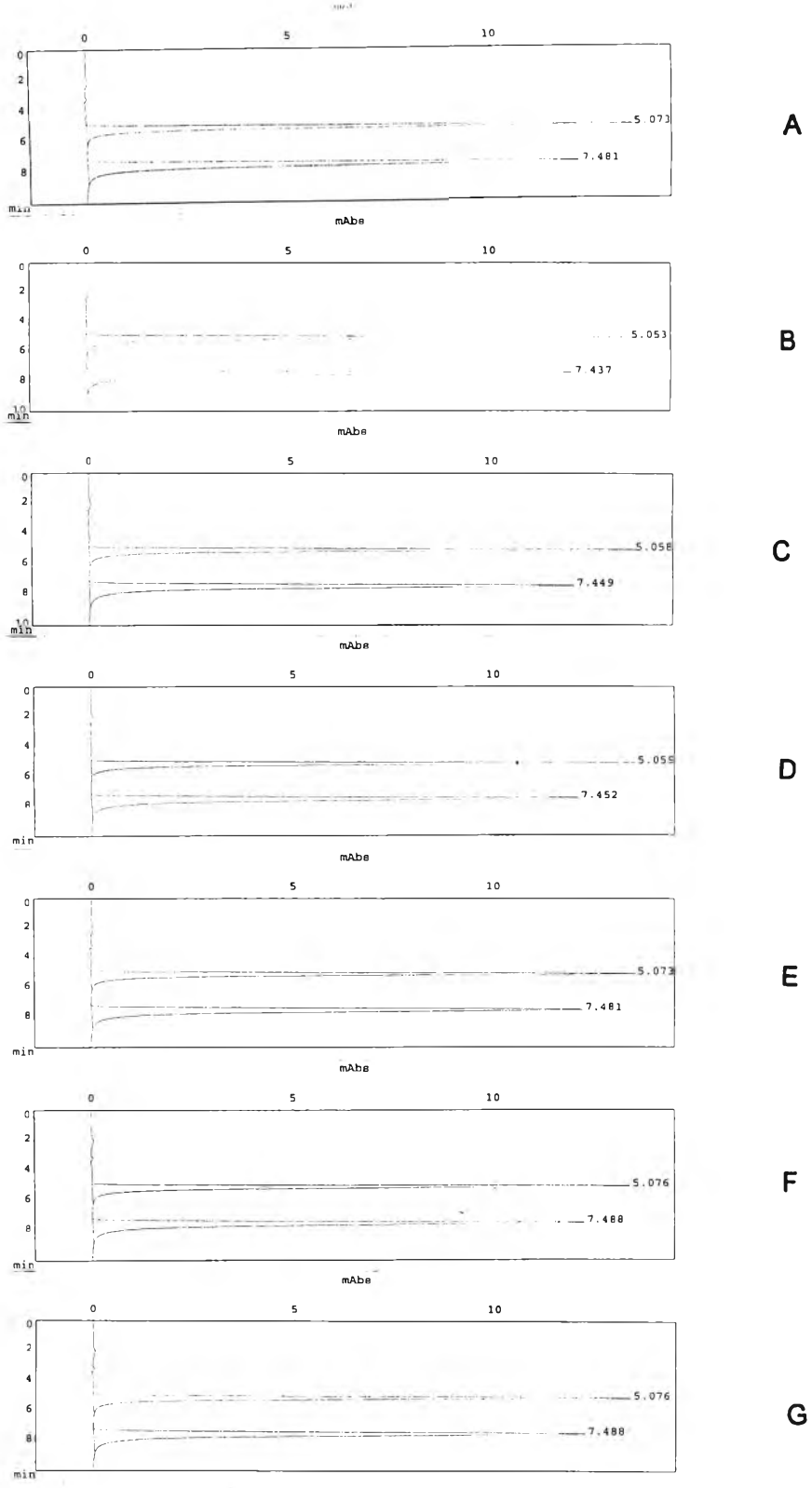

Figure 61. HPLC chromatograms of ranitidine HCl in buffer solutions pH 1-13. [0.30 M phosphate buffer pH 1, (A); 0.20 M phosphate buffer pH 3, (B); 0.30 M acetate buffer pH 5, (C); 0.20 M phosphate buffer pH 7, (D); 0.30 M glycine-NaOH buffer pH 9, (E); 0.30 M glycine-NaOH buffer pH11, (F); and 0.08 M phosphate buffer pH 13, (G)].

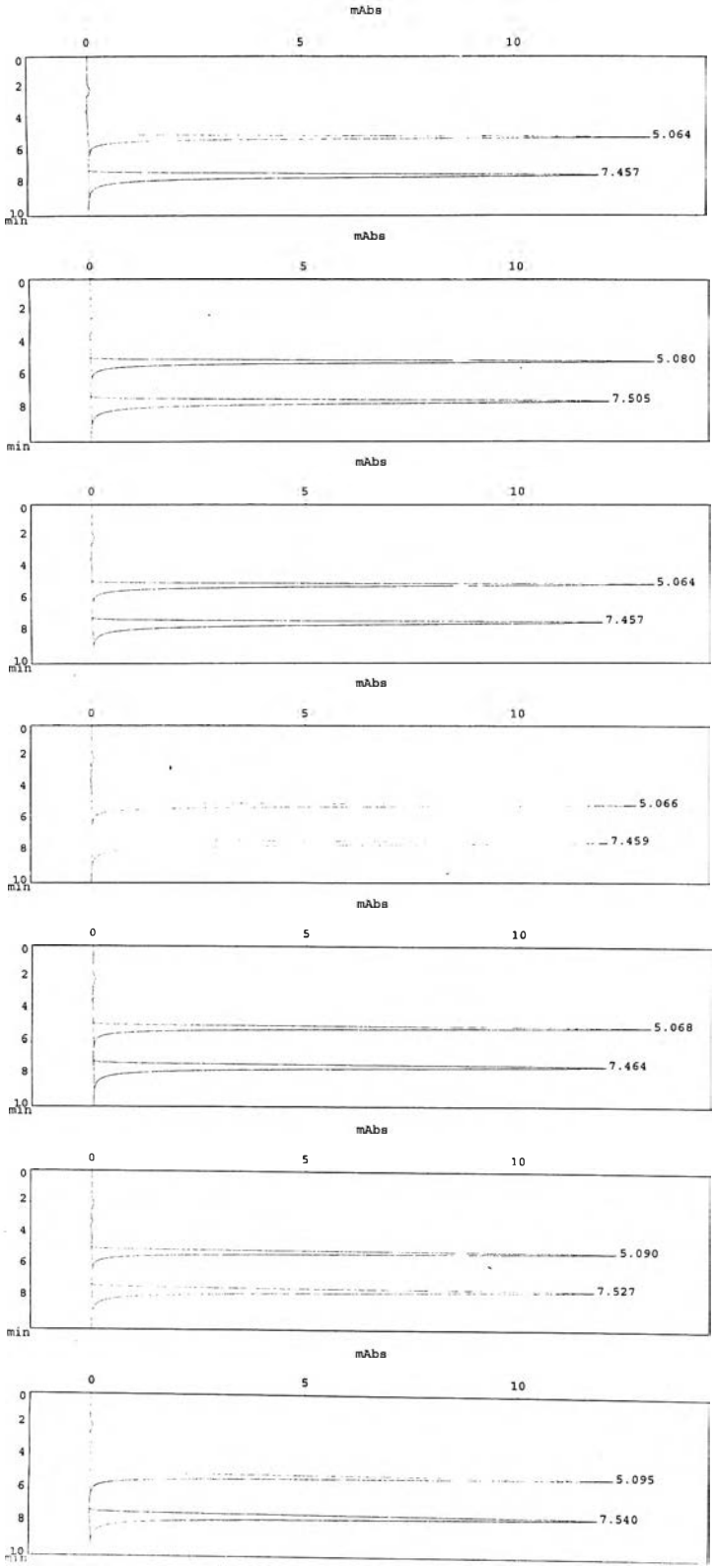

Figure 62. HPLC chromatograms of R:β-CD complex in buffer solutions pH 1-13. [0.30 M phosphate buffer pH 1, (A); 0.20 M phosphate buffer pH 3, (B); 0.30 M acetate buffer pH 5, (C); 0.20 M phosphate buffer pH 7, (D); 0.30 M glycine-NaOH buffer pH 9, (E); 0.30 M glycine-NaOH buffer pH11, (F); and 0.08 M phosphate buffer pH 13, (G)].

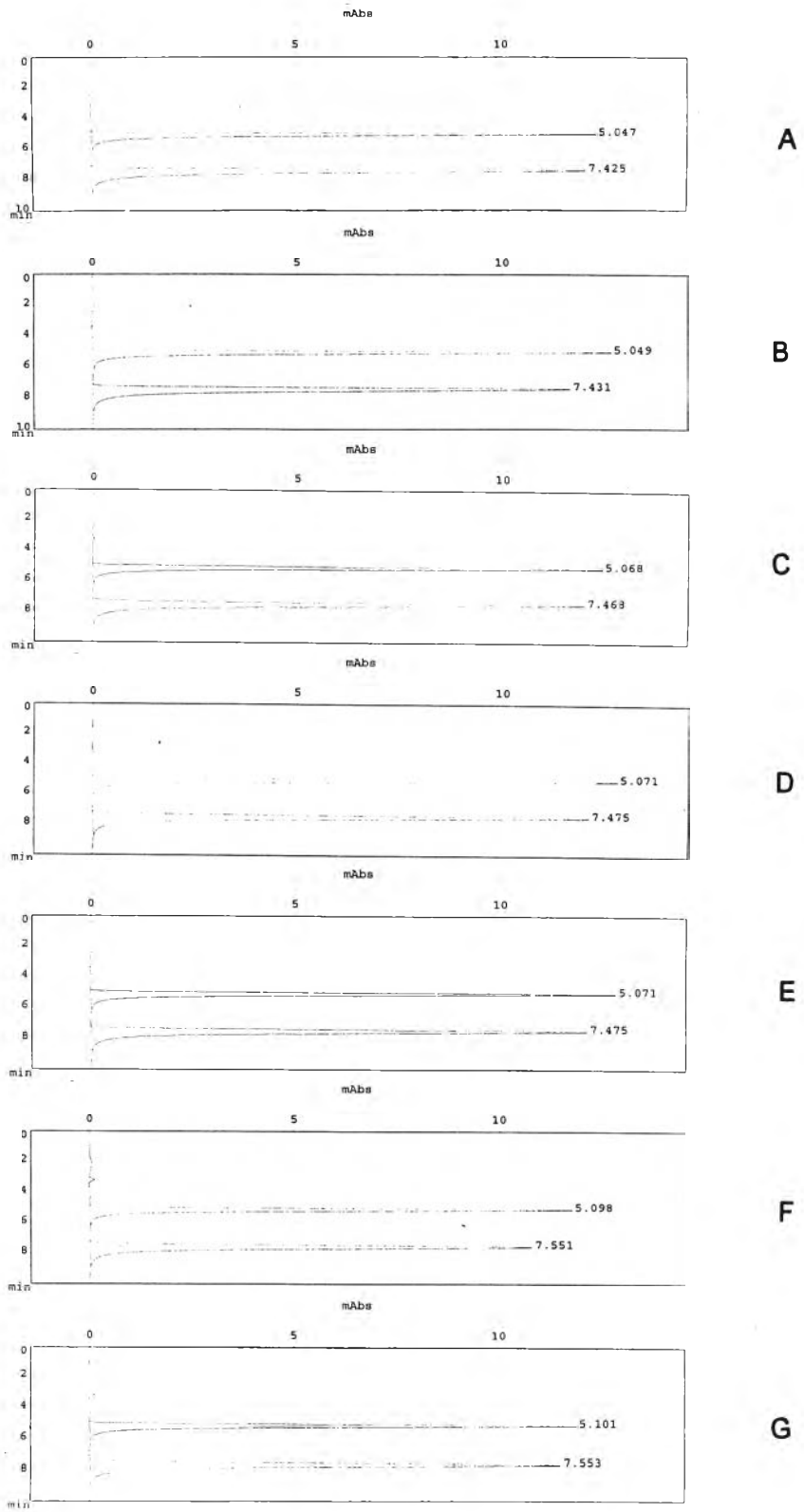

Figure 63. HPLC chromatograms of R:2HP-β-CD complex in buffer solutions pH 1-13. [0.30 M phosphate buffer pH 1, (A); 0.20 M phosphate buffer pH 3, (B); 0.30 M acetate buffer pH 5, (C); 0.20 M phosphate buffer pH 7, (D); 0.30 M glycine-NaOH buffer pH 9, (E); 0.30 M glycine-NaOH buffer pH11, (F); and 0.08 M phosphate buffer pH 13, (G)].

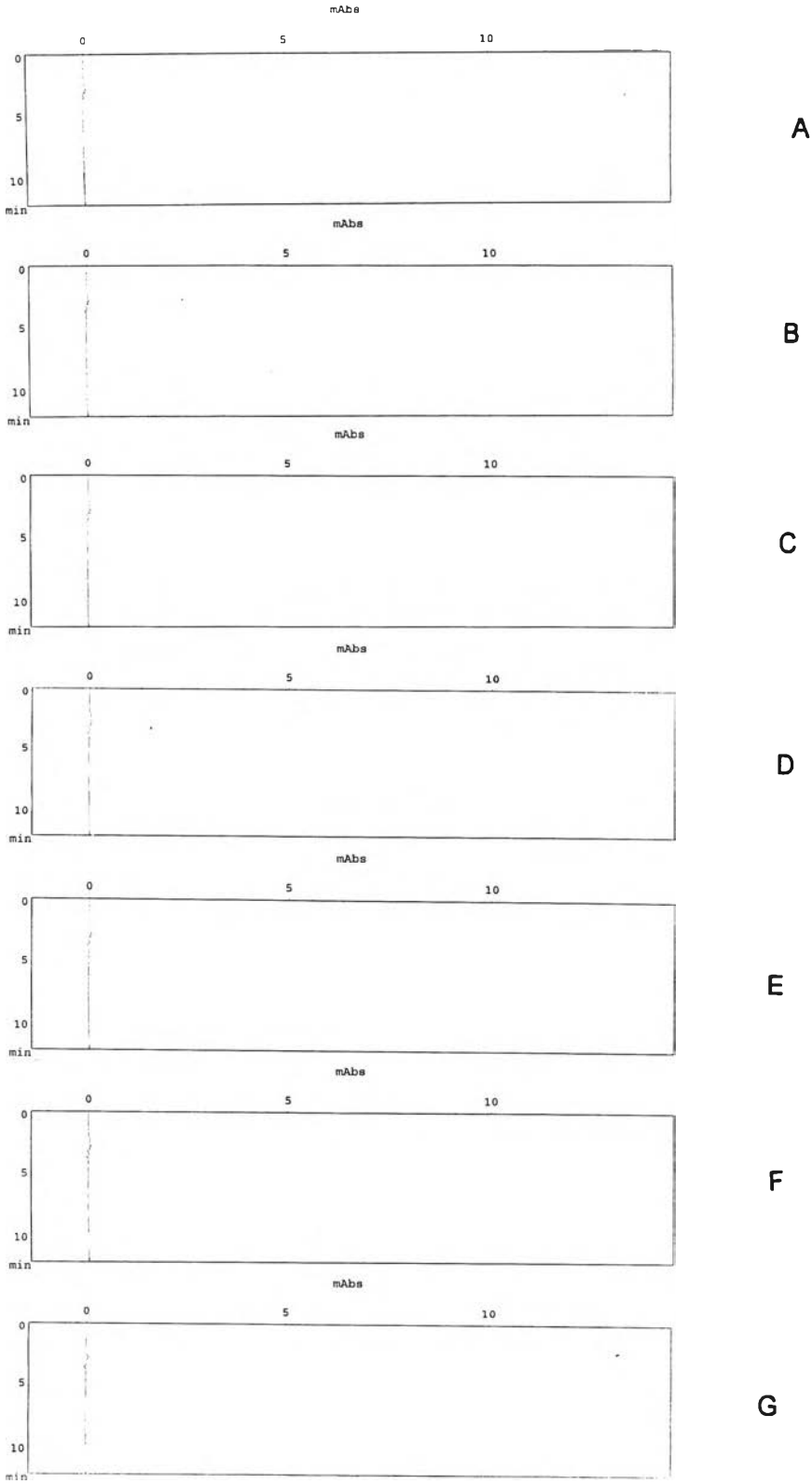

Figure 64. HPLC chromatograms of decomposed buffer solutions pH 1-13. [0.30 M phosphate buffer pH 1, (A); 0.20 M phosphate buffer pH 3, (B); 0.30 M acetate buffer pH 5, (C); 0.20 M phosphate buffer pH 7, (D); 0.30 M glycine-NaOH buffer pH 9, (E); 0.30 M glycine-NaOH buffer pH11, (F); and 0.08 M phosphate buffer pH 13, (G)].

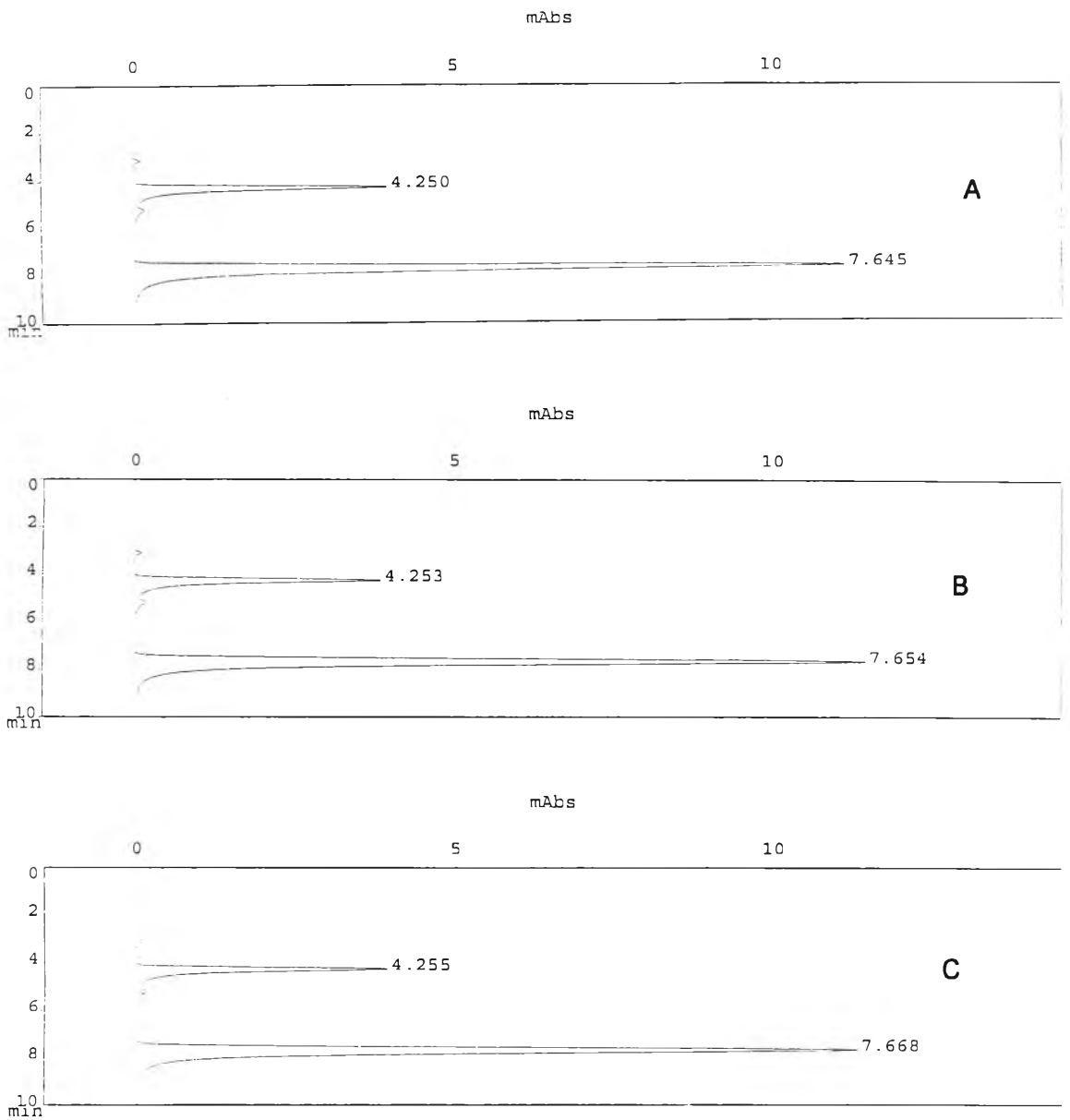

Figure 65. HPLC chromatograms of decomposed drug solutions in 0.30 **M** phosphate buffer pH 1. [ranitidine HCl, (A); R:β-CD complex, (B); R:2HP-β-CD complex, (C)].

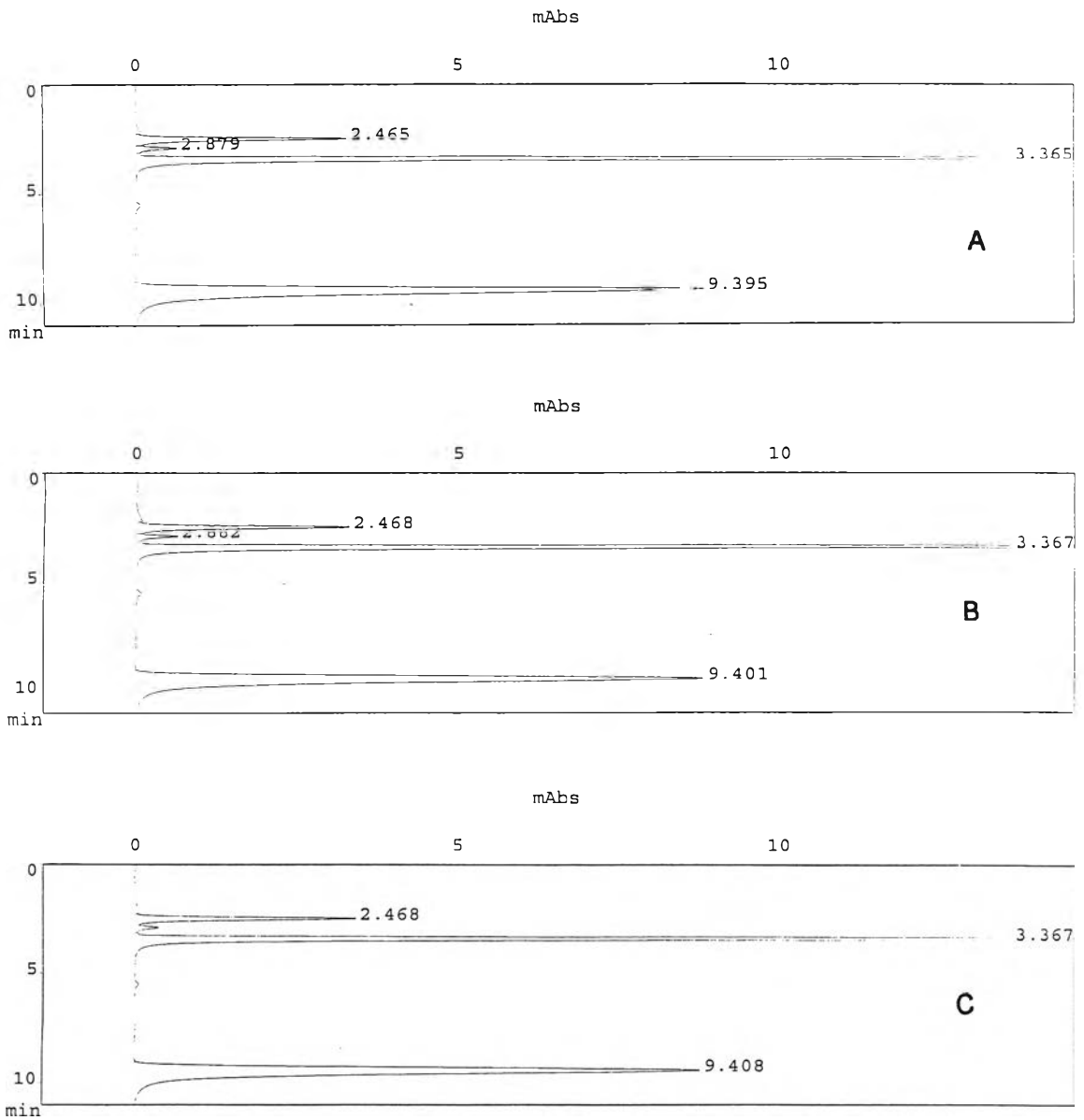

Figure 66. HPLC chromatograms of decomposed drug solutions in 0.08 M phosphate buffer pH 13. [ranitidine HCl, (A); R:β-CD complex, (B); R:2HP-β-CD complex, (C)].

phosphate buffer, similar results were also observed (Figure 66). The degradation product peaks were also eluted before ranitidine HCl peak which almost disappeared. Thus, this method could be used for analysis of ranitidine HCl, both in its free form or in R : CDs form, in the presence of its degradation products and it was not interfered by the decomposed buffer components.

6.2 Precision

The precision of an analytical method is the degree of agreement among individual test results when the procedure is applied repeatedly to multiple samplings of a homogeneous sample. The precision of an analytical method is usually expressed as the standard deviation or relative standard deviation (coefficient of variation).

Tables 27-28 illustrated the data of within and between run precisions, respectively. All coefficient of variation values were small indicating that the HPLC method used were precise for quantitation of ranitidine HCl concentrations in the range studied at any time.

6.3 Accuracy

The accuracy of an analytical method is the closeness of test results obtained by that method to the true value. Accuracy may often be expressed as percent recovery by the assay of known, added amounts of analyte. The percentages of analytical recovery of each drug concentration are shown in Table 29. All the percentage of analytical recoveries of all drug concentrations with a mean of 100.10% and a %CV of 0.94 indicated the high accuracy of this method. Thus, it could be used for analysis of ranitidine HCl in all concentrations studied.

Table 27. Data of within run precision.

Ranitidine HCl concentrations (μg/mL)	Peak area ratio				
	Set No. 1	Set No. 2	Set No. 3	Mean (SD)	%CV
2.00	0.0639	0.06304	0.0622	0.0630 (0.0009)	1.41
4.00	0.1286	0.1317	0.1298	0.1300 (0.0016)	1.23
8.00	0.2495	0.2565	0.2505	0.2522 (0.0038)	1.49
12.00	0.3748	0.3794	0.3830	0.3790 (0.0041)	1.08
16.00	0.5041	0.5084	0.5124	0.5083 (0.0042)	0.82
20.00	0.6426	0.6474	0.6477	0.6459 (0.0028)	0.44
24.00	0.7633	0.7629	0.7673	0.7645 (0.0024)	0.32

Table 28. Data of between run precision.

Ranitidine HCl concentrations (μg/mL)	Peak area ratio				
	Day 1	Day 2	Day 3	Mean (SD)	%CV
2.00	0.0653	0.0643	0.0649	0.0648 (0.0005)	0.79
4.00	0.1310	0.1314	0.1305	0.1310 (0.0004)	0.34
8.00	0.2554	0.2568	0.2606	0.2576 (0.0027)	1.05
12.00	0.3854	0.3816	0.3862	0.3844 (0.0025)	0.64
16.00	0.5148	0.5169	0.5224	0.5180 (0.0039)	0.76
20.00	0.6509	0.6454	0.6570	0.6511 (0.0058)	0.89
24.00	0.7729	0.7700	0.7780	0.7736 (0.0040)	0.52

Table 29. Percentages of analytical recovery of ranitidine HCl.

Known ranitidine HCl concentrations (μg/mL)	Calculated concentrations* (μg/mL)	% Analytical recovery
2.00	2.02	100.96
	1.99	99.38
	2.01	100.33
4.00	4.05	101.33
	4.06	101.61
	40.4	100.91
8.00	7.90	98.74
	7.94	99.26
	8.06	100.75
12.00	11.92	99.32
	11.80	98.36
	11.95	99.55
16.00	15.92	99.51
	15.99	99.93
	16.16	100.99
20.00	20.13	100.66
	19.96	99.81
	20.32	101.61
24.00	23.90	99.60
	23.81	99.23
	24.06	100.26
		Mean = 100.10
		SD = 0.9369
		%CV = 0.94

* Calculated from calibration curve.

6.4 Linearity

The linearity of an analytical method is its ability to elicit test results that are directly, or by a well-defined mathematical transformation, proportional to the concentration of analyte in samples within a given range. The linearity is usually expressed in terms of the variance around the slope of the regression line calculated according to an established mathematical relationship from test results obtained by the analysis of samples with varying concentrations of analyte. The calibration curve data is shown in Table 30. The plot of ranitidine HCl concentrations versus the peak area ratios of ranitidine HCl and its internal standard (Figure 67) illustrated the linear correlation in the concentration range studied, 2.00-24.00 μg/mL. The correlation coefficient (r) of this line was 0.9999.

Table 30. Data for calibration curve of ranitidine HCl.

Ranitidine HCl concentrations (μg/mL)	Peak area ratio				
	Set No. 1	Set No. 2	Set No. 3	Mean (SD)	%CV
2.00	0.0653	0.0643	0.0649	0.0648 (0.0005)	0.79
4.00	0.1310	0.1314	0.1305	0.1310 (0.0004)	0.34
8.00	0.2554	0.2568	0.2606	0.2576 (0.0027)	1.05
12.00	0.3854	0.3816	0.3862	0.3844 (0.0025)	0.64
16.00	0.5148	0.5169	0.5224	0.5180 (0.0039)	0.76
20.00	0.6509	0.6454	0.6570	0.6511 (0.0058)	0.89
24.00	0.7729	0.7700	0.7780	0.7736 (0.0040)	0.52

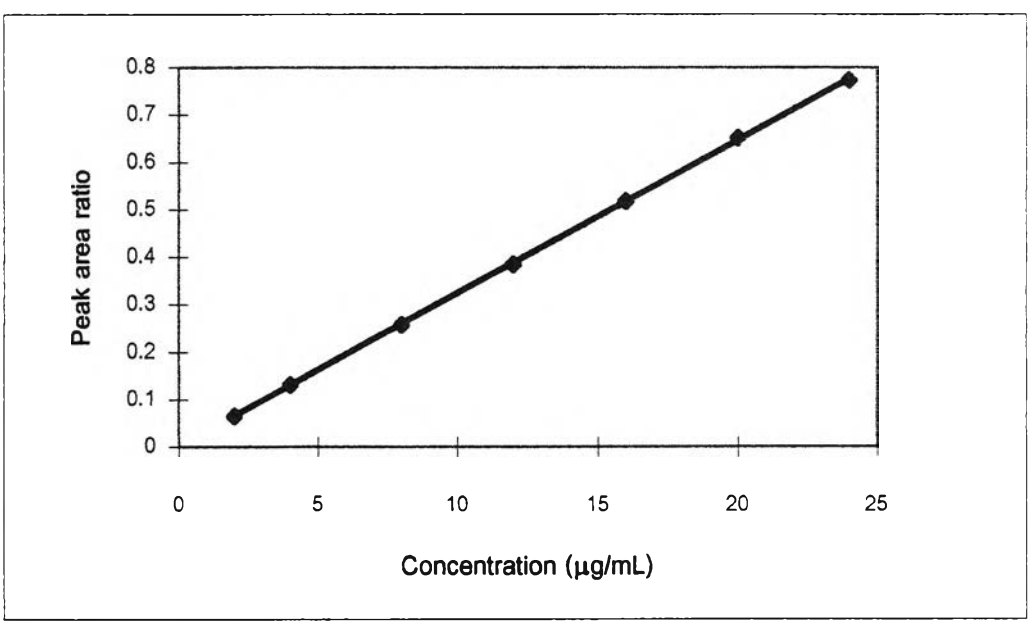

Figure 67. The calibration curve of ranitidine HCl.